

FrenchBic METBIO summer school

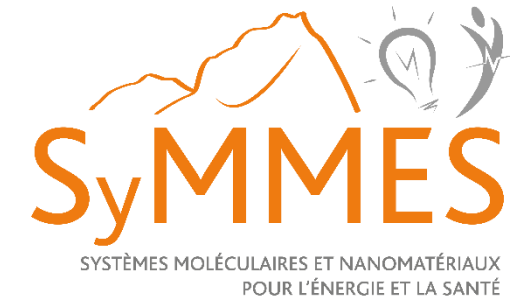
September 17-21, 2017

Lecture #3

Theoretical chemistry

Jean-Marie Mouesca

CEA/Univ Grenoble Alpes



Outline of the lecture

- ***Basic introduction to DFT***
 - ***Hartree-Fock versus DFT***
- ***Application : (mono-metal) g-tensors***
 - ***Relativistic origin***
 - ***Perturbative & self-consistent approaches***
 - ***When it does not work ...***
- ***Polymetallic complexes***
 - ***Spin-coupling***
 - ***g-tensor (dimer)***
 - ***Hyperfine couplings (dimer)***
 - ***More complex systems : hyperfine & Mössbauer***
- ***Conclusions***

DFT & (metal) spectroscopies :

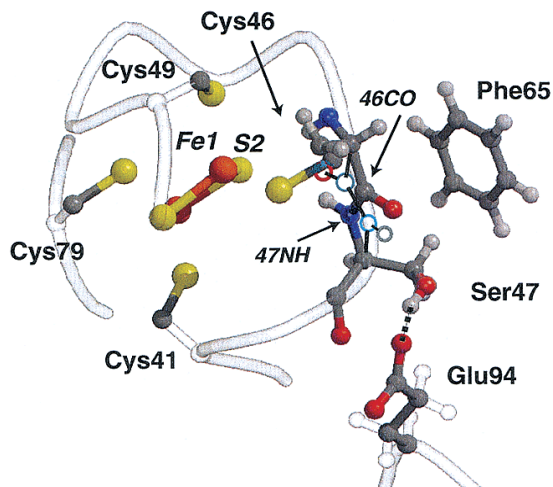
Molecular
structure

φ -chemical
properties

Crystallography
(X-ray)
Solution NMR

Spectroscopic
parameters

Redox potentials
Electron transfer
Magnetism



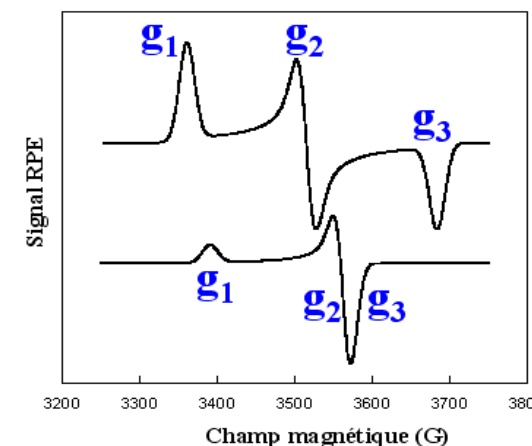
Chemical shifts : NMR

g-tensors : EPR

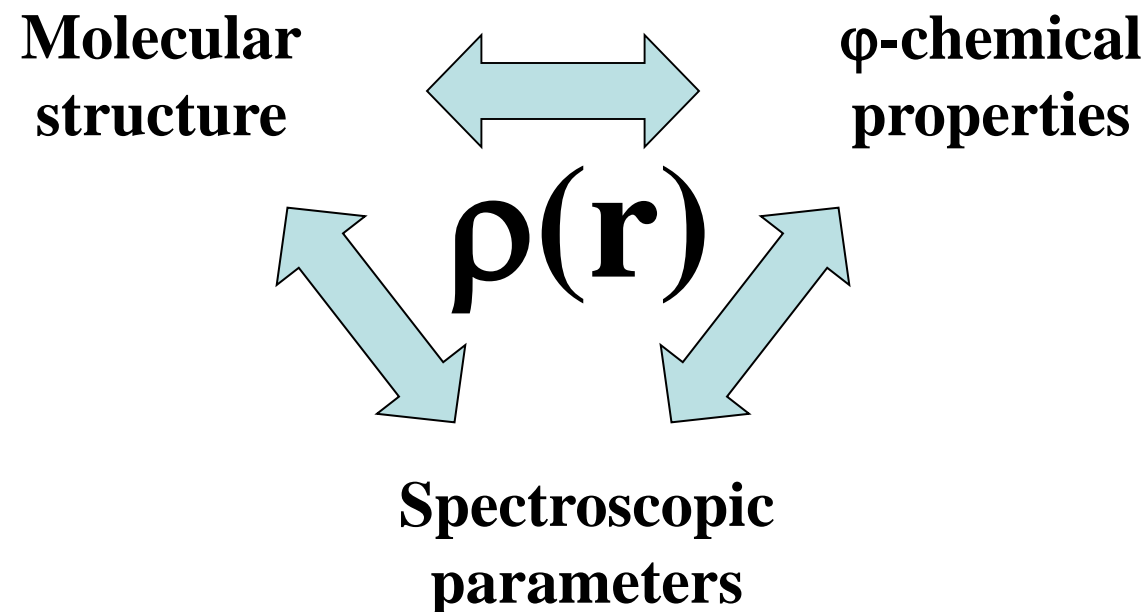
Hyperfine couplings: NMR/ EPR

But also

Mössbauer, etc



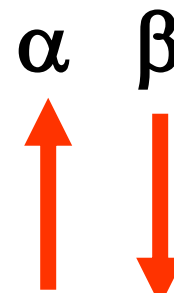
Density Functional Theory



Density function

$$\rho(\mathbf{r}) = \Psi^2(\mathbf{r})$$

- ↳ of charge : $\rho_e(\mathbf{r}) = \rho_\alpha(\mathbf{r}) + \rho_\beta(\mathbf{r})$
- ↳ of spin : $\rho_s(\mathbf{r}) = \rho_\alpha(\mathbf{r}) - \rho_\beta(\mathbf{r})$



+ « home-made » codes (spectroscopies)



Walter Kohn

Density Functional Theory

What can we compute ?

Charge (diamagnetic)

$$\rho_e(r) = \rho_\alpha(r) + \rho_\beta(r)$$

diamag. NMR

Spin (paramagnetic)

$$\rho_s(r) = \rho_\alpha(r) - \rho_\beta(r)$$

param. NMR (**hyperfine**)

EPR (g-tensors, **hyperfine**)

UV-vis

IR spectra

Mössbauer (δ , ΔE_Q)

Mössbauer (**hyperfine**)

SQUID (exchange J)

Redox potentials

etc.

etc.

etc.

Practical implementations

▼ Spectroscopic properties

- › IR spectra, (resonance) Raman, VROA, VCD
- › Time-dependent DFT
- › Excitation energies: UV/Vis, X-ray, CD, MCD
- Excited state (geometry) optimizations
- › vibrationally resolved electronic spectra
- › (Hyper-)Polarizabilities, ORD, magnetizabilities, Verdet constants

› Ligand Field and Density Functional Theory (LFDFT)

› NMR

› ESR/EPR

Nuclear Quadrupole Interaction (EFG)

Mössbauer spectroscopy

▼ ESR/EPR

ESR/EPR g-tensor and A-tensor

ESR/EPR Q-tensor

ESR/EPR Zero-field splitting (D-tensor)

▼ NMR

› NMR Chemical Shifts

Paramagnetic NMR Chemical Shifts

› NMR spin-spin coupling constants

▼ Excitation energies: UV/Vis, X-ray, CD, MCD

› Excitation energies, UV/Vis spectra

Excitation energies for open-shell systems

Spin-flip excitation energies

+ Solvent effects

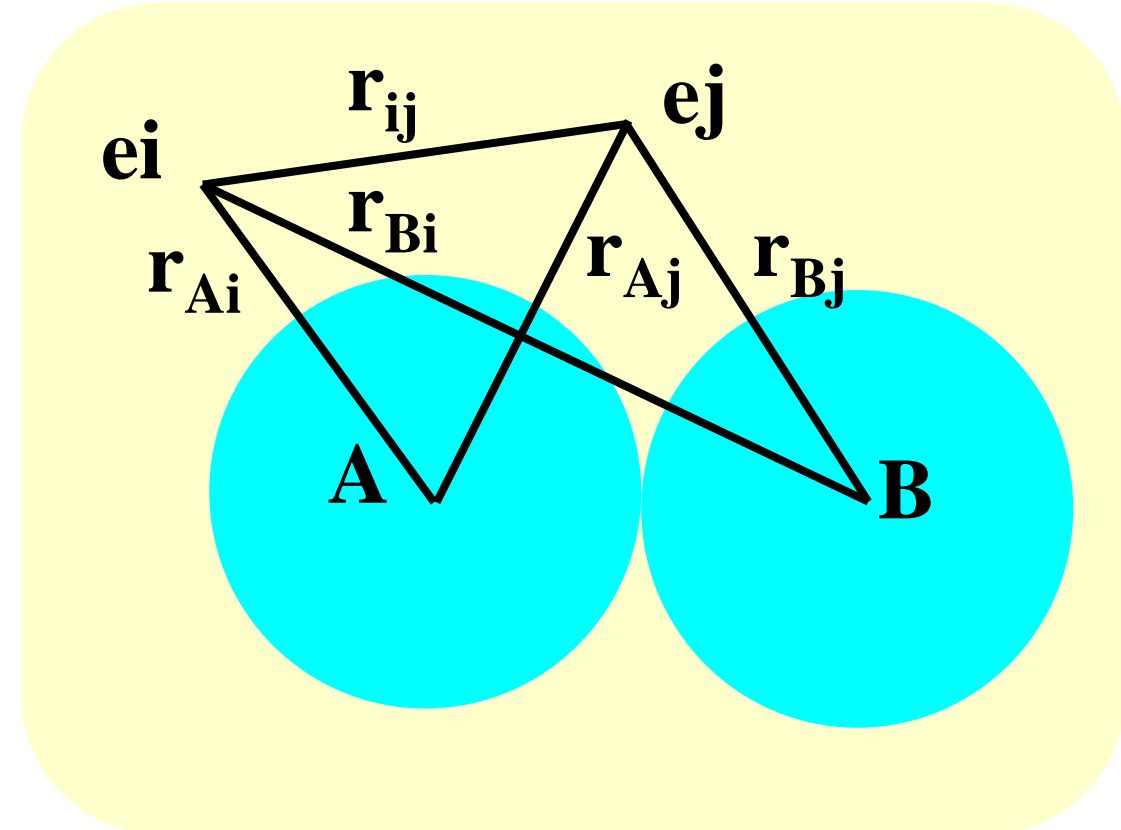
Schrödinger equation

(classical & time-independant)

$$H_T \Psi = E \Psi$$

$$\begin{aligned} H_T = & -\sum_A \frac{\hbar^2}{2M_A} \nabla_A^2 & -\sum_i \frac{\hbar^2}{2m_i} \nabla_i^2 \\ & + \sum_A \sum_{B>A} \frac{Z_A Z_B e^2}{|R_A - R_B|} & + \sum_i \sum_{j>i} \frac{e^2}{|r_i - r_j|} \\ & - \sum_A \sum_i \frac{Z_A e^2}{|R_A - r_i|} \end{aligned}$$

$$H_{\text{elec}} \Psi_{\text{elec}} = E_{\text{elec}} \Psi_{\text{elec}}$$



Schrödinger equation

(classical & time-independant)

$$H_T \Psi = E \Psi$$

$$\begin{aligned} H_{elec} = & -\sum_i \frac{\hbar^2}{2m_i} \nabla_i^2 \\ & + \sum_i \sum_{j>i} \frac{e^2}{|r_i - r_j|} \\ & - \sum_A \sum_i \frac{Z_A e^2}{|R_A - r_i|} \end{aligned}$$

$$\begin{aligned} H_{elec} \Psi_{elec} &= E_{elec} \Psi_{elec} \\ E_{tot} &= E_{elec} + E_{nuc} \end{aligned}$$

$$E_{test} \geq E_0 = \min_{\{\Psi\}} E[\Psi_{test}]$$

$$\{N, Z_A, R_A\} \Rightarrow H \Rightarrow \Psi_0 \Rightarrow E_0$$

$$\Psi(\mathbf{x}_i, \mathbf{x}_j) = -\Psi(\mathbf{x}_j, \mathbf{x}_i)$$

Hartree-Fock & Slater determinant

$$\Psi_{test} \approx \Psi_{Slater} = \frac{1}{\sqrt{N!}} \begin{vmatrix} \varphi_1(x_1) & \varphi_2(x_1) & \dots & \varphi_N(x_1) \\ \varphi_1(x_2) & \varphi_2(x_2) & \dots & \varphi_N(x_2) \\ \dots & \dots & \dots & \dots \\ \varphi_1(x_N) & \varphi_2(x_N) & \dots & \varphi_N(x_N) \end{vmatrix}$$

$$\varphi_1(x_1) \equiv \varphi_1(r_1, s_1) \approx \varphi_1(r_1) \sigma_1(s_1)$$

$$\begin{aligned}\sigma(\uparrow) &= \alpha \\ \sigma(\downarrow) &= \beta\end{aligned}$$

$$E_{HF} = \min_{\{\Psi_{Slater}\}} E[\Psi_{Slater}]$$

Hartree-Fock equations

$$\Psi_{test} \approx \Psi_{Slater} = \frac{1}{\sqrt{2!}} \begin{vmatrix} \varphi_1(r_1)\sigma_1(s_1) & \varphi_2(r_1)\sigma_2(s_1) \\ \varphi_1(r_2)\sigma_1(s_2) & \varphi_2(r_2)\sigma_2(s_2) \end{vmatrix}$$

$$E_{HF} = \langle \Psi_{Slater} | H_{elec} | \Psi_{Slater} \rangle =$$
$$\sum_{i=1}^2 \left\langle \varphi_i(x_1) \left| -\frac{\hbar^2}{2m_i} \nabla_i^2 - \sum_A \frac{Z_A e^2}{|R_A - r_i|} \right. \right\rangle \varphi_i(x_1)$$
$$+ \cancel{\left\langle \varphi_1(x_1)^2 \left| \frac{e^2}{|r_1 - r_2|} \right| \varphi_1(x_2)^2 \right\rangle} + \left\langle \varphi_1(x_1)^2 \left| \frac{e^2}{|r_1 - r_2|} \right| \varphi_2(x_2)^2 \right\rangle \quad \mathbf{K}_{12}$$
$$- \cancel{\left\langle \varphi_1(x_1)^2 \left| \frac{e^2}{|r_1 - r_2|} \right| \varphi_1(x_2)^2 \right\rangle} - \left\langle \varphi_1(x_1) \varphi_2(x_2) \left| \frac{e^2}{|r_1 - r_2|} \right| \varphi_2(x_1) \varphi_1(x_2) \right\rangle \quad \mathbf{J}_{12}$$

Case of 2 electrons : triplet state ($S=1$)

$$\det_1 = \frac{1}{\sqrt{2}} \begin{vmatrix} \varphi_1(r_1)\alpha_1(s_1) & \varphi_2(r_1)\alpha_2(s_1) \\ \varphi_1(r_2)\alpha_1(s_2) & \varphi_2(r_2)\alpha_2(s_2) \end{vmatrix}$$



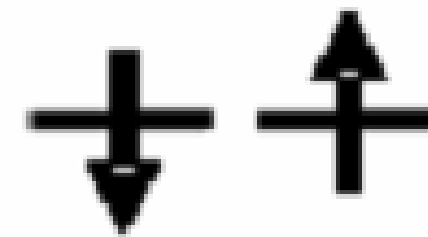
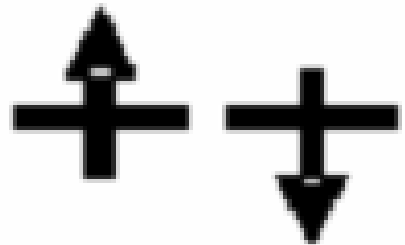
$$[\Phi_1(r_1)\Phi_2(r_2) - \Phi_2(r_1)\Phi_1(r_2)]\alpha(1)\alpha(2)$$

$$E_{HF}^{\alpha\alpha} = h_1 + h_2 + K_{12} - J_{12}$$

Case of 2 electrons : singlet state ($S=0$)

$$\det_2 = \frac{1}{\sqrt{2}} \begin{vmatrix} \Phi_1(r_1)\alpha(1) & \Phi_1(r_2)\alpha(2) \\ \Phi_2(r_1)\beta(1) & \Phi_2(r_2)\beta(2) \end{vmatrix}$$

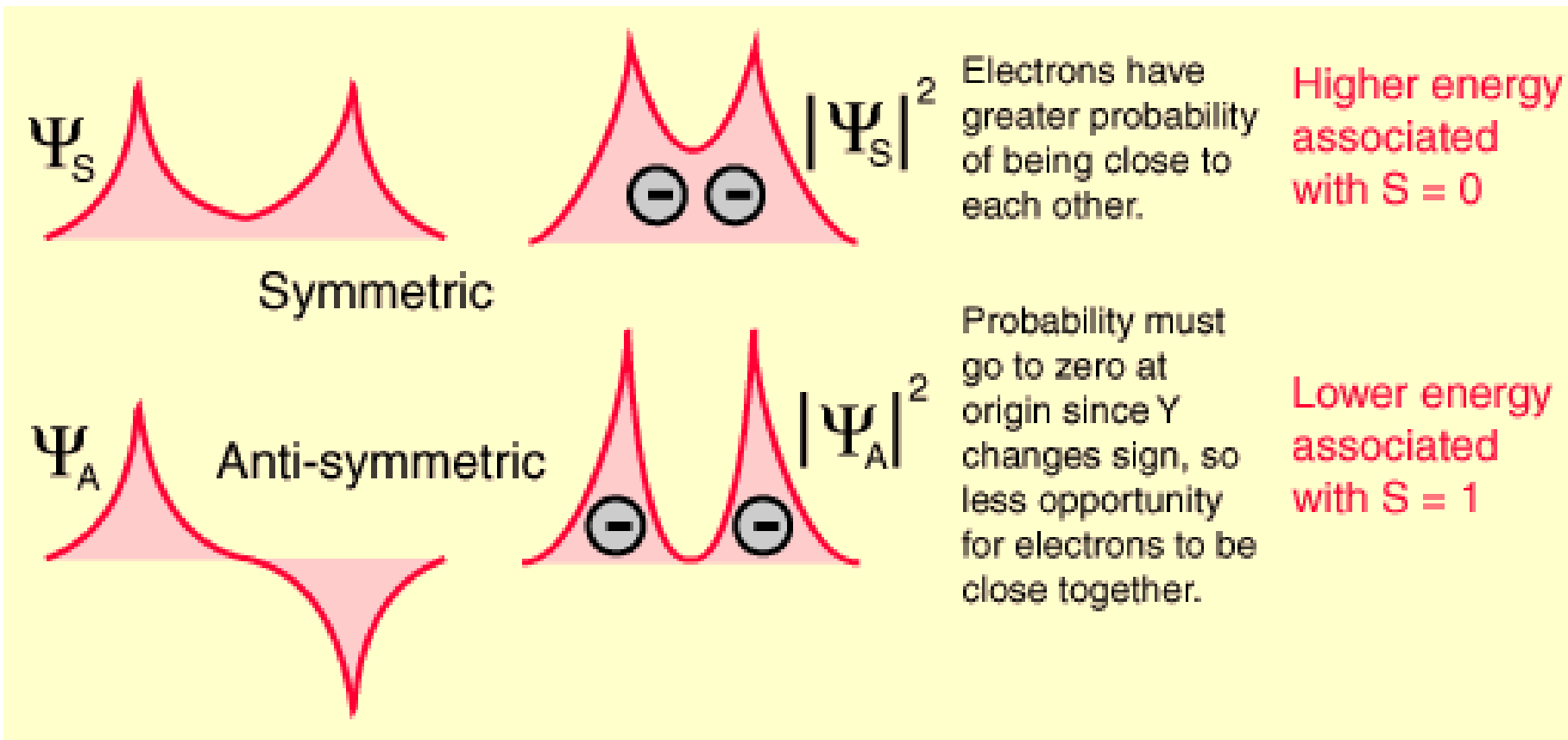
$$\det_3 = \frac{1}{\sqrt{2}} \begin{vmatrix} \Phi_1(r_1)\beta(1) & \Phi_1(r_2)\beta(2) \\ \Phi_2(r_1)\alpha(1) & \Phi_2(r_2)\alpha(2) \end{vmatrix}$$



$$[\Phi_1(r_1)\Phi_2(r_2) + \Phi_2(r_1)\Phi_1(r_2)] [\alpha(1)\beta(2) - \beta(1)\alpha(2)]$$

$$E_{HF}^{\alpha\beta} = h_1 + h_2 + K_{12}$$

Exchange term



Triplet state



$$E_{HF}^{\alpha\alpha} = h_1 + h_2 + K_{12} - J_{12}$$

Singlet state



$$E_{HF}^{\alpha\beta} = h_1 + h_2 + K_{12}$$

What about electronic correlation ?

$$E_{correlation} \equiv E_0 - E_{HF} < 0$$

$$\Psi_{test} = c_0 \Psi_0 + \sum_k c_k \Psi_k$$

Dynamic correlation :
Instantaneous repulsion

Static correlation :
Orbital degenerescence

$$(c_0)^2 \gg (c_k)^2$$

$$\rho_{CI} = \left(c_0 \Psi_0 + \sum_k c_k \Psi_k \right)^2$$

$$(c_0)^2 \sim (c_k)^2$$

Basis of DFT

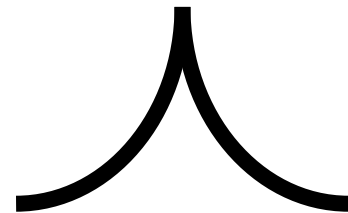
(Density Functional Theory)

$\Psi(r,s)$ not observable,
in contrast to
 $\rho(r,s) = \Psi(r,s)^2$

$$\int \rho(r) dr = N$$

$\rho(r)$ non differentiable in R_A

$\rho(r)$ en $R_A \rightarrow Z_A$



Basis of DFT

(Density Functional Theory)

Thomas-Fermi model (1927)

Kinetic energy:

$$\frac{3}{10} (3\pi^2)^{2/3} \int \rho^{5/3}(r) dr$$

Electron-nucleus :

$$-Z \int \frac{\rho(r)}{r} dr$$

Electron-electron :

$$\frac{1}{2} \iint \frac{\rho(r_1)\rho(r_2)}{r_{12}} dr_1 dr_2$$

Basis of DFT

(Density Functional Theory)

Slater's model (1951) HFS ($X\alpha$)

Goal : simplify Hartree-Fock's exchange

$$\frac{1}{2} \sum_{i=1}^N \sum_{j=1}^N \left\langle \varphi_j(x_1) \varphi_i(x_2) \left| \frac{e^2}{|r_1 - r_2|} \right| \varphi_i(x_1) \varphi_j(x_2) \right\rangle$$



$$E_{X\alpha}[\rho] = -\frac{9}{8} \left(\frac{3}{\pi} \right)^{1/3} \alpha \int \rho(r)^{4/3} dr$$

Basis of DFT

(Density Functional Theory)

**Existence theorem :
Hohenberg-Kohn (1964)**

The external potential V_{ext} is a unique functional of the density $\rho(r)$. Since V_{ext} determines the hamiltonian H_{elec} , the fundamental state is a functional of the density.

$$H = T + V_{ee} + V_{ext}$$

$$\rho_0 \Rightarrow \{N, Z_A, R_A\} \Rightarrow H \Rightarrow \Psi_0 \Rightarrow E_0$$

Basis of DFT

$$H = T + V_{ee} + V_{ext}$$



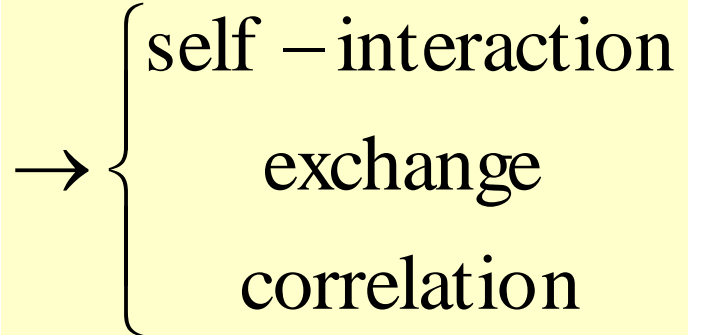
$$E_0[\rho_0] = T[\rho_0] + E_{ee}[\rho_0] + \int V_{ext} \rho_0(r) dr$$



Molecule

$$F_{HK}[\rho_0]$$

$$E_{ee}[\rho] = \underbrace{\frac{1}{2} \iint \frac{\rho(r_1)\rho(r_2)}{r_{12}} dr_1 dr_2}_{K[\rho]} + \boxed{E_{XC}[\rho]}$$


→ { self – interaction
 exchange
 correlation

Basis of DFT

(Density Functional Theory)

Kohn-Sham (1965)

Reference : non-interacting electrons (Slater determinant)

$$\hat{F}_{HF} \varphi_i^{HF} = \varepsilon_i^{HF} \varphi_i^{HF} \leftrightarrow \hat{F}_{KS} \varphi_i^{KS} = \varepsilon_i^{KS} \varphi_i^{KS}$$

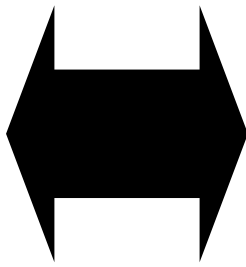
$$F_{HK}[\rho] = T_{KS}[\rho] + K[\rho] + \int V_{ext} \rho(r) dr + E_{XC}[\rho]$$

Practical implementations

$$F_{HK}[\rho] = T_{KS}[\rho] + K[\rho] + \int V_{ext} \rho(r) dr + E_{XC}[\rho]$$

- **Density Functionals (XC)**

- LDA
- GGA
- MetaGGA
- Hartree-Fock
- Hybrid
- Meta-Hybrid
- Range separated hybrids
- Notes on Hartree-Fock and (meta-)hybrid functionals
- Model Potentials



Available LDA functionals:

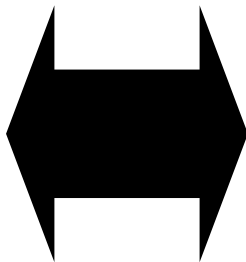
- **Xonly:** The pure-exchange electron gas formula. Technically this is identical to the Xalpha form (see next) with a value 2/3 for the X-alpha parameter.
- **Xalpha:** The scaled (parametrized) exchange-only formula. When this option is used you may (optionally) specify the X-alpha *parameter* by typing a numerical value after the string Xalpha (separated by a blank). If omitted this parameter takes the default value 0.7
- **VWN:** The parametrization of electron gas data given by Vosko, Wilk and Nusair (ref [20], formula version V). Among the available LDA options this is the more advanced one, including correlation effects to a fair extent.
- **PW92:** the parametrization of electron gas data given by Perdew and Wang (ref [288]).

Practical implementations

$$F_{HK}[\rho] = T_{KS}[\rho] + K[\rho] + \int V_{ext} \rho(r) dr + E_{XC}[\rho]$$

- **Density Functionals (XC)**

- LDA
- GGA
- MetaGGA
- Hartree-Fock
- Hybrid
- Meta-Hybrid
- Range separated hybrids
- Notes on Hartree-Fock and
(meta-)hybrid functionals
- Model Potentials



For the exchange part the options are:

- Becke: Becke (1988) [22].
- PW86x: Perdew-Wang (1986) [23].
- PW91x: Perdew-Wang (1991) [24]
- mPWx: Modified PW91 by Adamo-Barone (1998) [25]
- PBEx: Perdew-Burke-Ernzerhof (1996) [26]
- RPBEx: revised PBE by Hammer-Hansen-Nørskov (1999) [27]
- revPBEx: revised PBE by Zhang-Wang (1998) [28]
- mPBEx: Modified PBE by Adamo-Barone (2002) [174]
- PBEsolx: Perdew-Ruzsinszky-Csonka-Vydrov-Scuseria (2008) [285]
- HTBSx: [437]
- OPTX: Handy-Cohen (2001) [29]
- BEE: Mortensen-Kaasbjerg-Frederiksen-Nørskov-Sethna-Jacobsen (2005) [284]

For the correlation part the options are:

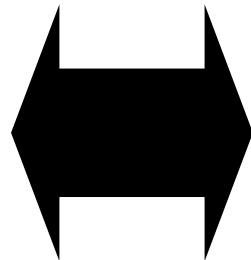
- Perdew: Perdew (1986) [30].
- PBEc: Perdew-Burke-Ernzerhof (1996) [26].
- PBEsolc: The PBEsol correlation correction by Perdew-Ruzsinszky-Csonka-Vydrov-Scuseria (2008) [285]
- PW91c: Perdew-Wang (1991), see [24].
- LYP: Lee-Yang-Parr (1988) correlation correction [31-33].

Practical implementations

$$F_{HK}[\rho] = T_{KS}[\rho] + K[\rho] + \int V_{ext} \rho(r) dr + E_{XC}[\rho]$$

- **Density Functionals (XC)**

- LDA
- **GGA**
- MetaGGA
- Hartree-Fock
- Hybrid
- Meta-Hybrid
- Range separated hybrids
- Notes on Hartree-Fock and
(meta-)hybrid functionals
- Model Potentials



Available GGA functionals:

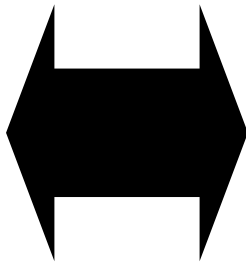
- BP86: Exchange: Becke, Correlation: Perdew
- PW91: Exchange: pw91x, Correlation: pw91c
- mPW: Exchange: mPWx, Correlation: pw91c
- PBE: Exchange: PBEx, Correlation: PBEc
- RPBE: Exchange: RPBEx, Correlation: PBEc
- revPBE: Exchange: revPBEx, Correlation: PBEc
- mPBE: Exchange: mPBEx, Correlation: PBEc
- PBEsol: Exchange: PBEsolx, Correlation: PBEsolc
- HTBS: Exchange: HTBSx, Correlation: PBEc
- BLYP: Exchange: Becke, Correlation: LYP
- OLYP: Exchange: OPTX, Correlation: LYP
- OPBE: Exchange: OPTX, Correlation: PBEc [175]
- BEE: Exchange: BEEx, Correlation: PBEc
- XLYP: Exchange: XLYPx [172] (exchange, not available separately from LYP) + LYP

Practical implementations

$$F_{HK}[\rho] = T_{KS}[\rho] + K[\rho] + \int V_{ext} \rho(r) dr + E_{XC}[\rho]$$

- **Density Functionals (XC)**

- LDA
- GGA
- MetaGGA
- Hartree-Fock
- **Hybrid**
- Meta-Hybrid
- Range separated hybrids
- Notes on Hartree-Fock and
(meta-)hybrid functionals
- Model Potentials



Available Hybrid functionals:

- **B3LYP**: ADF uses VWN5 in B3LYP functional (20% HF exchange) by Stephens-Devlin-Chabłowski-Frisch [176].
- **B3LYP***: Modified B3LYP functional (15% HF exchange) by Reiher-Salomon-Hess [177].
- **B1LYP**: Functional (25% HF exchange) by Adamo-Barone [178].
- **KMLYP**: Functional (55.7% HF exchange) by Kang-Musgrave [179].
- **O3LYP**: Functional (12% HF exchange) by Cohen-Handy [180].
- **X3LYP**: Functional (21.8% HF exchange) by Xu-Goddard [172].
- **BHandH**: 50% HF exchange, 50% LDA exchange, and 100% LYP correlation.
- **BHandHLYP**: 50% HF exchange, 50% LDA exchange, 50% Becke88 exchange, and 100% LYP correlation.
- **B1PW91**: Functional by (25% HF exchange) Adamo-Barone [178].
- **mPW1PW**: Functional (42.8% HF exchange) by Adamo-Barone [25].
- **mPW1K**: Functional (25% HF exchange) by Lynch-Fast-Harris-Truhlar [181].
- **PBE0**: Functional (25% HF exchange) by Ernzerhof-Scuseria [211] and by Adamo-Barone [212], hybrid form of PBE.
- **OPBE0**: Functional (25% HF exchange) by Swart-Ehlers-Lammertsma [175], hybrid form of OPBE.
- **S12H**: Dispersion corrected (Grimme-D3) functional (25% HF exchange) by Swart [367].

Comparaison between HF and DFT

$$\rho^{HF} = (\Psi^{HF})^2$$

$$\Psi_{CI} = c_0 \Psi_0 + \sum_k c_k \Psi_k$$

- Ψ^{HF} contains no correlation
- ρ^{HF} is not the ‘true’ density ρ^{CI}

$$\Psi^{KS} \leftarrow \rho^{KS}$$

$$\rho_{CI} = \left(c_0 \Psi_0 + \sum_k c_k \Psi_k \right)^2$$

- Ψ^{KS} is not the wave function
- ρ^{KS} close to the ‘true’ density ρ^{CI}

Case of 2 electrons : triplet state ($S=1$)

$$\Psi_1 = \frac{1}{\sqrt{2}} \begin{vmatrix} \varphi_1(r_1)\alpha_1(s_1) & \varphi_2(r_1)\alpha_2(s_1) \\ \varphi_1(r_2)\alpha_1(s_2) & \varphi_2(r_2)\alpha_2(s_2) \end{vmatrix}$$



$$[\Phi_1(r_1)\Phi_2(r_2) - \Phi_2(r_1)\Phi_1(r_2)]\alpha(1)\alpha(2)$$

$$\rho^{HF} \sim (\Psi_1)^2$$

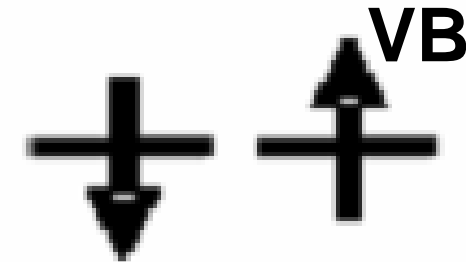
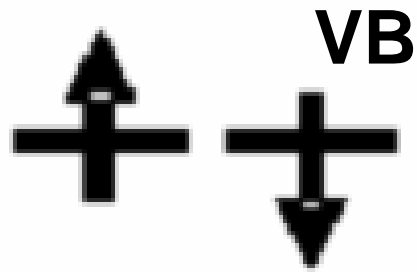
High-spin state :
~ one determinant

$$\rho^{KS} = (\Psi^{KS})^2$$

Case of 2 electrons : singlet state ($S=0$)

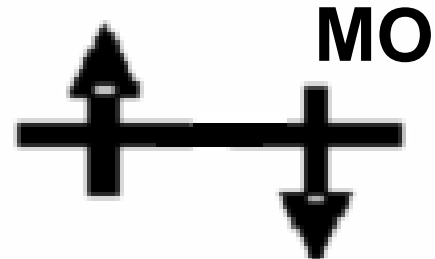
$$\Psi_2 = \frac{1}{\sqrt{2}} \begin{vmatrix} \Phi_1(r_1)\alpha(1) & \Phi_1(r_2)\alpha(2) \\ \Phi_2(r_1)\beta(1) & \Phi_2(r_2)\beta(2) \end{vmatrix}$$

$$\Psi_3 = \frac{1}{\sqrt{2}} \begin{vmatrix} \Phi_1(r_1)\beta(1) & \Phi_1(r_2)\beta(2) \\ \Phi_2(r_1)\alpha(1) & \Phi_2(r_2)\alpha(2) \end{vmatrix}$$



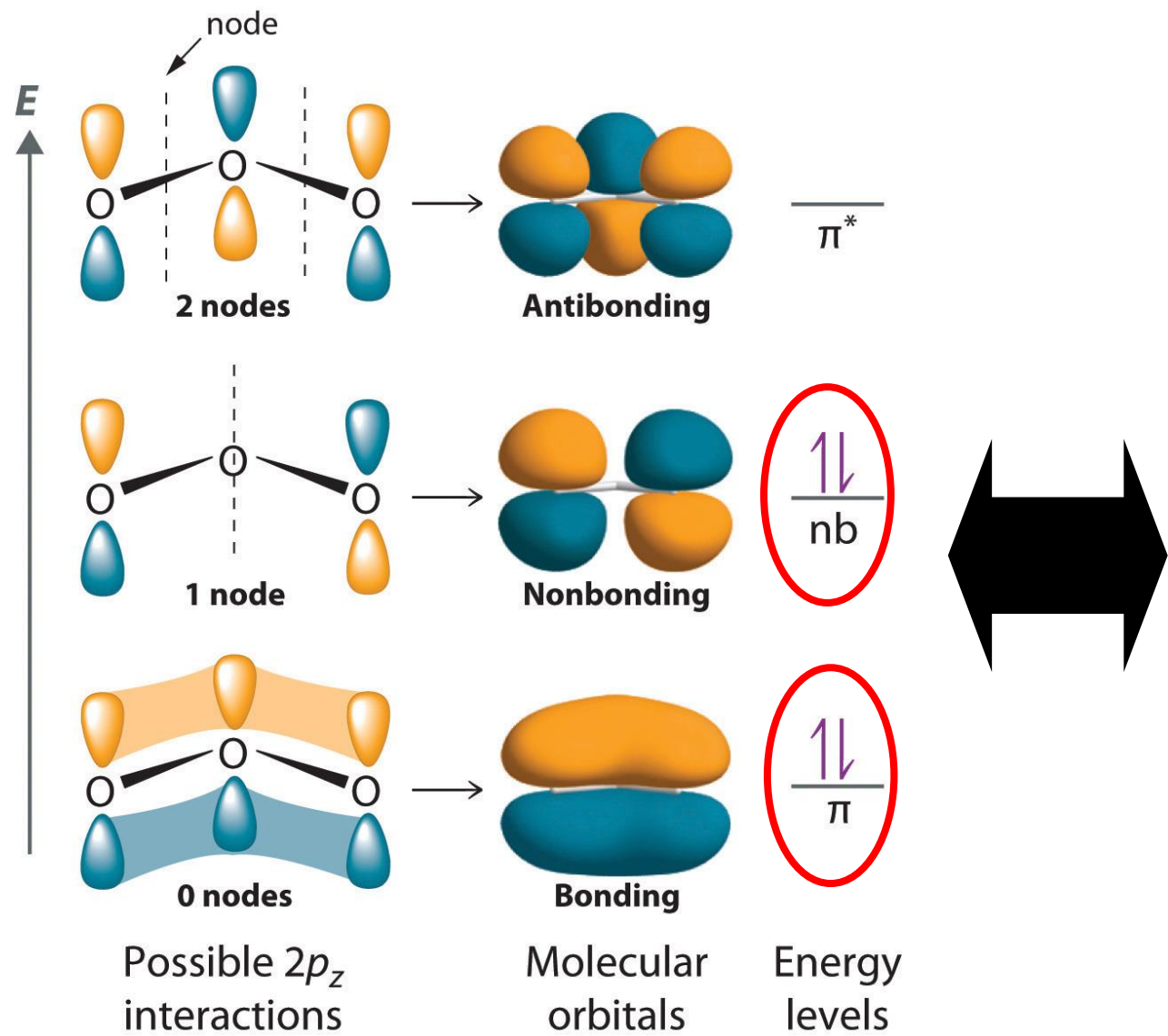
$$[\Phi_1(r_1)\Phi_2(r_2) + \Phi_2(r_1)\Phi_1(r_2)] [\alpha(1)\beta(2) - \beta(1)\alpha(2)]$$

$$\rho^{HF} \sim (\Psi_2 - \Psi_3)^2$$

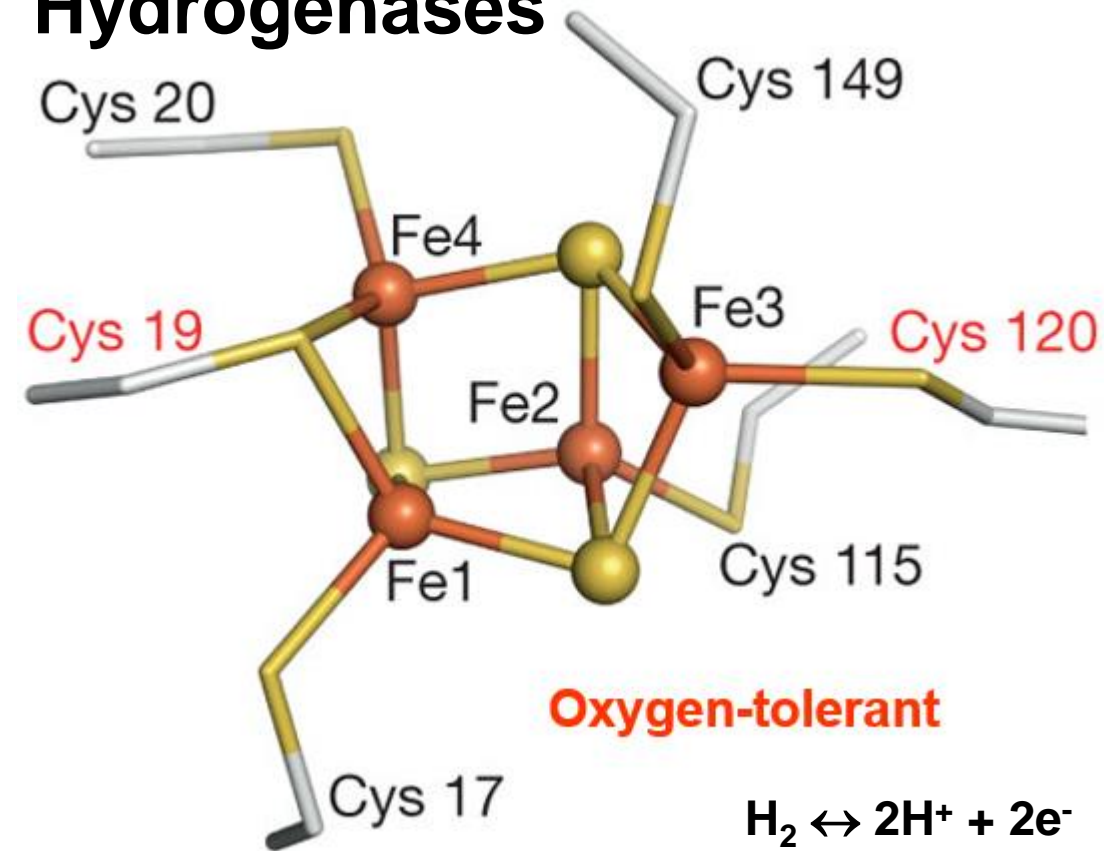


$$\rho^{KS} = (\Psi^{KS})^2$$

Organic molecules versus (poly)metallic complexes



Hydrogenases



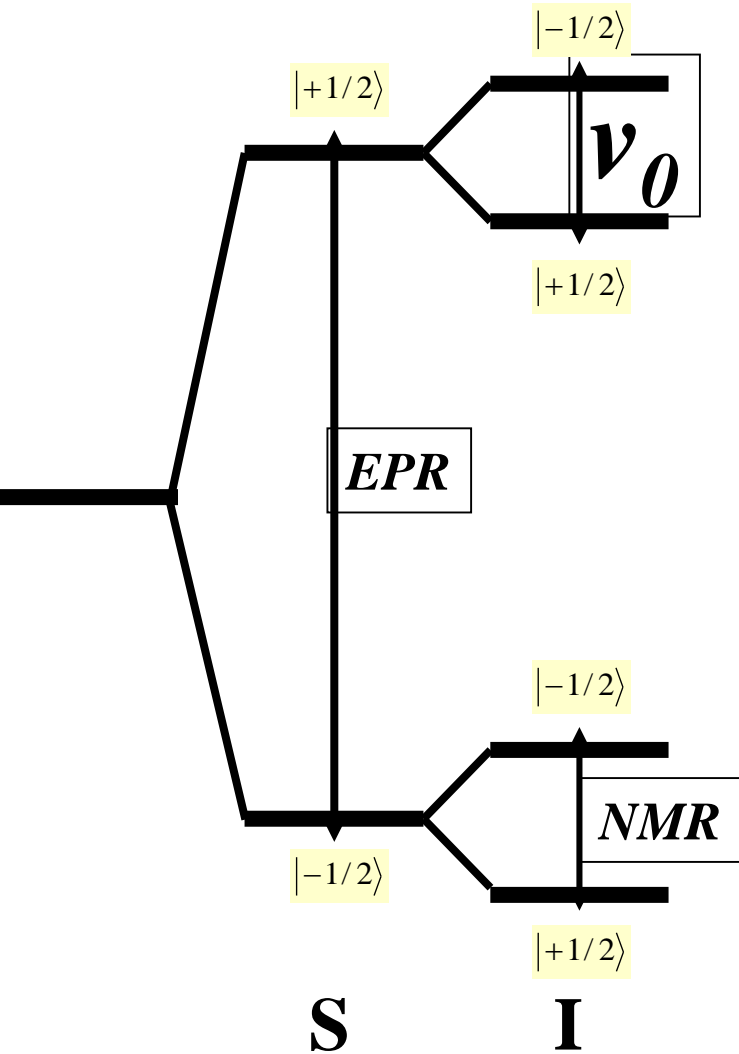
charge : $\rho_e(r) = \rho_\alpha(r) + \rho_\beta(r)$

spin : $\rho_s(r) = \rho_\alpha(r) - \rho_\beta(r)$

Outline of the lecture

- ***Basic introduction to DFT***
 - Hartree-Fock versus DFT
- ***Application : (mono-metal) g-tensors***
 - Relativistic origin
 - Perturbative & self-consistent approaches
 - When it does not work ...
- ***Polymetallic complexes***
 - Spin-coupling
 - g-tensor (dimer)
 - Hyperfine couplings (dimer)
 - More complex systems : hyperfine & Mössbauer
- ***Conclusions***

Zeeman interactions



Between nuclear spins {I}
and the magnetic field H

→ NMR : *chemical shifts*

$$g_I \beta_I \vec{B} \cdot \vec{I}$$

Between electronic spins S
and the magnetic field H

→ EPR : *g tensors*

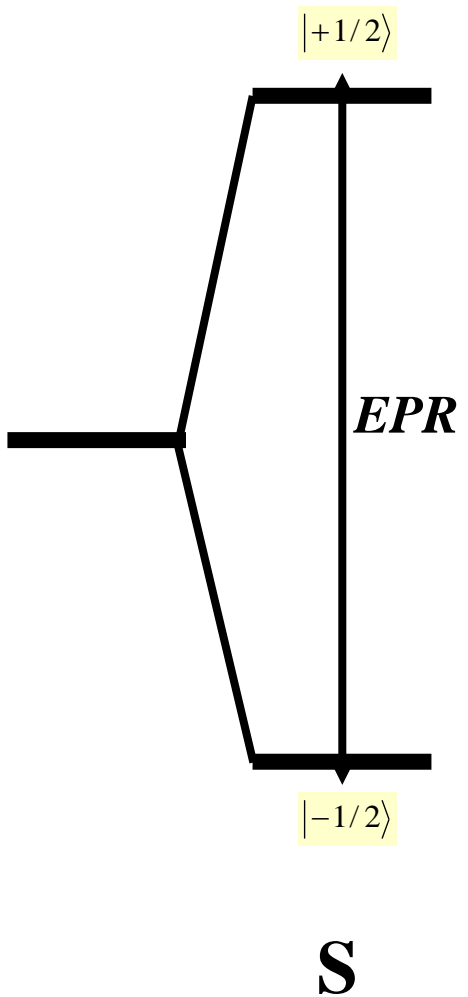
$$g_e \beta_e \vec{B} \cdot \vec{S}$$

The « g » tensor

The origin of the signal is therefore the **electron**. In fact, since many students of chemistry are much more familiar with NMR, one way of describing EPR is as if it were NMR *with the electron as the observe nucleus*. To extend this analogy a little further:

NMR property	EPR equivalent
• observe nucleus (e.g. ^1H , ^{77}Se)	• one or more unpaired electrons
• magnetic dipole vs. magnetic quadrupole	• $m_s = \pm \frac{1}{2}$ (i.e. resembles spin- $\frac{1}{2}$ nuclei)
• chemical shift (i.e. field/frequency ratio)	• <i>g</i> -value (i.e. field/frequency ratio)
• homo-nuclear coupling	• <i>normally not seen - all electrons equivalent</i>
• hetero-nuclear coupling (<i>always</i> first-order)	• hyperfine splitting (<i>always</i> first-order)

Zeeman interactions



$$g_e \beta_e \vec{B} \cdot \vec{s}$$

Electron $spin : \vec{s}$
orbital moment : $\vec{\ell}$

$$H_{Zeeman} = \beta_e (\vec{\ell} + g_e \vec{s}) \cdot \vec{B}$$

$$+ \zeta \vec{\ell} \cdot \vec{s} \quad (\text{spin - orbit})$$

$$\Rightarrow \beta_e \vec{B} \cdot \tilde{\vec{g}} \cdot \vec{s}$$

$g_e \sim 2$

Introduction to the spin (Dirac theory for one electron)

Non linear $\frac{E^2}{c^2} - p^2 = m^2 c^2$

Linear $-\frac{\hbar^2}{2m} \nabla^2 \phi = i\hbar \frac{\partial}{\partial t} \phi$

$$(\nabla^2 - \frac{1}{c^2} \frac{\partial^2}{\partial t^2}) \phi = \frac{m^2 c^2}{\hbar^2} \phi$$

Linearized $\nabla^2 - \frac{1}{c^2} \frac{\partial^2}{\partial t^2} = (A\partial_x + B\partial_y + C\partial_z + \frac{i}{c} D\partial_t)(A\partial_x + B\partial_y + C\partial_z + \frac{i}{c} D\partial_t)$ **Pauli**

$$\sigma_k = \begin{pmatrix} 0 & 1 \\ 1 & 0 \end{pmatrix}, \begin{pmatrix} 0 & -i \\ i & 0 \end{pmatrix}, \begin{pmatrix} 1 & 0 \\ 0 & -1 \end{pmatrix}$$

$$\left(\beta mc^2 + \sum_{k=1}^3 \alpha_k p_k c \right) \psi(\mathbf{x}, t) = i\hbar \frac{\partial \psi}{\partial t}(\mathbf{x}, t)$$

$2s_y$	$ \alpha\rangle$	$+i \beta\rangle$	$2s_x$	$ \alpha\rangle$	$+i \beta\rangle$	$2s_z$	$ \alpha\rangle$	$+i \beta\rangle$
$\langle\alpha $	0	1	$\langle\alpha $	0	$+i$	$\langle\alpha $	1	0
$-i\langle\beta $	1	0	$-i\langle\beta $	$-i$	0	$-i\langle\beta $	0	-1

Introduction to the spin (approximated Dirac's theory : Breit equation)

$$H_e = \sum_i \frac{p_i^2}{2m_i} + \sum_i \sum_{j>i} \frac{e^2}{|r_i - r_j|} - \sum_A \sum_i \frac{Z_A e^2}{|R_A - r_i|}$$

$$H_1^e = \sum_i \pi^2(i)/2m$$

$$H_7^e = (e^2/2) \sum'_{i,j} (1/r_{ij})$$

$$H_1^{en} = -e^2 \sum_{i,n} Z_n/r_{ni}$$

Introduction to the spin (approximated Dirac's theory : Breit equation)

$$H_S^e = g\beta \sum_i \mathbf{S}(i) \cdot \mathbf{B}(i)$$

$$H_2^n = -\beta_p \sum_n g_n \mathbf{I}(n) \cdot \mathbf{B}(n)$$

$$\sim g_e \beta_e \bar{B} \cdot \bar{s}$$

$$\sim g_I \beta_I \vec{B} \cdot \vec{I}$$

Zeeman terms

$$H_{11}^e = -(g^2 \beta^2 / 2) \sum'_{i,j} r_{ij}^{-5} [3(\mathbf{S}(j) \cdot \mathbf{r}_{ij})(\mathbf{S}(i) \cdot \mathbf{r}_{ij}) - r_{ij}^2 \mathbf{S}(i) \cdot \mathbf{S}(j)]$$

$$H_{12}^e = -(4\pi g^2 \beta^2 / 3) \sum'_{i,j} \mathbf{S}(i) \cdot \mathbf{S}(j) \delta(\mathbf{r}_i - \mathbf{r}_j).$$

Spin-spin term

$$\vec{S} \cdot \tilde{D} \cdot \vec{S}$$

$$H_9^e = -(g\beta^2/\hbar) \sum'_{i,j} r_{ij}^{-3} [2\mathbf{S}(i) \cdot \mathbf{r}_{ij} \times \boldsymbol{\pi}(j) + \mathbf{S}(j) \cdot \mathbf{r}_{ij} \times \boldsymbol{\pi}(j)]$$

$$+ \zeta \vec{\ell} \cdot \vec{s}$$

$$H_5^{en} = (\beta^2/\hbar) \sum_{i,n} Z_n r_{ni}^{-3} [\mathbf{S}(i) \cdot \mathbf{r}_{ni} \times \boldsymbol{\pi}(i)]$$

Spin-orbit coupling

Spin-orbit coupling

$$H_9^e = -(g\beta^2/\hbar) \sum'_{i,j} r_{ij}^{-3} [2\mathbf{S}(i) \cdot \mathbf{r}_{ij} \times \boldsymbol{\pi}(j) + \mathbf{S}(j) \cdot \mathbf{r}_{ij} \times \boldsymbol{\pi}(j)]$$

$$H_5^{en} = (\beta^2/\hbar) \sum_{i,n} Z_n r_{ni}^{-3} [\mathbf{S}(i) \cdot \mathbf{r}_{ni} \times \boldsymbol{\pi}(i)]$$

$$H_{Zeeman} = \beta_e (\vec{\ell} + g_e \vec{s}) \cdot \vec{B}$$

$$H_{SO} = \sum_i \zeta_i(r_i) \vec{\ell}_i \cdot \vec{s}_i$$

$$\vec{L} = \sum_i \vec{\ell}_i$$

$$\vec{S} = \sum_i \vec{s}_i$$

$$H_{SO} \rightarrow \lambda \vec{L} \cdot \vec{S}$$

$$\lambda \equiv \pm \frac{\zeta(r)}{2S} \sim \left\langle \frac{1}{r_{Ai}^3} \right\rangle$$

Russel-Saunders' scheme



$$+ \zeta \vec{\ell} \cdot \vec{s} \quad (\text{spin - orbit})$$



$$\Rightarrow \beta_e \vec{B} \cdot \tilde{\vec{g}} \cdot \vec{s}$$

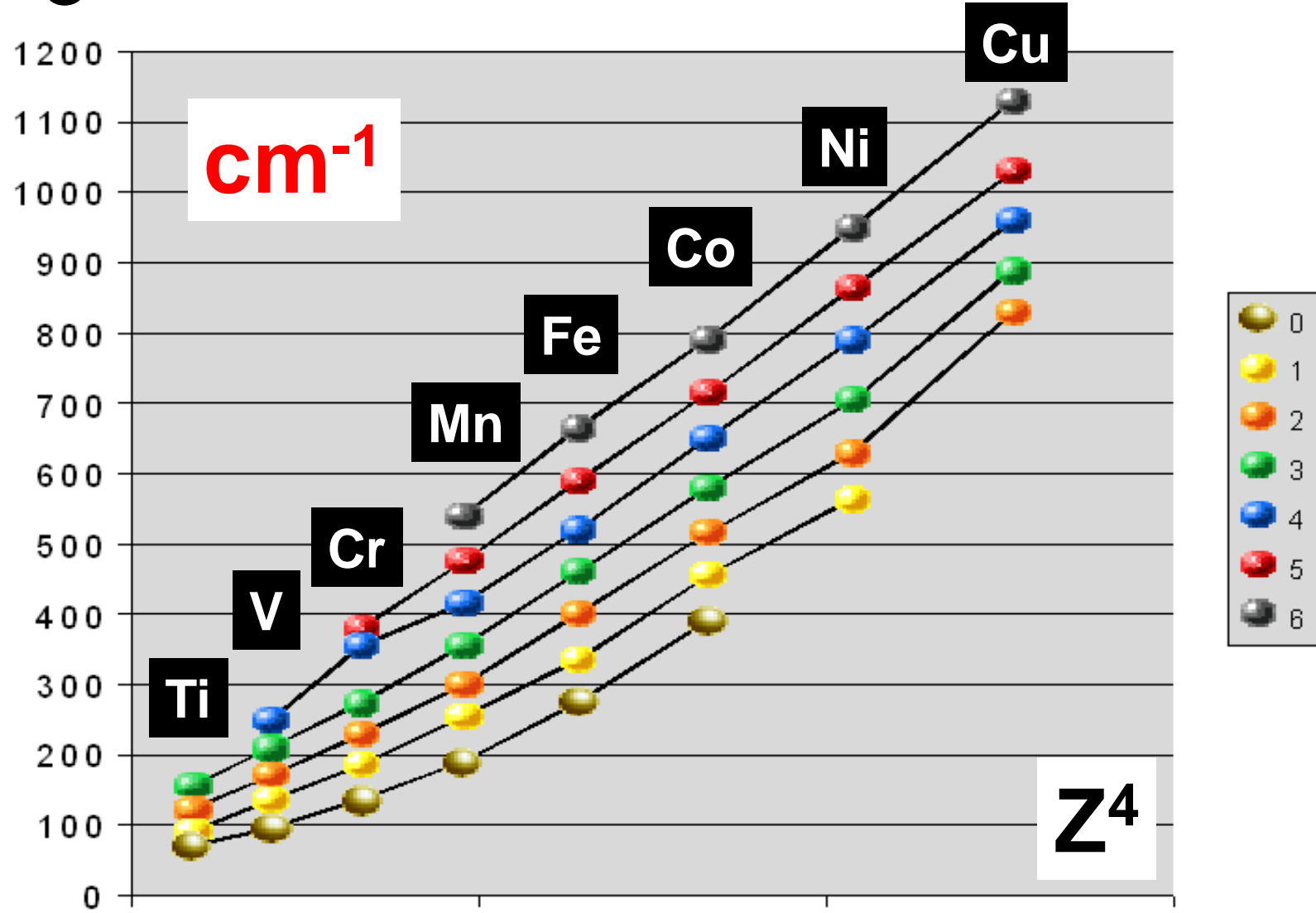
$$+ \vec{S} \cdot \tilde{\vec{D}} \cdot \vec{S}$$

$$\Rightarrow \beta_e \vec{B} \cdot \tilde{\vec{g}}_{\text{eff}} \cdot \vec{s}$$

SKIP !**n=3**

Spin-orbit coupling (mono-electronic)

$$\lambda = \pm \frac{\zeta_{3d}}{2S}$$



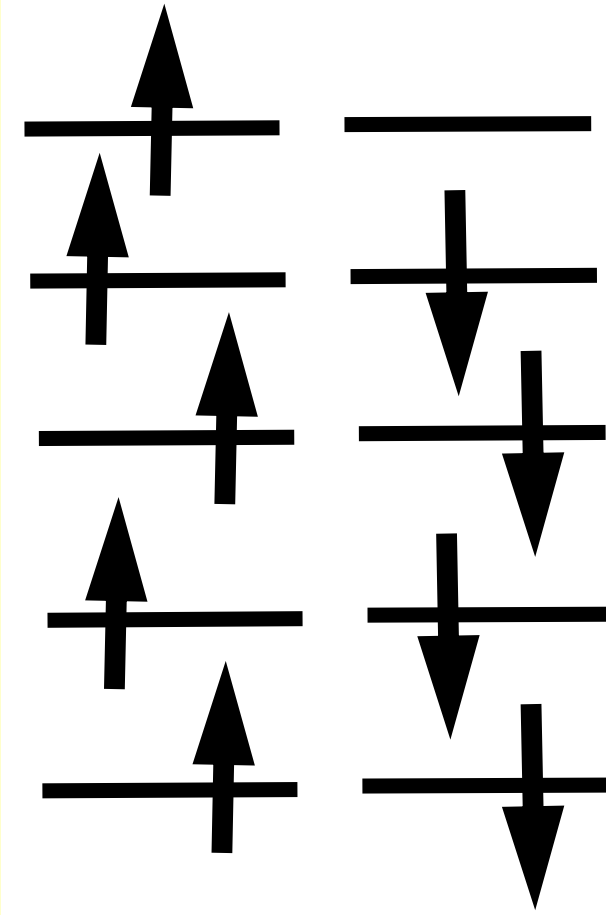
n=3

Spin-orbit coupling (mono-electronic)

$$\lambda = \pm \frac{\zeta_{3d}}{2S}$$

Métal	0	+1	+2	+3	+4	+5	+6
Ti	0.009	0.011	0.015	0.019			
V	0.012	0.017	0.021	0.026	0.031		
Cr	0.017	0.023	0.029	0.034	0.044	0.047	
Mn	0.024	0.032	0.037	0.044	0.051	0.059	0.067
Fe	0.034	0.042	0.050	0.057	0.064	0.073	0.082
Co	0.048	0.056	0.064	0.072	0.081	0.089	0.098
Ni		0.070	0.078	0.087	0.098	0.107	0.118
Cu			0.103	0.110	0.119	0.128	0.128

eV



Orbitals

▼ ESR/EPR

ESR/EPR g-tensor and
A-tensor

ESR/EPR Q-tensor

ESR/EPR Zero-field splitting
(D-tensor)

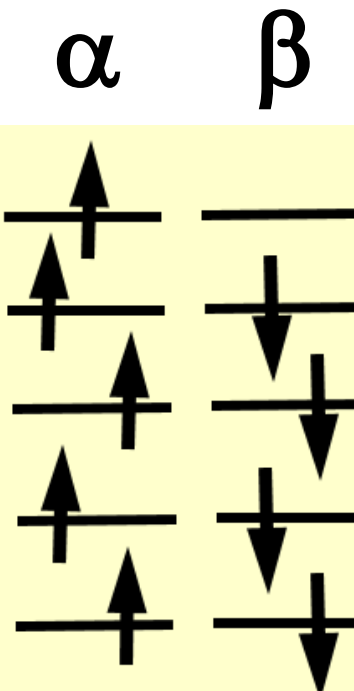
Treatment of Spin-orbit coupling

$$H_{SO} \rightarrow \lambda \vec{L} \cdot \vec{S}$$

Practical implementations

g-tensor, perturbative inclusion spin-orbit coupling

```
$ADFBIN/adf << eor
CHARGE charge spinpolarization
unrestricted
Relativistic scalar ZORA
Symmetry NOSYM
...
eor
```

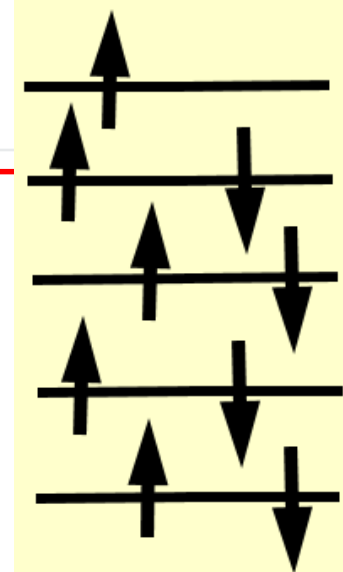


```
$ADFBIN/nmr << eor
nmr
g factors
u1k best
calc all
out iso tens
end
end input
eor
```

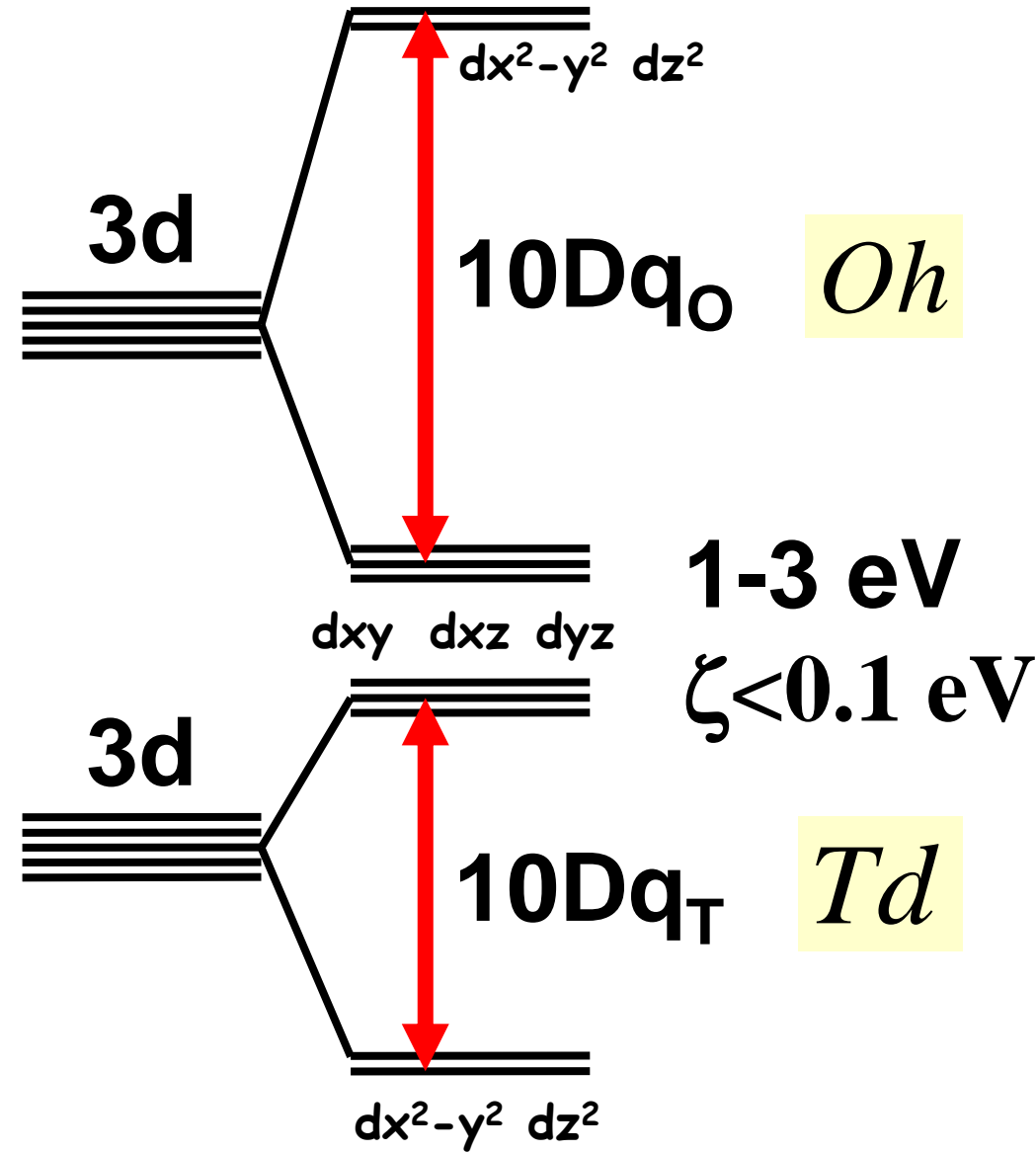
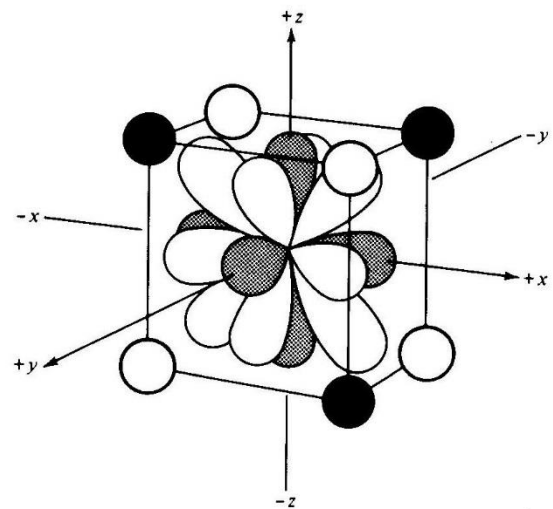
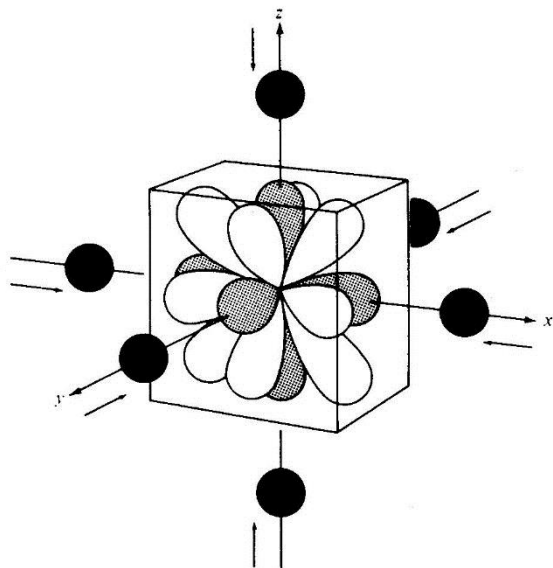
g-tensor and A-tensor, self consistent spin-orbit coupling

```
$ADFBIN/adf << eor
ESR
END
CHARGE charge
unrestricted
Relativistic spinorbit ZORA
Collinear
Symmetry NOSYM
eor
```

Spin- orbitals

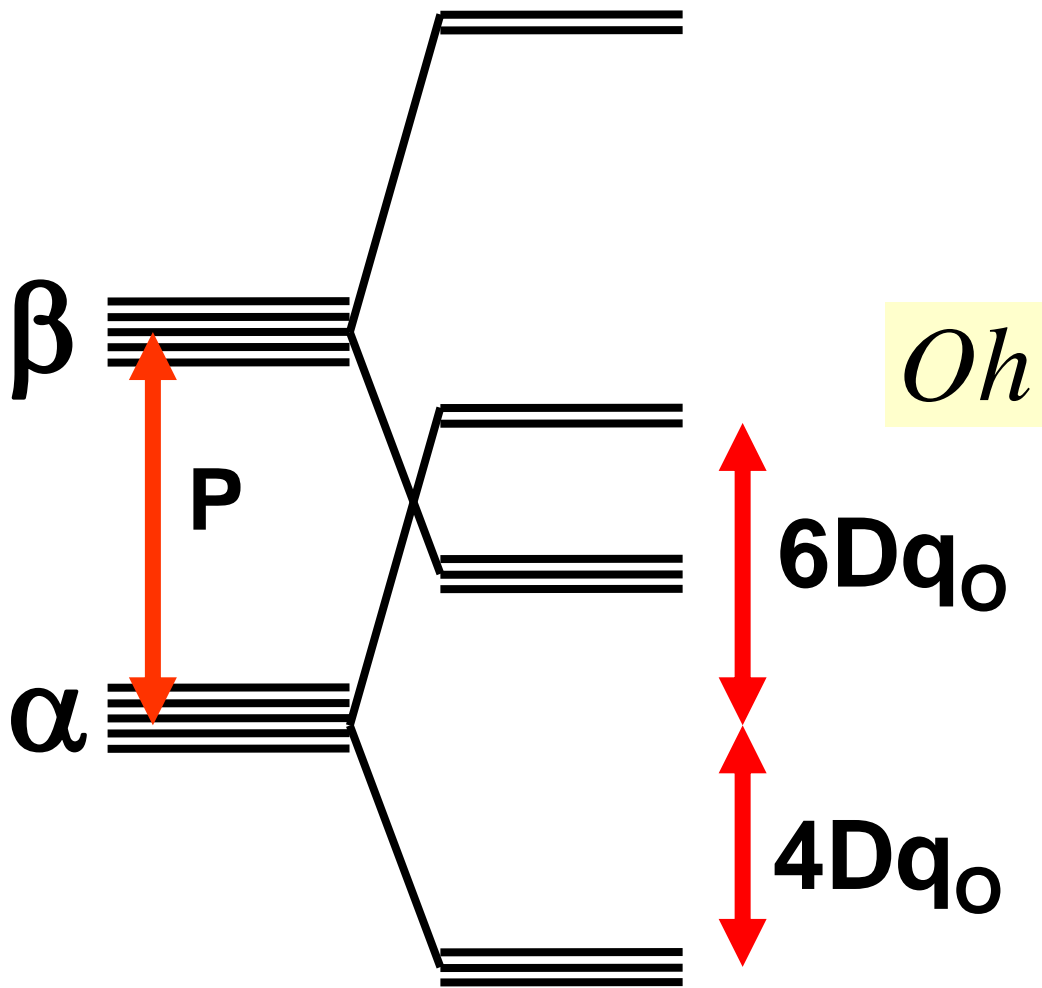


Ligand field theory



SKIP !

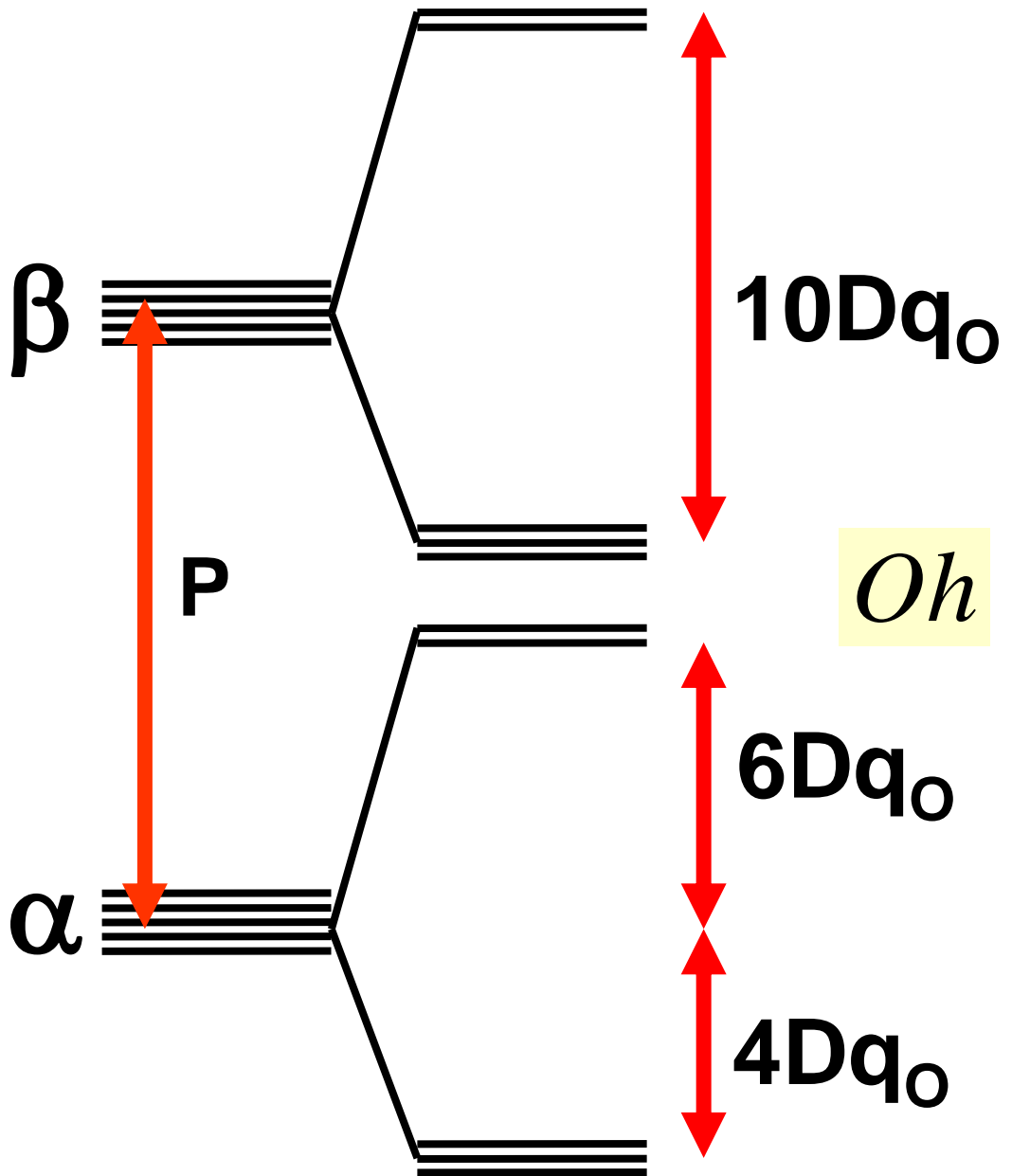
Strong ligand field



d^n	$CFSE$	$nb.$	$Spin$
d^1	$-4Dq$	1	$1/2$
d^2	$-8Dq$	2	1
d^3	$-12Dq$	3	$3/2$
d^4	$-16Dq + P$	2	1
d^5	$-20Dq + 2P$	1	$1/2$
d^6	$-24Dq + 2P$	0	0
d^7	$-18Dq + P$	1	$1/2$
d^8	$-12Dq$	2	1
d^9	$-6Dq$	1	$1/2$
d^{10}	$0Dq$	0	0

SKIP !

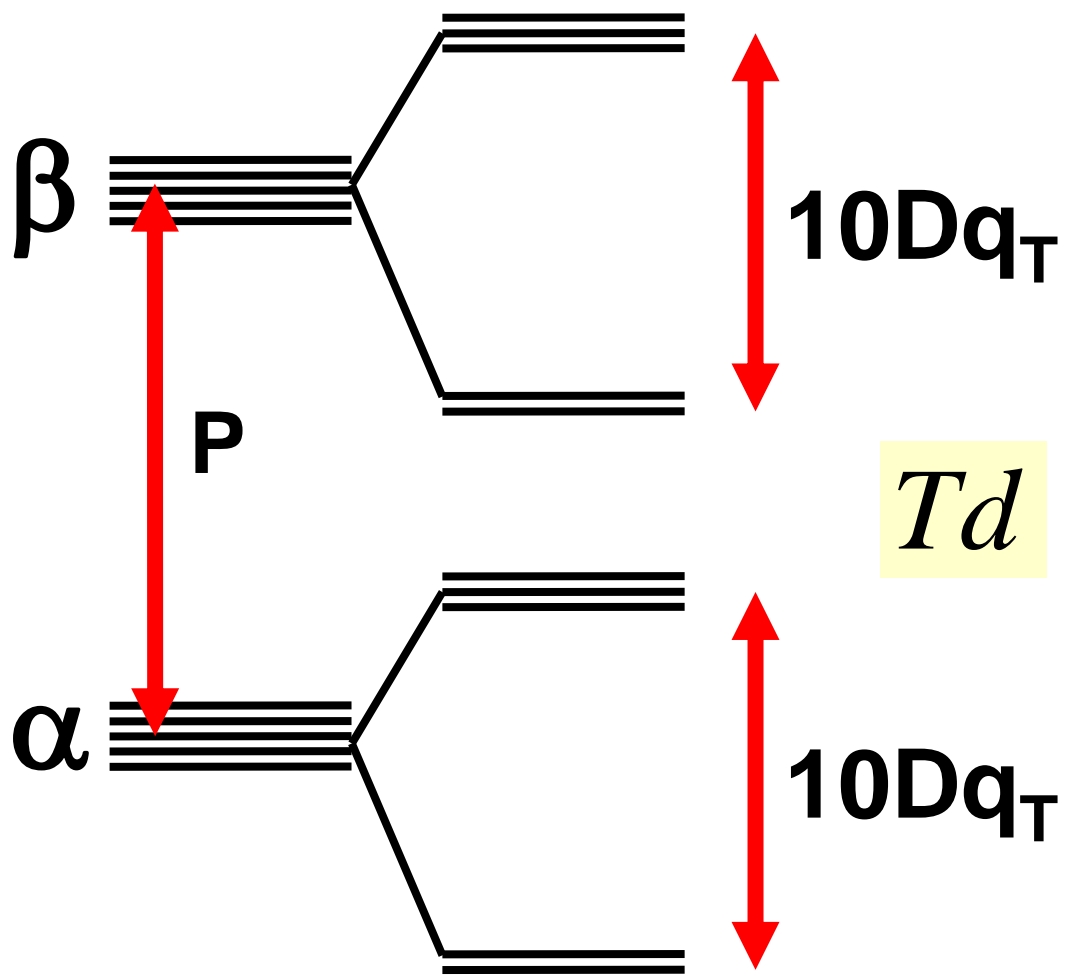
Weak ligand field



d^n	$CFSE$	$nb.$	$Spin$
d^1	$-4Dq$	1	$1/2$
d^2	$-8Dq$	2	1
d^3	$-12Dq$	3	$3/2$
d^4	$-6Dq$	4	2
d^5	$0Dq$	5	$5/2$
d^6	$-4Dq$	4	2
d^7	$-8Dq$	3	$3/2$
d^8	$-12Dq$	2	1
d^9	$-6Dq$	1	$1/2$
d^{10}	$0Dq$	0	0

SKIP !

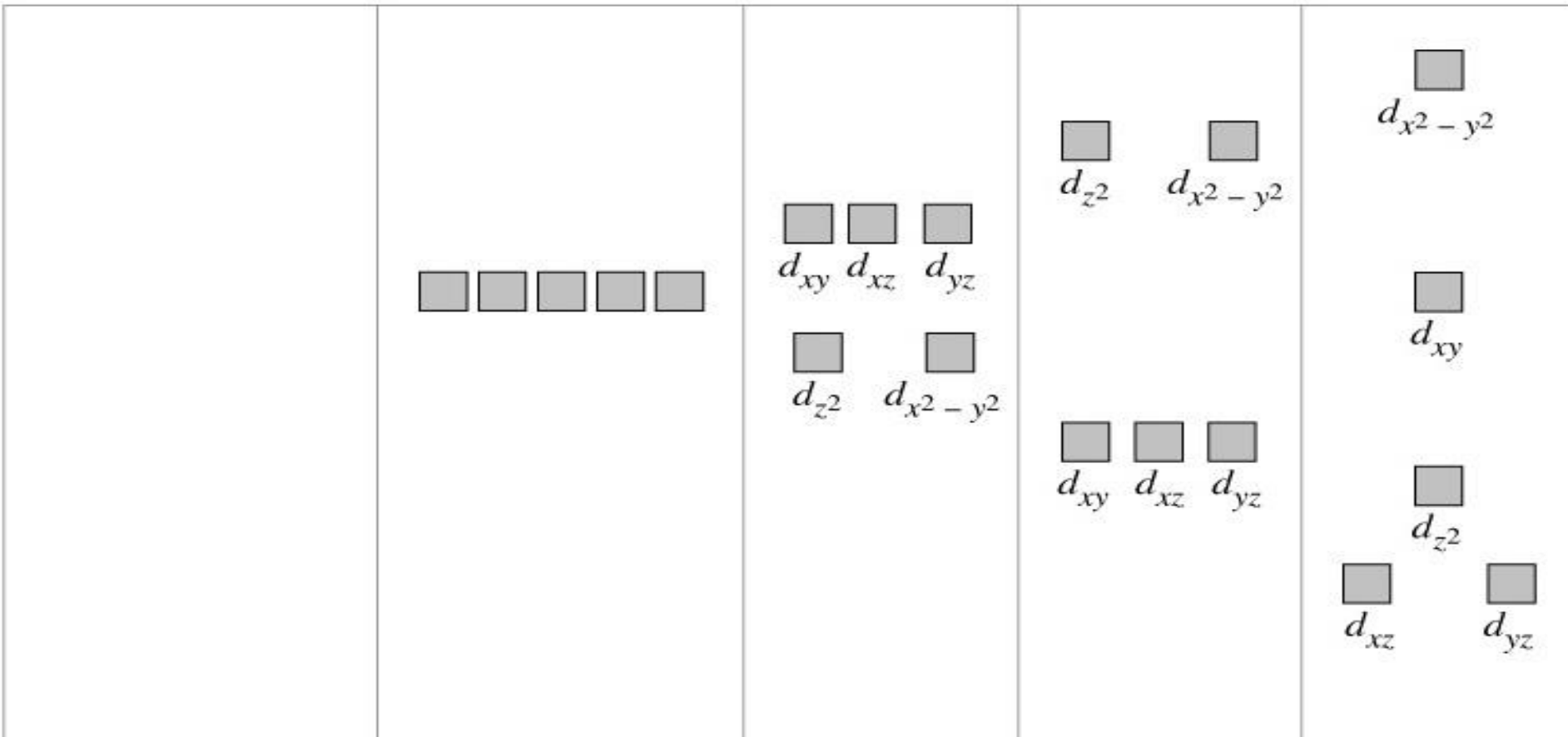
Weak ligand field



d^n	$CFSE$	$nb.$	$Spin$
d^1	$-6Dq$	1	$1/2$
d^2	$-12Dq$	2	1
d^3	$-8Dq$	3	$3/2$
d^4	$-4Dq$	4	2
d^5	$0Dq$	5	$5/2$
d^6	$-6Dq$	4	2
d^7	$-12Dq$	3	$3/2$
d^8	$-8Dq$	2	1
d^9	$-4Dq$	1	$1/2$
d^{10}	$0Dq$	0	0

SKIP !

Ligand field



d -orbital energies
in "free" metal
atom or ion

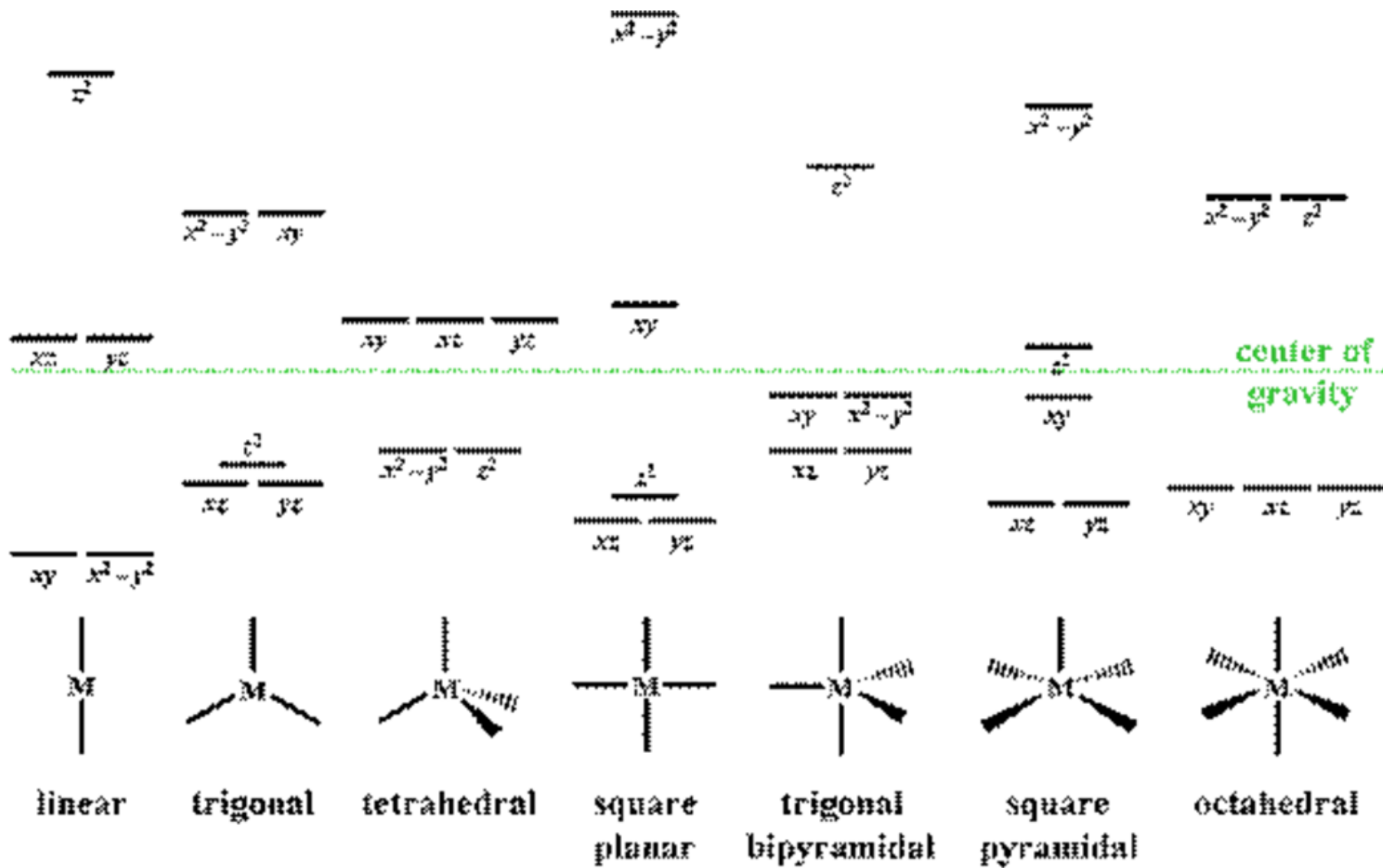
Average energy
of d orbitals in
the presence of
ligands

(a) d orbitals
in tetrahedral
complex

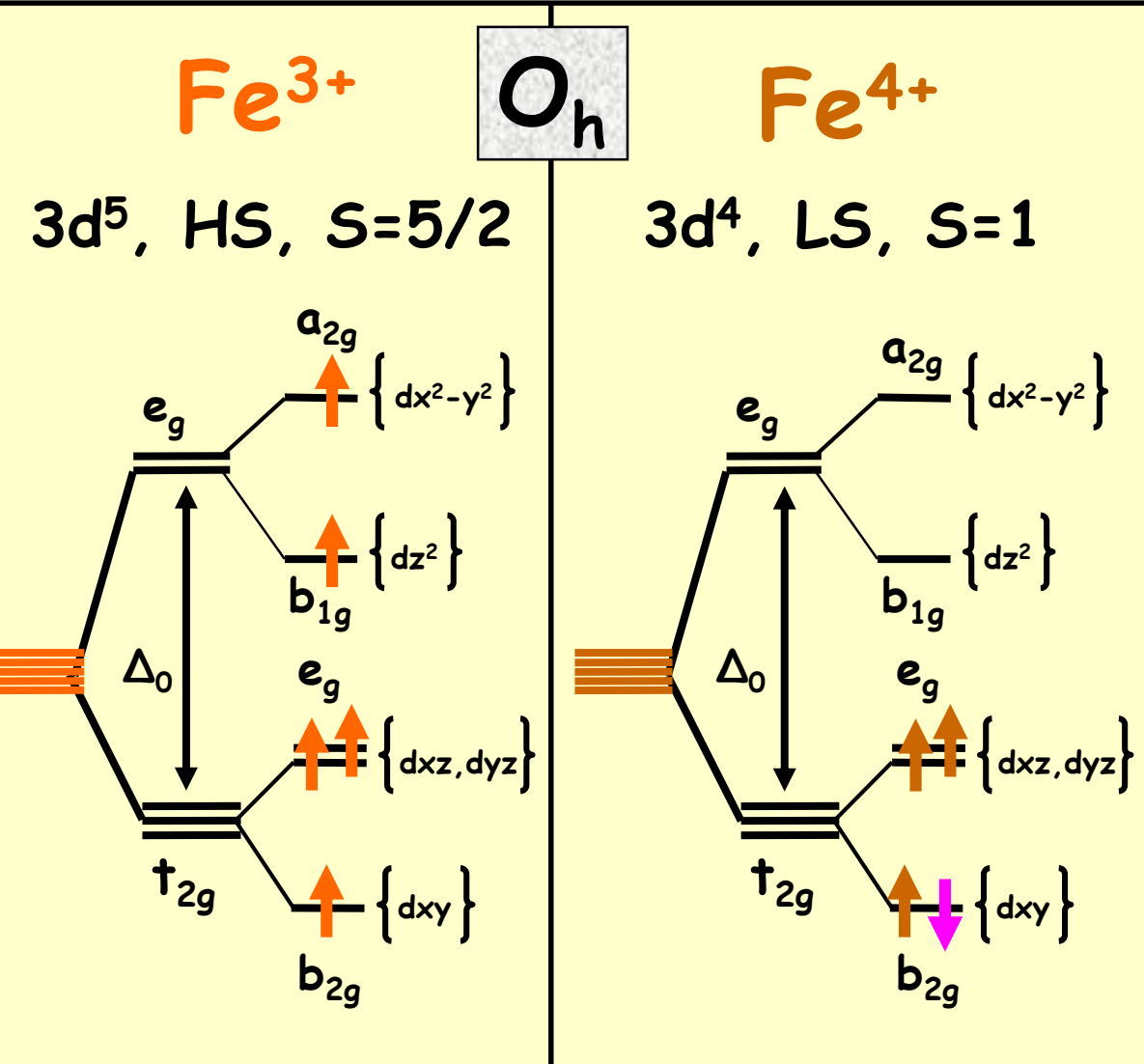
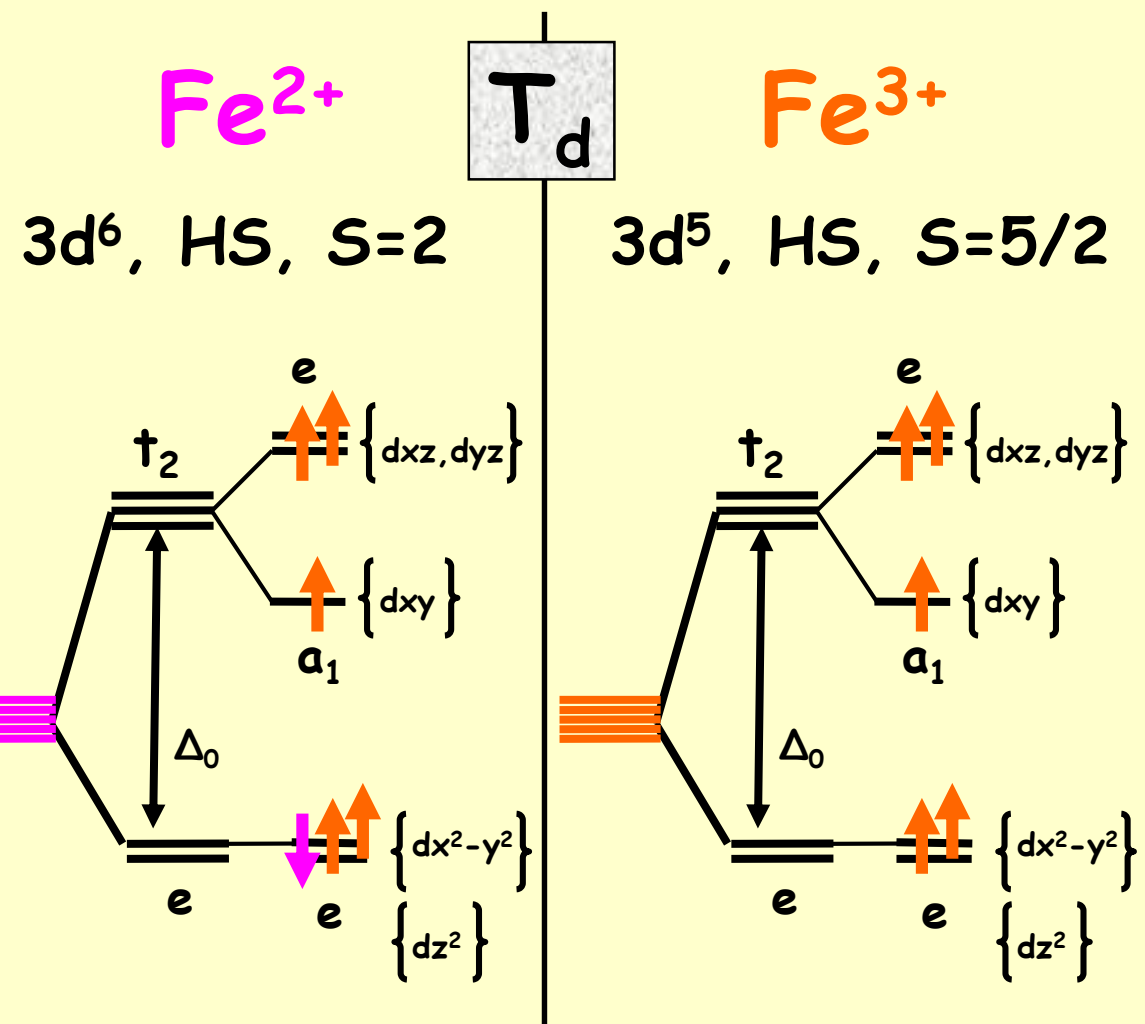
(b) d orbitals
in octahedral
complex

(c) d orbitals
in square
planar
complex

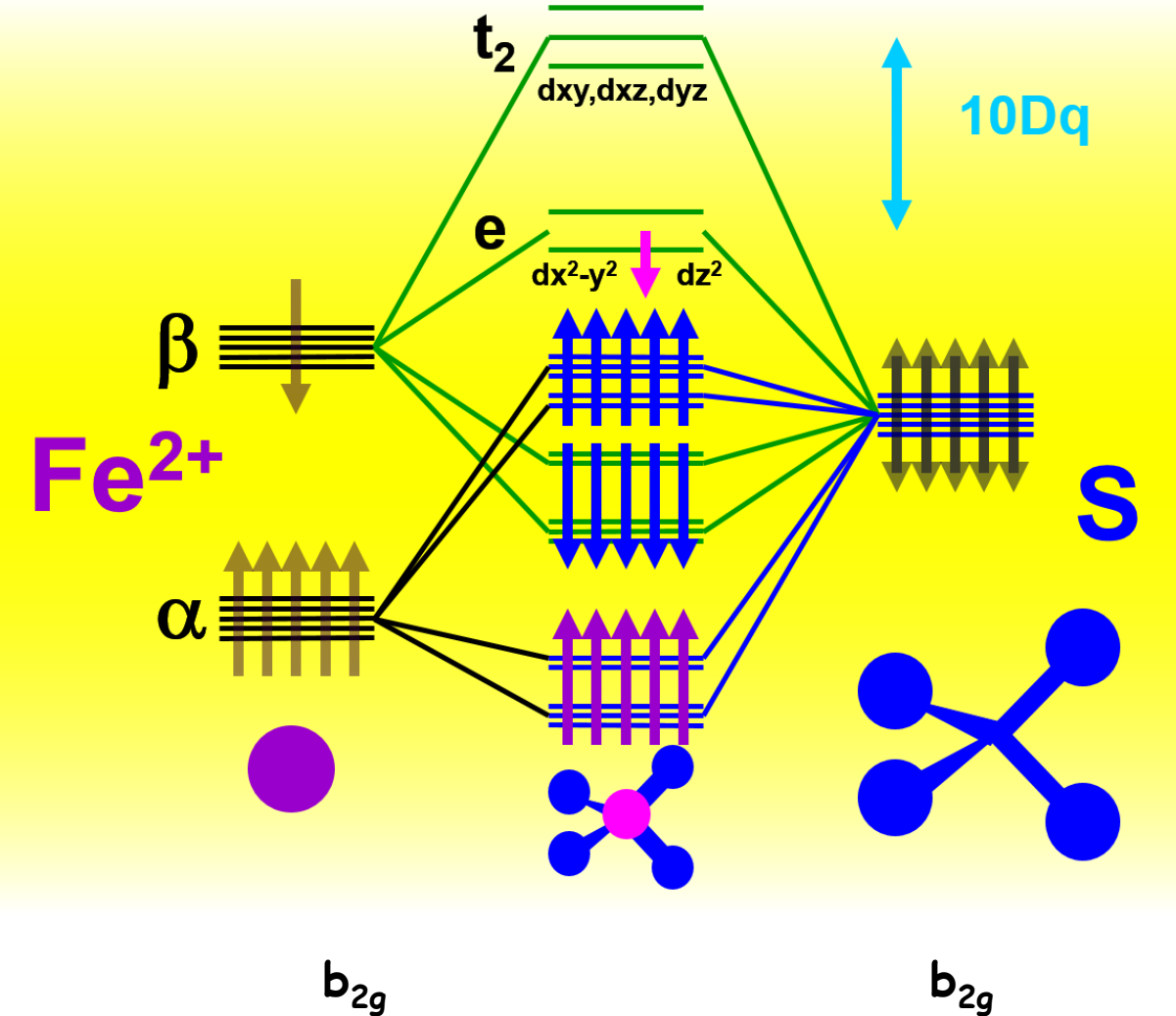
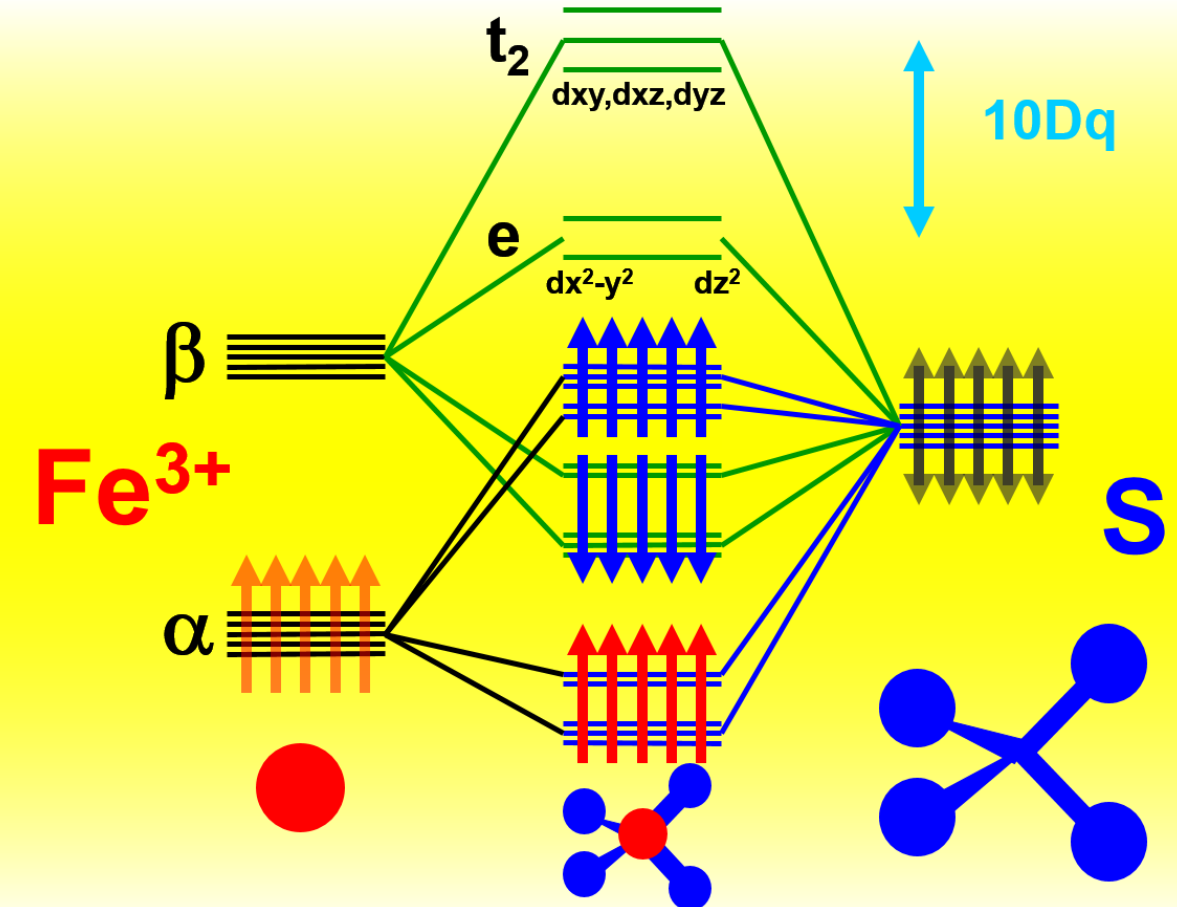
Ligand field



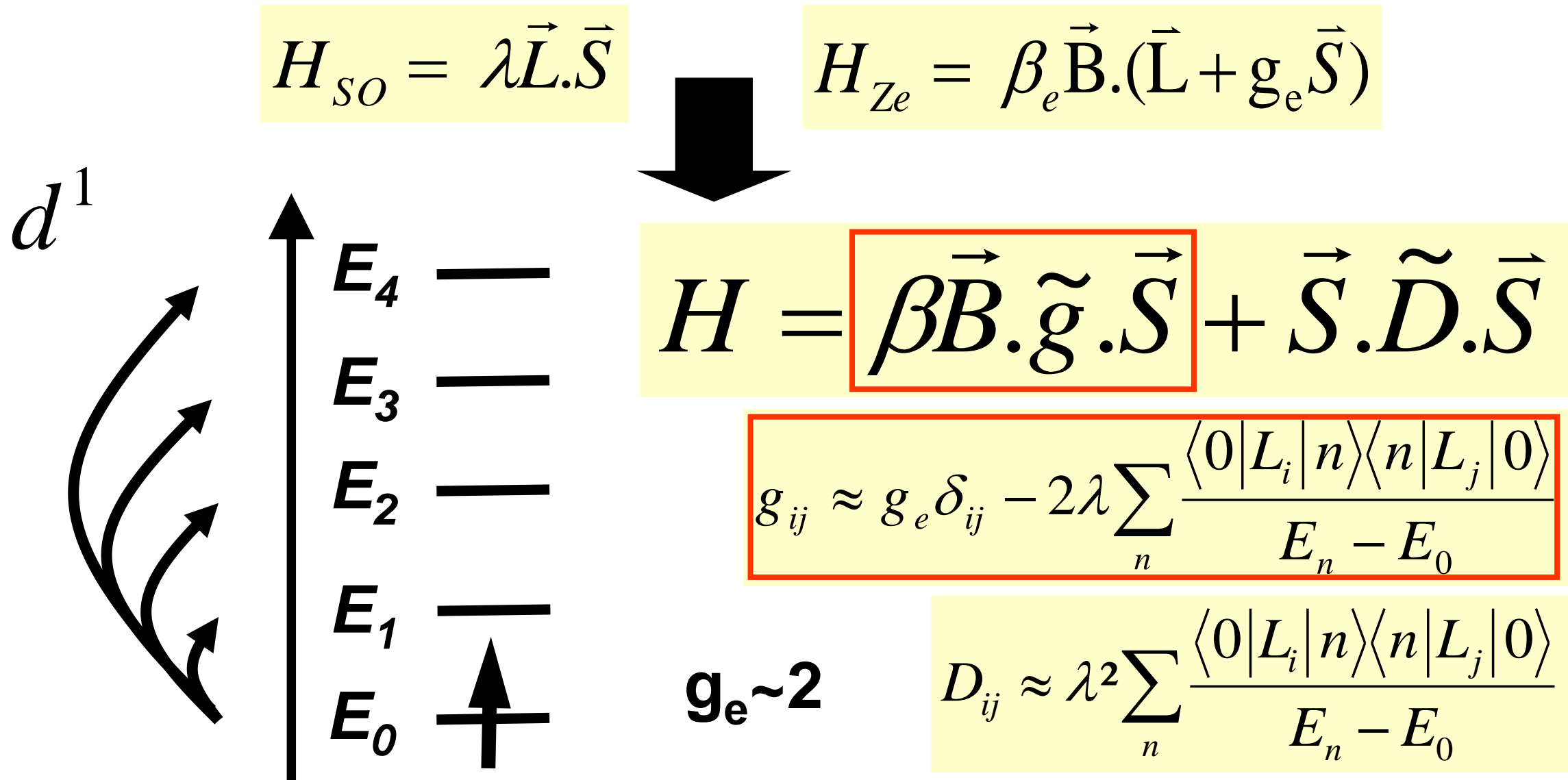
Ligand field



Ligand field in DFT : Anti-bonding set of molecular orbitals



(Perturbative) calculation of the g-tensor



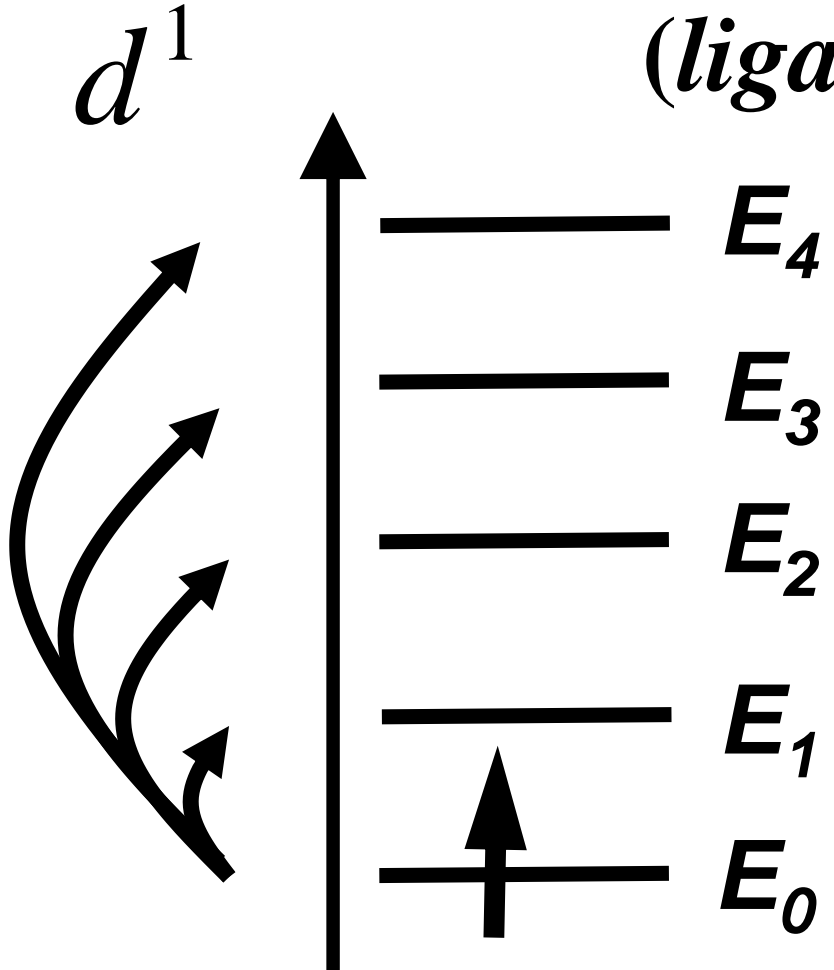
(Perturbative) calculation of the g-tensor

	L_x	L_y	L_z
z^2	$-i\sqrt{3}(yz)$	$i\sqrt{3}(xz)$	0
$x^2 - y^2$	$-i(yz)$	$-i(xz)$	$+2(xy)$
xy	$+i(xz)$	$-i(yz)$	$-2(x^2 - y^2)$
xz	$i(x^2 - y^2) + i\sqrt{3}(z^2)$	$+i(xy)$	$-i(xz)$
yz	$-i(xy)$	$-i\sqrt{3}(z^2) + i(x^2 - y^2)$	$+i(yz)$

$$g_{ij} \approx g_e \delta_{ij} - \frac{2\zeta_{3d}}{2S} \left(\sum_{\alpha} - \sum_{\beta} \right) \sum_n \frac{\langle 0 | L_i | n \rangle \langle n | L_j | 0 \rangle}{E_n - E_0}$$

g tensor calculation (ligand field)

$$\lambda = +\frac{\zeta_{3d}}{2S}$$



$$g_x \approx g_e - \frac{2\zeta_{3d}}{2S} \left(\frac{1}{E_1 - E_0} \right)$$

$$g_y \approx g_e - \frac{2\zeta_{3d}}{2S} \left(\frac{1}{E_2 - E_0} \right)$$

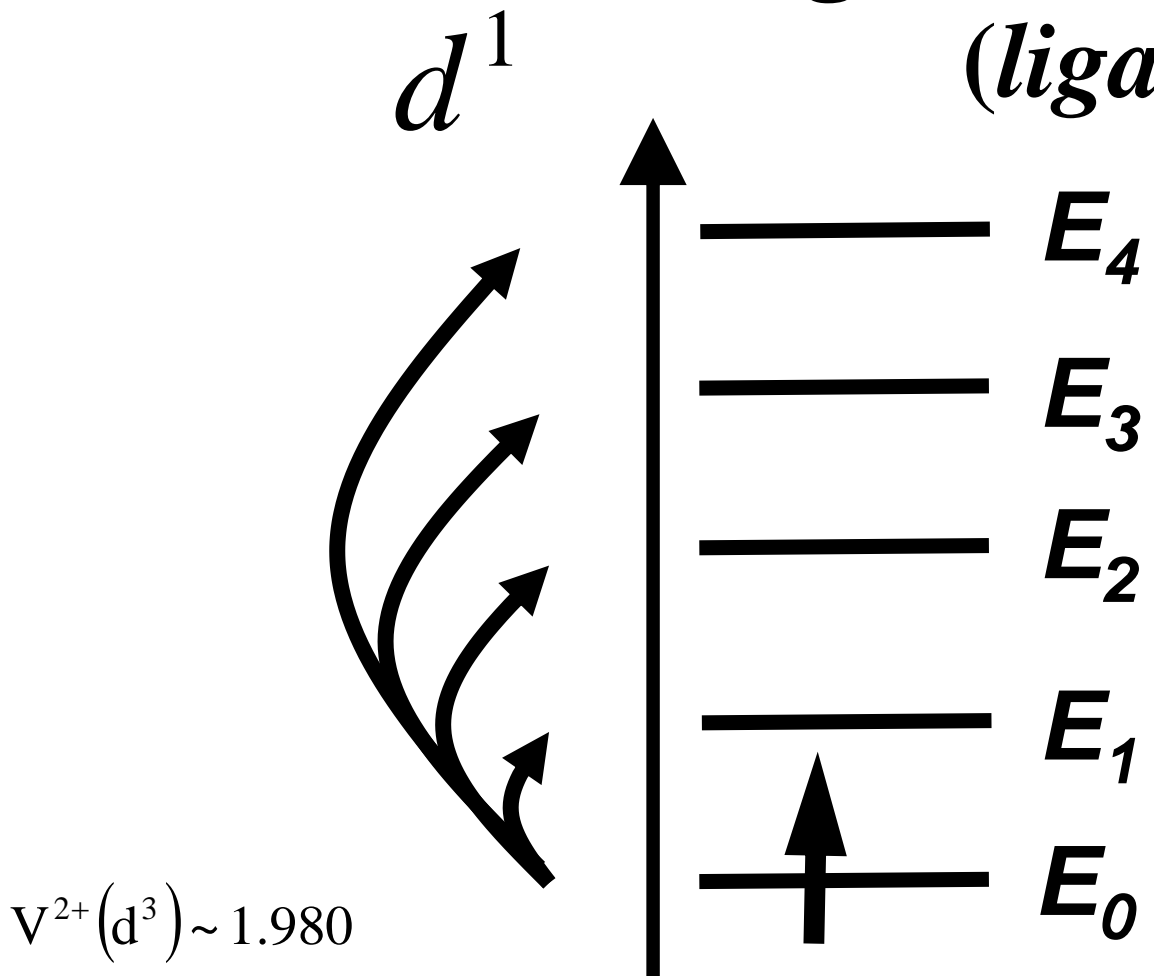
$$g_z \approx g_e - \frac{2\zeta_{3d}}{2S} \left(\frac{4}{E_4 - E_0} \right)$$

g_e~2

$$g_{ij} \approx g_e \delta_{ij} - \frac{2\zeta_{3d}}{2S} \left(\sum_{\alpha} - \sum_{\beta} \right) \sum_n \frac{\langle 0 | L_i | n \rangle \langle n | L_j | 0 \rangle}{E_n - E_0}$$

g tensor calculation (ligand field)

$$\lambda = +\frac{\zeta_{3d}}{2S}$$



$V^{2+}(d^3) \sim 1.980$

DFT: $V^{2+}(H_2O)_6$

1.977

1.980

1.981

$Ti^{3+}(d^1)$	g_1	g_2	g_3	$Sc^{2+}(H_2O)_6$
TiO_6	1.828	1.898	1.979	1.971
TiO_6	1.921	1.921	2.000	1.974
TiO_4F_2	1.932	1.932	1.968	1.980
$Ticp_2F_2$	1.979	1.988	1.998	$Ti^{3+}(H_2O)_6$
$Ticp_2Ge_2$	1.977	1.993	2.001	1.953
$Ticp_2H_2$	1.994	1.994	1.994	1.966
$Ticp_2H_2$	1.992	1.992	1.992	1.970

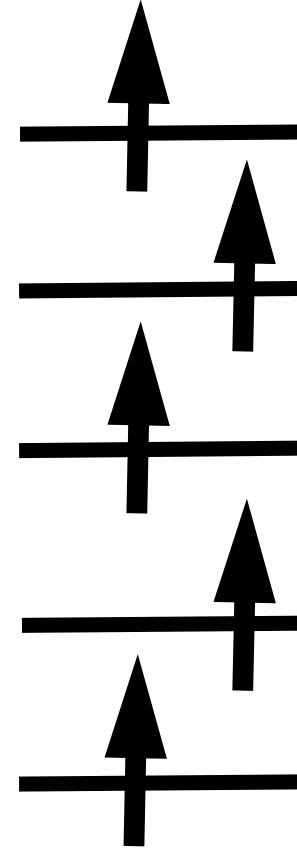
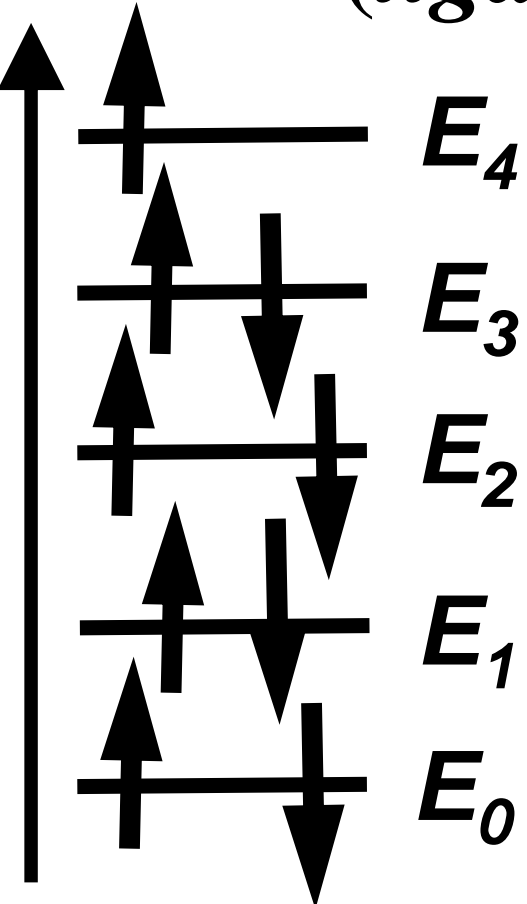
$$g_{ij} \approx g_e \delta_{ij} - \frac{2\zeta_{3d}}{2S} \left(\sum_{\alpha} \right)_n \sum \frac{\langle 0 | L_i | n \rangle \langle n | L_j | 0 \rangle}{E_n - E_0}$$

$V^{4+}(H_2O)_6$
1.930
1.930
1.992

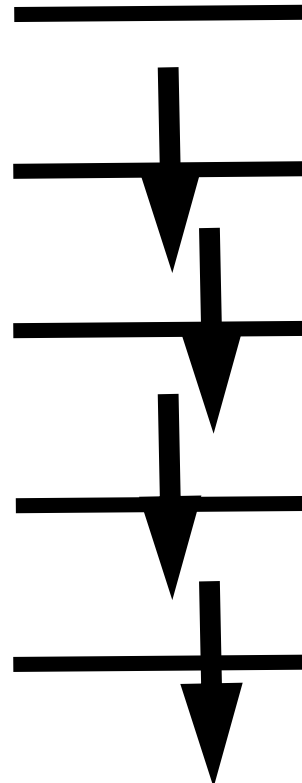
g tensor calculation (ligand field)

$$\lambda = \pm \frac{\zeta_{3d}}{2S}$$

d^9



&

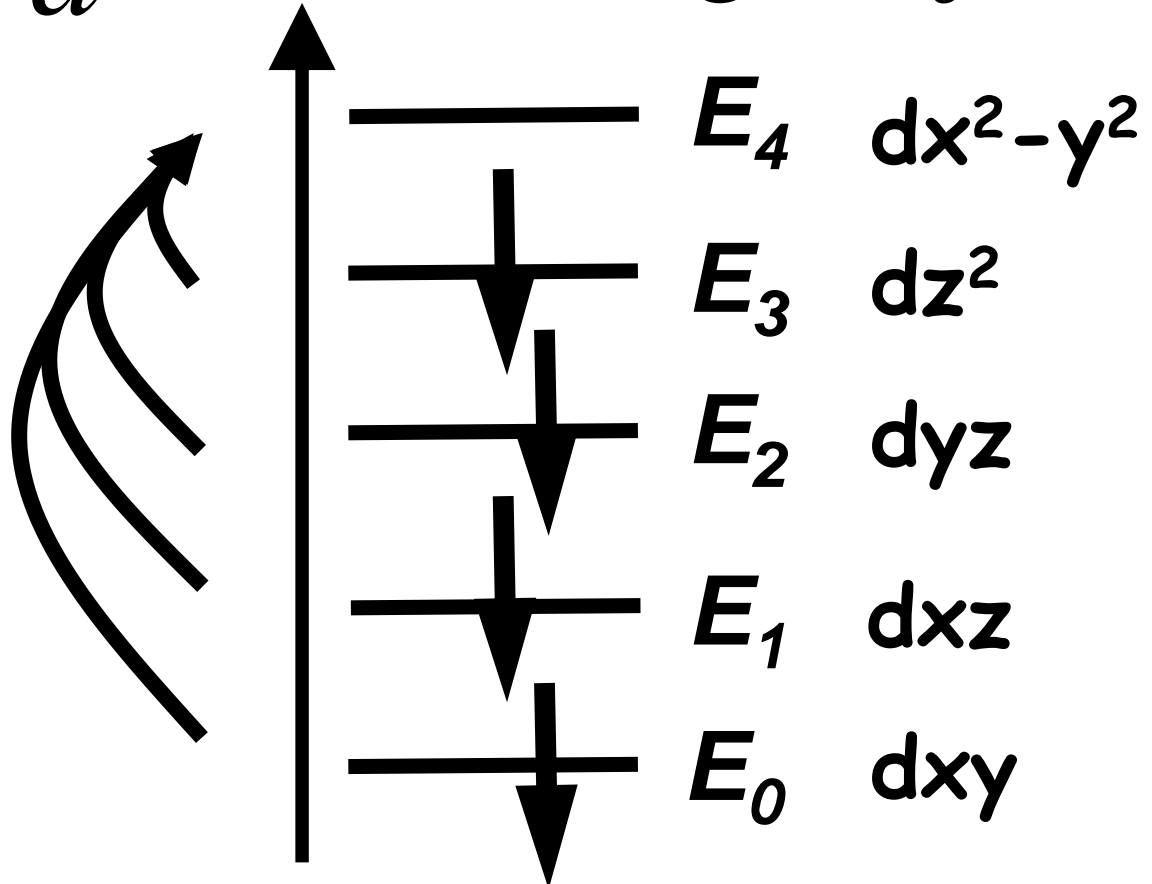


$$g_{ij} \approx g_e \delta_{ij} - \frac{2\zeta_{3d}}{2S} \left(\sum_{\alpha} \left[- \sum_{\beta} \right] \right)_n \frac{\langle 0 | L_i | n \rangle \langle n | L_j | 0 \rangle}{E_n - E_0}$$

g tensor calculation (ligand field)

$$\lambda = -\frac{\zeta_{3d}}{2S}$$

d^9



$$g_x \approx g_e + \frac{2\zeta_{3d}}{2S} \left(\frac{1}{E_4 - E_2} \right)$$

$$g_y \approx g_e + \frac{2\zeta_{3d}}{2S} \left(\frac{1}{E_4 - E_1} \right)$$

$$g_z \approx g_e + \frac{2\zeta_{3d}}{2S} \left(\frac{4}{E_4 - E_0} \right)$$

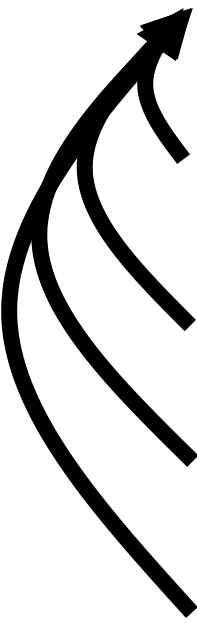
$$g_{ij} \approx g_e \delta_{ij} + \frac{2\zeta_{3d}}{2S} \left(\sum_{\beta} \right)_n \sum \frac{\langle 0 | L_i | n \rangle \langle n | L_j | 0 \rangle}{E_n - E_0}$$

$\mathbf{g_e} \sim 2$

g tensor calculation (ligand field)

$$\lambda = -\frac{\zeta_{3d}}{2S}$$

d^9



$\text{Co}^{2+}(\text{d}^7) \sim 2.29 (\text{g}_{\text{real}})$

DFT: $\text{Co}^{2+}(\text{H}_2\text{O})_6$

2.016

2.106

2.117

No ZFS !

$$g_{ij} \approx g_e \delta_{ij} + \frac{2\zeta_{3d}}{2S} \left(\sum_{\beta} \right)_n \sum \frac{\langle 0 | L_i | n \rangle \langle n | L_j | 0 \rangle}{E_n - E_0}$$

$\text{Cu}^{2+}(\text{d}^9)$

g_1

g_2

g_3

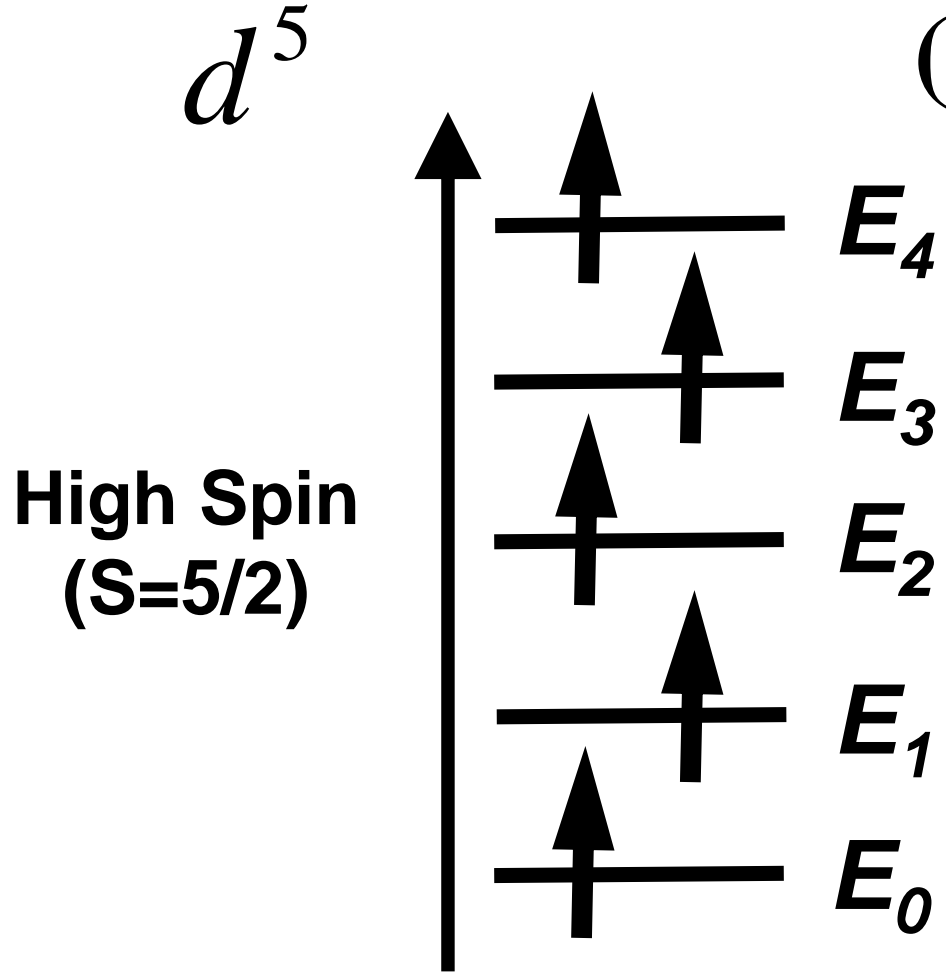
$\text{Cu}^{2+}(\text{H}_2\text{O})_6$

2.077

2.077

2.214

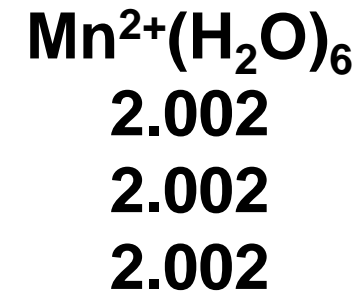
g tensor calculation (ligand field)



$$g_x \approx g_e$$

$$g_y \approx g_e$$

$$g_z \approx g_e$$

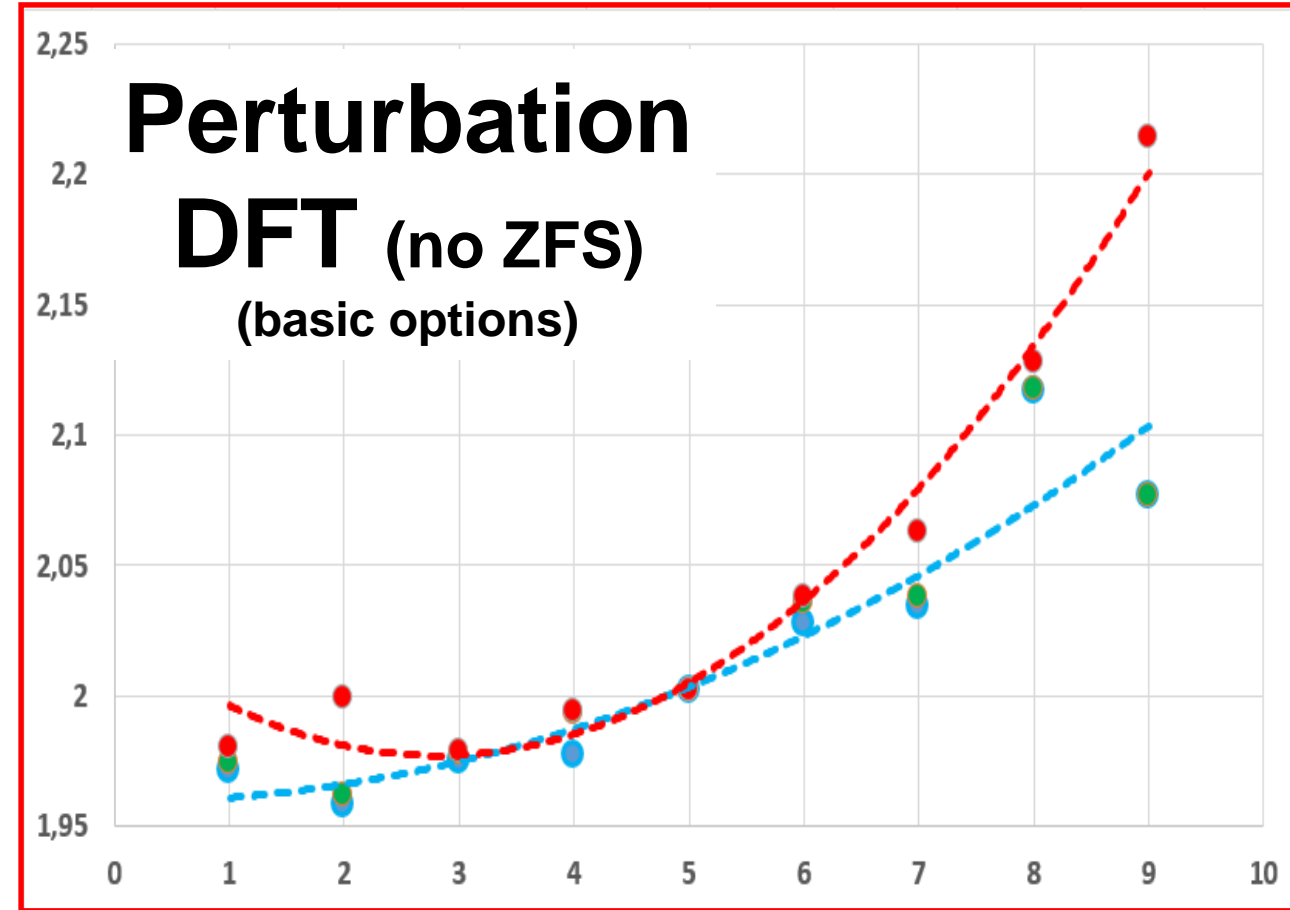


$$g_{ij} \approx g_e \delta_{ij} - \frac{2\zeta_{3d}}{2S} \left(\sum_{\alpha} - \sum_{\beta} \right) \sum_n \frac{\langle 0 | L_i | n \rangle \langle n | L_j | 0 \rangle}{E_n - E_0}$$

$\mathbf{g_e} \sim 2$

Perturbative treatment of spin-orbit coupling

M_2+	d_n	g_min	g_int	g_max	g-av
Sc	1	1,971	1,974	1,98	1,975
Ti	2	1,958	1,962	1,999	1,973
V	3	1,975	1,978	1,979	1,977
Cr	4	1,977	1,993	1,994	1,988
Mn	5	2,002	2,002	2,002	2,002
Fe	6	2,028	2,036	2,038	2,034
Co	7	2,034	2,038	2,063	2,045
Ni	8	2,117	2,118	2,128	2,121
Cu	9	2,077	2,077	2,214	2,123



$$g_{ij} \approx g_e \delta_{ij} - \frac{2\zeta_{3d}}{2S} \left(\sum_{\alpha} - \sum_{\beta} \right)_n \frac{\langle 0 | L_i | n \rangle \langle n | L_j | 0 \rangle}{E_n - E_0}$$

**High-spin
M²⁺(H₂O)₆**

Self-consistent inclusion of spin-orbit coupling

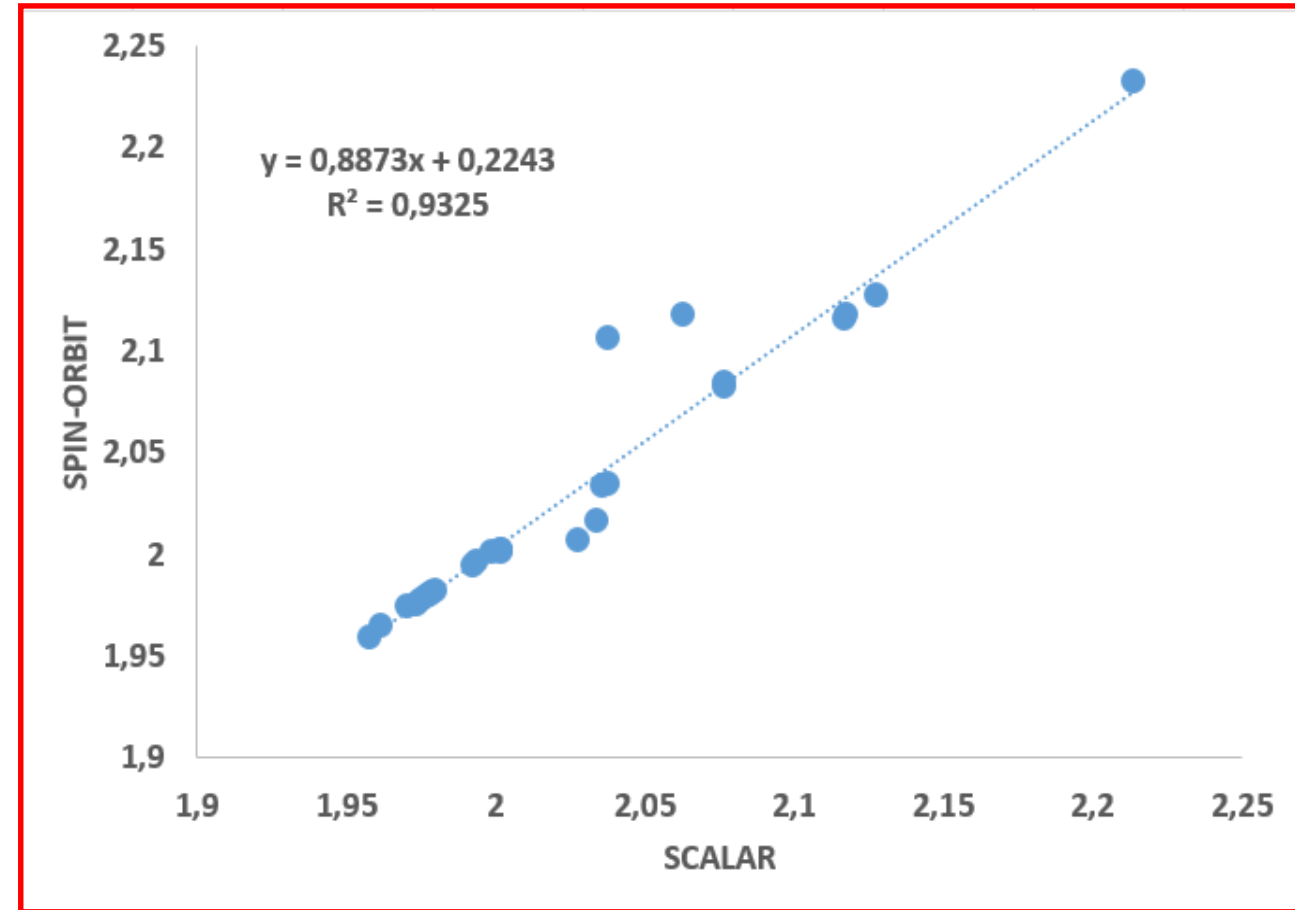
M_2+	d_n	g_min	g_int	g_max	g-av
Sc	1	1,974	1,975	1,982	1,977
Ti	2	1,959	1,964	2,001	1,975
V	3	1,977	1,98	1,981	1,979
Cr	4	1,979	1,994	1,996	1,990
Mn	5	2,001	2,002	2,002	2,002
Fe	6	2,006	2,033	2,034	2,024
Co	7	2,016	2,106	2,117	2,080
Ni	8	2,115	2,117	2,127	2,120
Cu	9	2,082	2,084	2,232	2,133

$$g_{\text{eff}(x)} = g_{\text{real}(x)}(1 \pm \{[1 + 3(E/D)]/\sqrt{[1 + 3(E/D)^2]}\}) \quad \sim 2.2$$

Co²⁺(H₂O)₆

$$g_{\text{eff}(y)} = g_{\text{real}(y)}(1 \pm \{[1 - 3(E/D)]/\sqrt{[1 + 3(E/D)^2]}\}) \quad \sim 3.9$$

$$g_{\text{eff}(z)} = g_{\text{real}(z)}(1 \pm \{(-2)/\sqrt{[1 + 3(E/D)^2]}\}) \quad \sim 5.2$$



$$g_{ij} \approx g_e \delta_{ij} - \frac{2\zeta_{3d}}{2S} \left(\sum_{\alpha} - \sum_{\beta} \right)_n \frac{\langle 0 | L_i | n \rangle \langle n | L_j | 0 \rangle}{E_n - E_0}$$

**High-spin
M²⁺(H₂O)₆**

Density Functional Calculations of Electronic *g*-Tensors Using Spin–Orbit Pseudopotentials and Mean-Field All-Electron Spin–Orbit Operators

Olga L. Malkina,^{†,‡} Juha Vaara,[§] Bernd Schimmelpfennig,^{||} Markéta Munzarová,[⊥] Vladimir G. Malkin,^{*,†} and Martin Kaupp^{*,#}

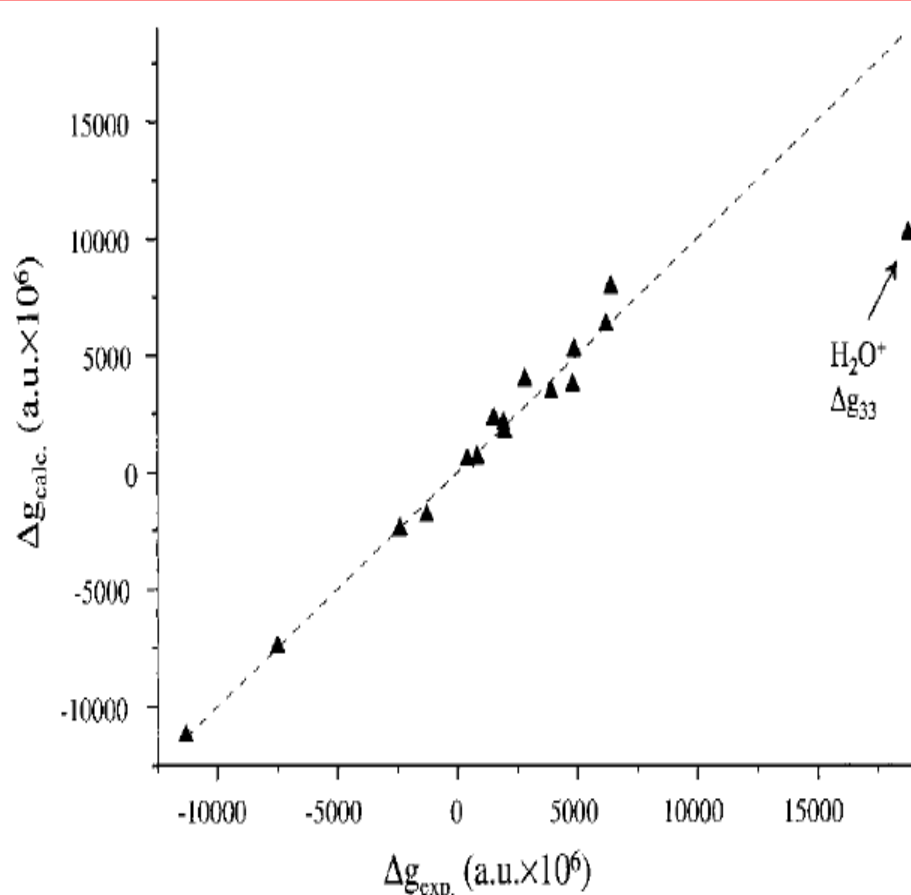


Table 3. *g*-Tensor Components (ppm) for Some Light Main Group Radicals^a

		this work ^b	SZ ^c	Lushington (MRCI) ^d	exp. ^e	
H_2O^+	Δg_{11}	-142	103	-292	200	gas phase
	Δg_{22}	3702	5126	4217	4800	
	Δg_{33}	10205	13824	16019	18800	
CO^+	Δg_{\perp}	-2458	-3129	-2674	-2400	gas phase
	Δg_{\parallel}	-93	-138	-178	-	
HCO	Δg_{11}	-224	-270	-	0	matrix
	Δg_{22}	2275	2749	-	1500	
	Δg_{33}	-7476	-9468	-	-7500	
C_3H_5	Δg_{11}	-65	-115	-	0	matrix
	Δg_{22}	497	660	-	400	
	Δg_{33}	603	769	-	800	
NO_2	Δg_{11}	-688	-760	-235	-300	gas phase
	Δg_{22}	3400	4158	3806	3900	
	Δg_{33}	-11229	-13717	-10322	-11300	
NF_2	Δg_{11}	-617	-738	-	-100	matrix
	Δg_{22}	3928	4678	-	2800	
	Δg_{33}	6288	7619	-	6200	
MgF	Δg_{\perp}	-1869	-2178	-1092	-1300	matrix
	Δg_{\parallel}	14	-60	-59	-300	

^a UDFT-BP86 results. ^b Basis BIII, UDFT-IGLO, AMFI approximation. ^c UDFT-GIAO.¹² ^d Multireference configuration interaction results.⁷ ^e Experimental data as quoted in refs. 7,12.

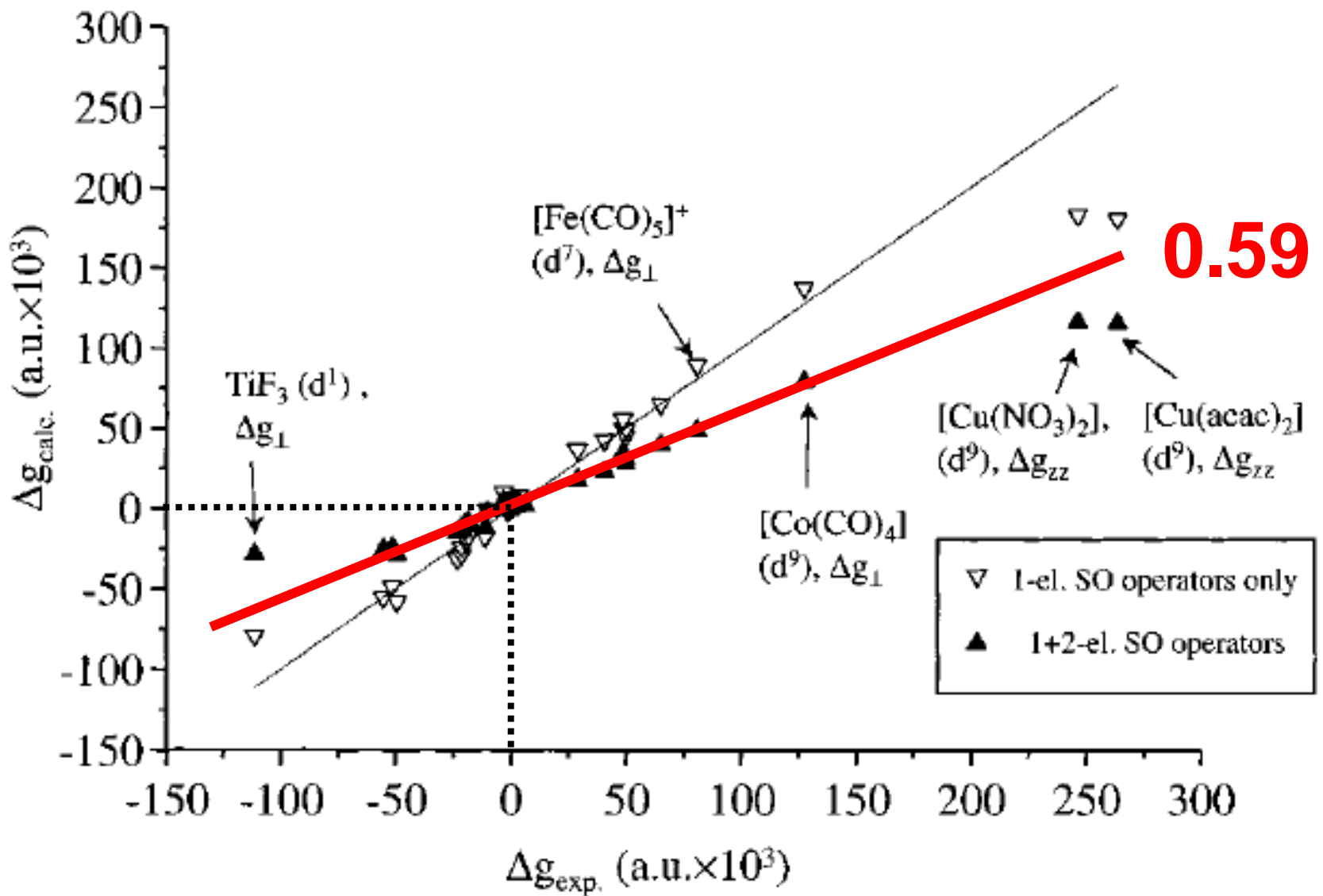
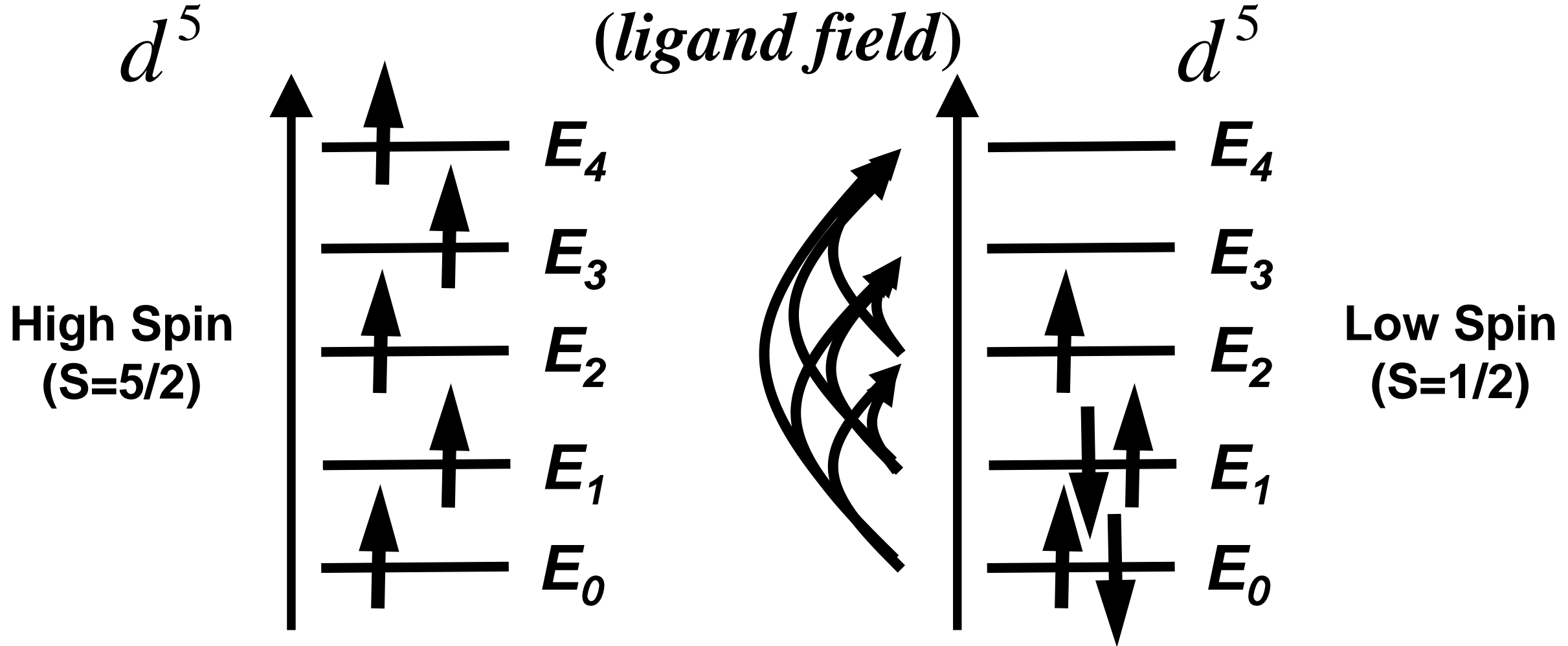


Figure 2. Comparison of calculated and experimental g -shift tensor components (ppt) for 3d transition metal complexes (cf. Table 10).

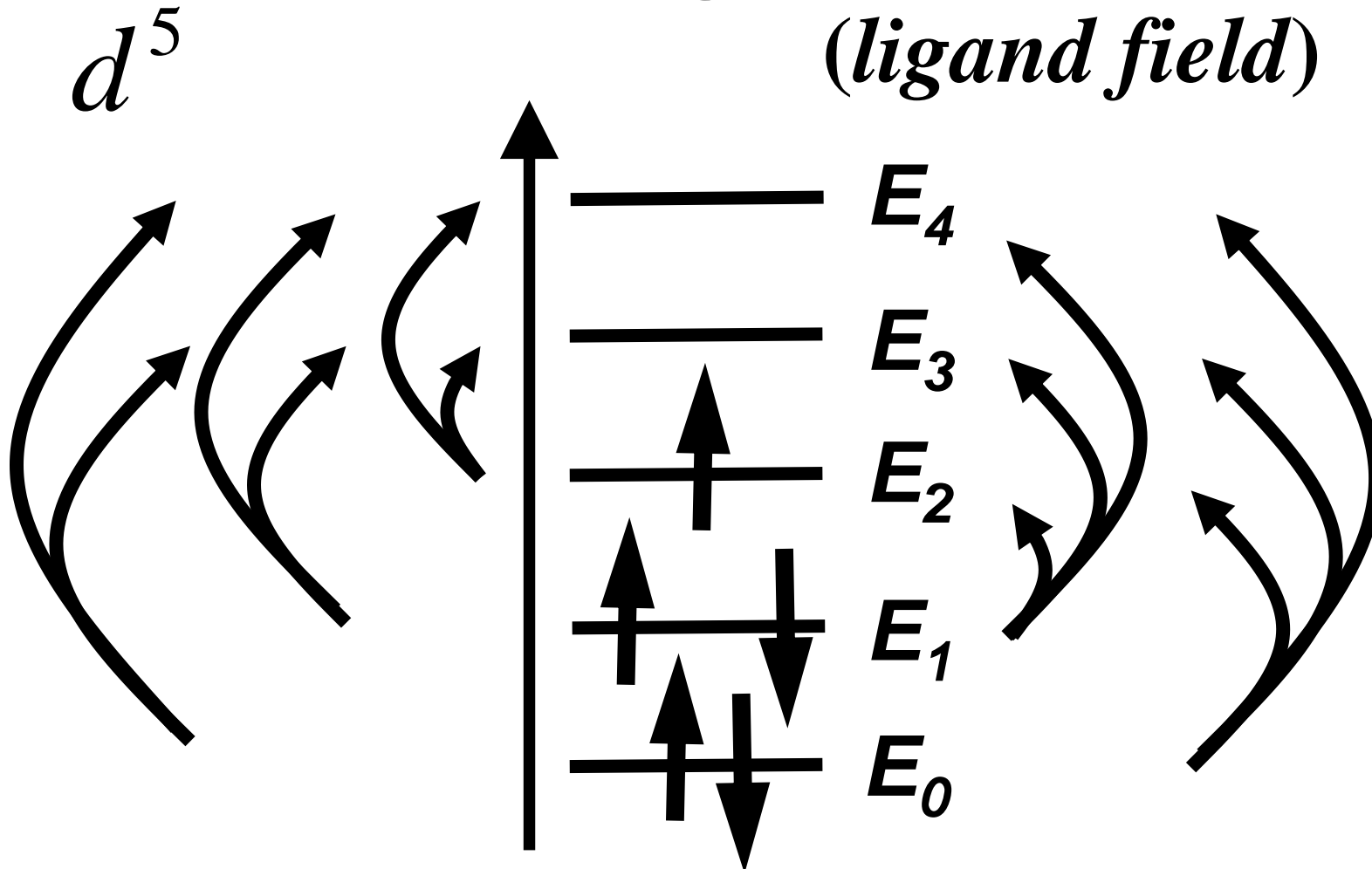
g tensor calculation

(ligand field)



$$g_{ij} \approx g_e \delta_{ij} - \frac{2\zeta_{3d}}{2S} \left(\sum_{\alpha} - \sum_{\beta} \right) \sum_n \frac{\langle 0 | L_i | n \rangle \langle n | L_j | 0 \rangle}{E_n - E_0}$$

g tensor calculation (ligand field)



$Fe^{3+}(d^5)$

FeC_6

FeC_5N

FeC_4N_2

FeC_4N_2

FeN_6

FeN_6

FeN_6

FeN_6

Low Spin
($S=1/2$)

	g_1	g_2	g_3
FeC_6	2.10	0.91	2.35
FeC_5N	2.177	0.845	2.995
FeC_4N_2	2.50	2.50	1.65
FeC_4N_2	2.7	2.7	1.6
FeN_6	2.615	2.727	1.459
FeN_6	2.61	2.61	1.61
FeN_6	2.64	2.64	1.38
FeN_6	2.60	2.60	1.60

$$g_{ij} \approx g_e \delta_{ij} - \frac{2\zeta_{3d}}{2S} \left(\sum_{\alpha} - \sum_{\beta} \right) \sum_n \frac{\langle 0 | L_i | n \rangle \langle n | L_j | 0 \rangle}{E_n - E_0}$$

$Fe^{3+}(H_2O)_6$
1.935
2.072
2.110

When it does not work as simply ...

Angew. Chem. Int. Ed. 2000, 39

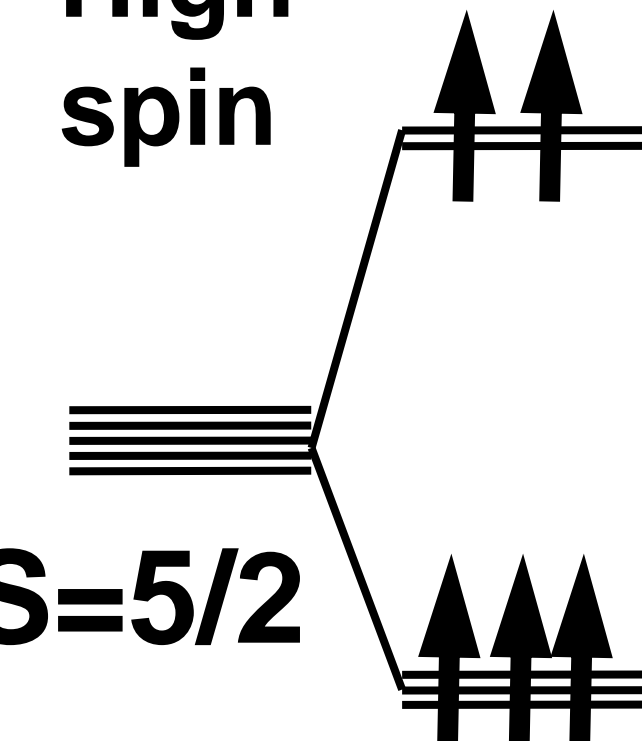
Jean-Jacques Girerd & Marie-Laure Boillot

Dalton Trans., 2005, 1734-1742

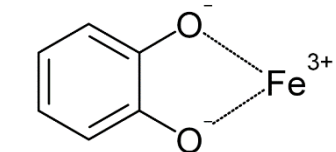
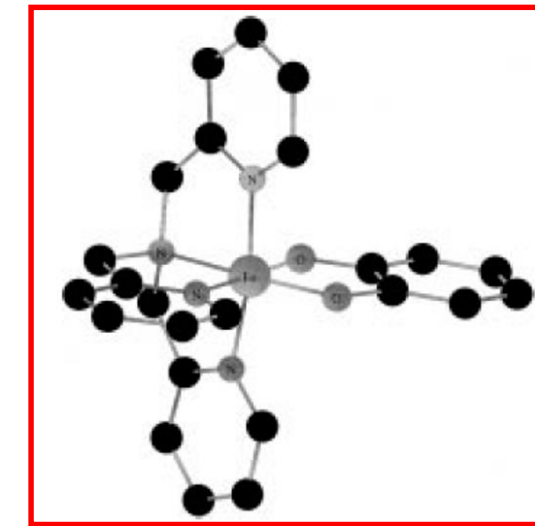
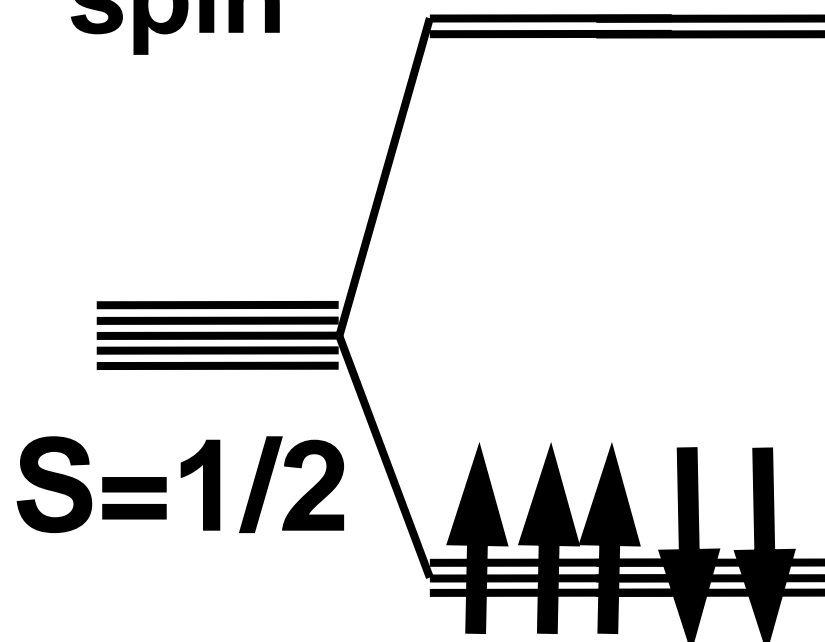
Inorganica Chimica Acta 361 (2008) 4012-4016

'High spin' versus 'low spin'

High
spin



Low
spin



DBC : 2 x *ter*-Bu
CAT : 2 x H
TCC : 4 x Cl
DNC : 2 x NO₂

Experimental g tensors for a series of catecholate spin transition complexes

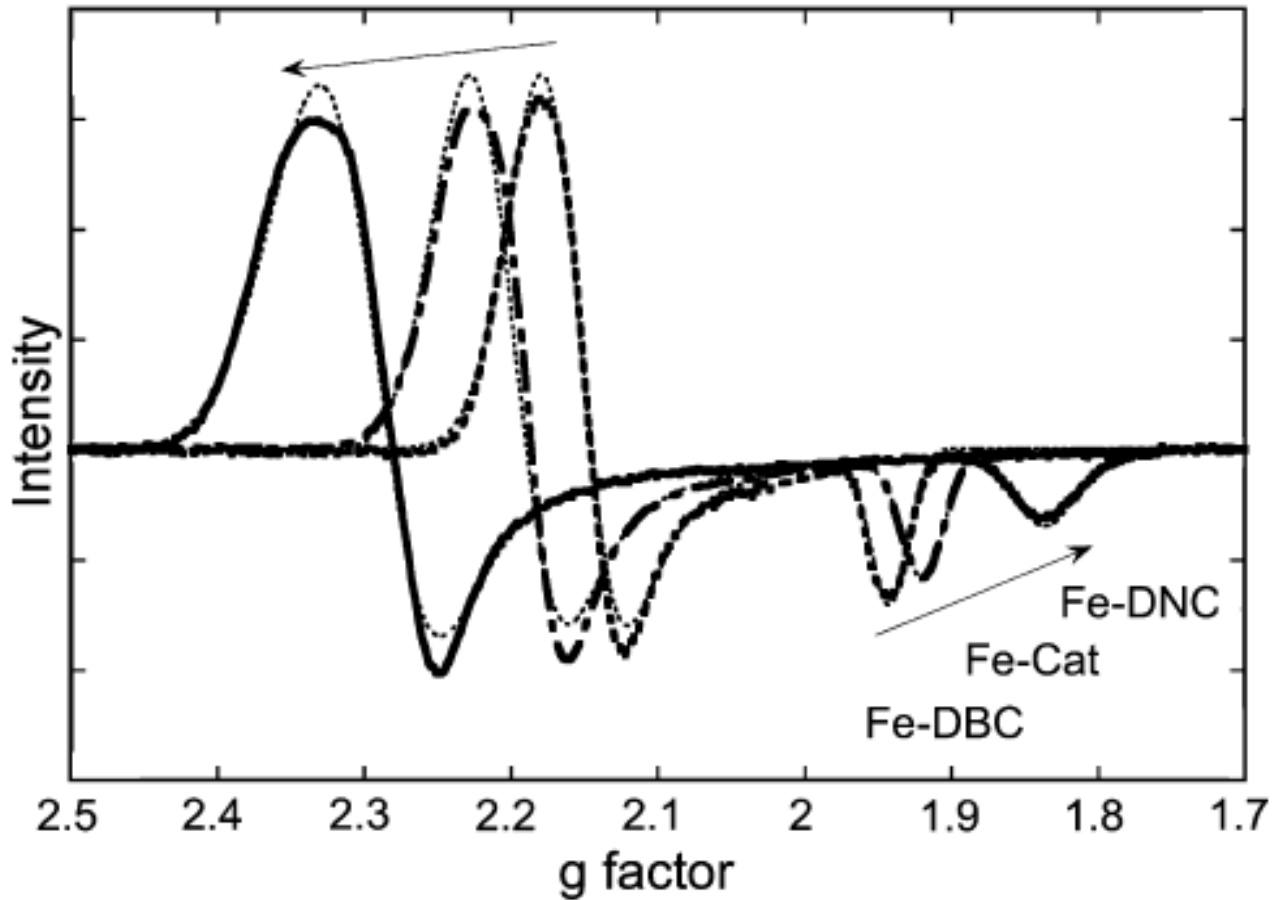
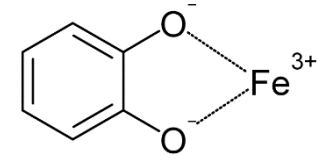
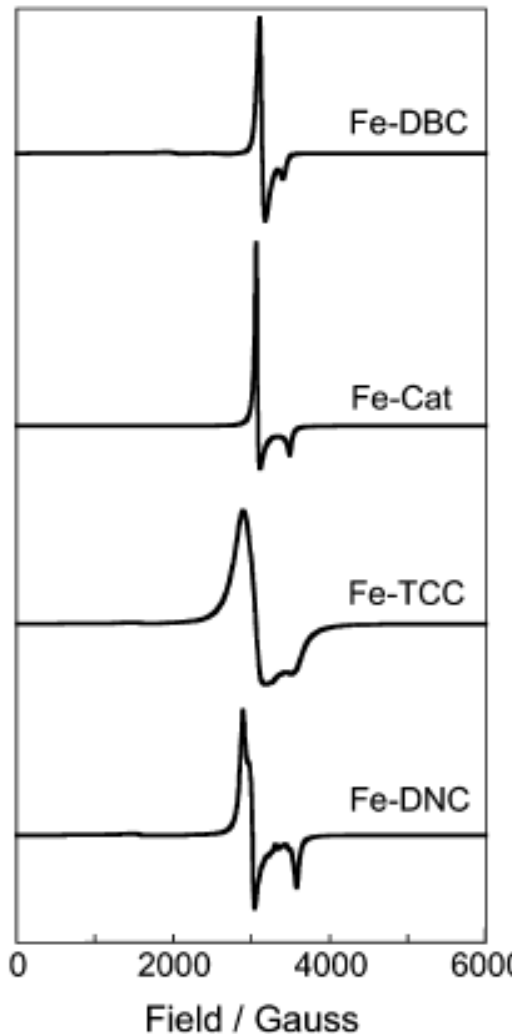


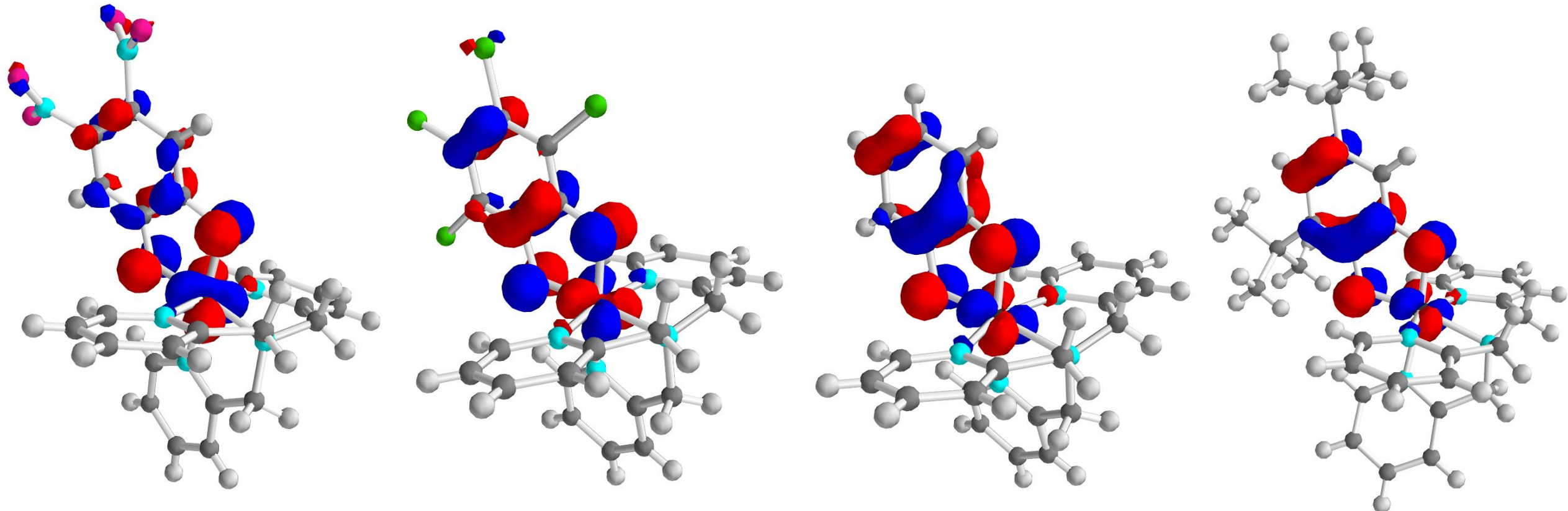
Fig. 4. Experimental LS spectra of $[(\text{TPA})\text{Fe}(\text{R-Cat})]\text{BPh}_4$ in frozen butyronitrile solutions, $T = 5 \text{ K}$; the dotted lines are used for the simulated spectra.



$$[g] = \lambda^2 [g_{\text{Fe(II)}\text{SQ}}] + (1 - \lambda^2) [g_{\text{Fe(III)}\text{Cat}}]$$

PERTURB.	EXP
DBC	1,986
DBC	2,012
DBC	2,059
CAT	2,002
CAT	2,018
CAT	2,053
TCC	2,003
TCC	2,014
TCC	2,057
DNC	2,002
DNC	2,033
DNC	2,066
	1,942
	2,155
	2,175
	1,918
	2,190
	2,228
	1,905
	2,235
	2,290
	1,826
	2,278
	2,353

Molecular orbital delocalisation for a series of catecholate spin transition complexes



DNC

TCC

CAT

DBC

Analytical calculation of the g tensor

$$\begin{cases} \Psi_n = \alpha_n \cdot dz^2 + \beta_n \cdot dx^2 - y^2 + \gamma_n \cdot dxy + \delta_n \cdot dxz + \varepsilon_n \cdot dyz \\ \Psi_o = \alpha_o \cdot dz^2 + \beta_o \cdot dx^2 - y^2 + \gamma_o \cdot dxy + \delta_o \cdot dxz + \varepsilon_o \cdot dyz \end{cases}$$

$L_{Fe} \cdot S_{Fe}$	Ψ_0^α	Ψ_0^β	Ψ_n^α	Ψ_n^β
$\Psi_0^{\alpha*}$	E_o	0	$-i.c$	$-a + i.b$
$\Psi_0^{\beta*}$	0	E_o	$a + i.b$	$i.c$
$\Psi_n^{\alpha*}$	$i.c$	$a - i.b$	E_1	0
$\Psi_n^{\beta*}$	$-a - i.b$	$-i.c$	0	E_1

$$H_{SO} = \lambda L \cdot S = \lambda \left[L_z S_z + \frac{1}{2} (L^+ S^- + L^- S^+) \right]$$

Analytical calculation of the g tensor

Spin-orbitals

$$\begin{array}{c} |\alpha\rangle \left(\begin{array}{c} \frac{\beta_0 - i\gamma_0}{\sqrt{2}} |2\rangle \\ \frac{i\varepsilon_0 - \delta_0}{\sqrt{2}} |1\rangle \\ \alpha_0 |0\rangle \\ \frac{i\varepsilon_0 + \delta_0}{\sqrt{2}} |-1\rangle \\ \frac{\beta_0 + i\gamma_0}{\sqrt{2}} |-2\rangle \\ 0 \\ 0 \\ 0 \\ 0 \\ 0 \end{array} \right) \left(\begin{array}{c} 0 \\ 0 \\ 0 \\ 0 \\ \frac{\beta_0 - i\gamma_0}{\sqrt{2}} |2\rangle \\ \frac{i\varepsilon_0 - \delta_0}{\sqrt{2}} |1\rangle \\ \alpha_0 |0\rangle \\ \frac{i\varepsilon_0 + \delta_0}{\sqrt{2}} |-1\rangle \\ \frac{\beta_0 + i\gamma_0}{\sqrt{2}} |-2\rangle \\ 0 \\ 0 \\ 0 \\ 0 \\ 0 \end{array} \right) \left(\begin{array}{c} \frac{\beta_n - i\gamma_n}{\sqrt{2}} |2\rangle \\ \frac{i\varepsilon_n - \delta_n}{\sqrt{2}} |1\rangle \\ \alpha_0 |0\rangle \\ \frac{i\varepsilon_n + \delta_n}{\sqrt{2}} |-1\rangle \\ \frac{\beta_n + i\gamma_n}{\sqrt{2}} |-2\rangle \\ 0 \\ 0 \\ 0 \\ 0 \\ 0 \end{array} \right) \left(\begin{array}{c} 0 \\ 0 \\ 0 \\ 0 \\ \frac{\beta_n - i\gamma_n}{\sqrt{2}} |2\rangle \\ \frac{i\varepsilon_n - \delta_n}{\sqrt{2}} |1\rangle \\ \alpha_0 |0\rangle \\ \frac{i\varepsilon_n + \delta_n}{\sqrt{2}} |-1\rangle \\ \frac{\beta_n + i\gamma_n}{\sqrt{2}} |-2\rangle \\ 0 \\ 0 \\ 0 \\ 0 \\ 0 \end{array} \right) \\ |\beta\rangle \left(\begin{array}{c} \frac{\beta_0 - i\gamma_0}{\sqrt{2}} |2\rangle \\ \frac{i\varepsilon_0 - \delta_0}{\sqrt{2}} |1\rangle \\ \alpha_0 |0\rangle \\ \frac{i\varepsilon_0 + \delta_0}{\sqrt{2}} |-1\rangle \\ \frac{\beta_0 + i\gamma_0}{\sqrt{2}} |-2\rangle \\ 0 \\ 0 \\ 0 \\ 0 \\ 0 \end{array} \right) \left(\begin{array}{c} 0 \\ 0 \\ 0 \\ 0 \\ \frac{\beta_0 - i\gamma_0}{\sqrt{2}} |2\rangle \\ \frac{i\varepsilon_0 - \delta_0}{\sqrt{2}} |1\rangle \\ \alpha_0 |0\rangle \\ \frac{i\varepsilon_0 + \delta_0}{\sqrt{2}} |-1\rangle \\ \frac{\beta_0 + i\gamma_0}{\sqrt{2}} |-2\rangle \\ 0 \\ 0 \\ 0 \\ 0 \\ 0 \end{array} \right) \left(\begin{array}{c} \frac{\beta_n - i\gamma_n}{\sqrt{2}} |2\rangle \\ \frac{i\varepsilon_n - \delta_n}{\sqrt{2}} |1\rangle \\ \alpha_0 |0\rangle \\ \frac{i\varepsilon_n + \delta_n}{\sqrt{2}} |-1\rangle \\ \frac{\beta_n + i\gamma_n}{\sqrt{2}} |-2\rangle \\ 0 \\ 0 \\ 0 \\ 0 \\ 0 \end{array} \right) \left(\begin{array}{c} 0 \\ 0 \\ 0 \\ 0 \\ \frac{\beta_n - i\gamma_n}{\sqrt{2}} |2\rangle \\ \frac{i\varepsilon_n - \delta_n}{\sqrt{2}} |1\rangle \\ \alpha_0 |0\rangle \\ \frac{i\varepsilon_n + \delta_n}{\sqrt{2}} |-1\rangle \\ \frac{\beta_n + i\gamma_n}{\sqrt{2}} |-2\rangle \\ 0 \\ 0 \\ 0 \\ 0 \\ 0 \end{array} \right) \end{array}$$

Kramers doublet

$$\left\{ \Psi_K, \Psi_K^* \right\}$$

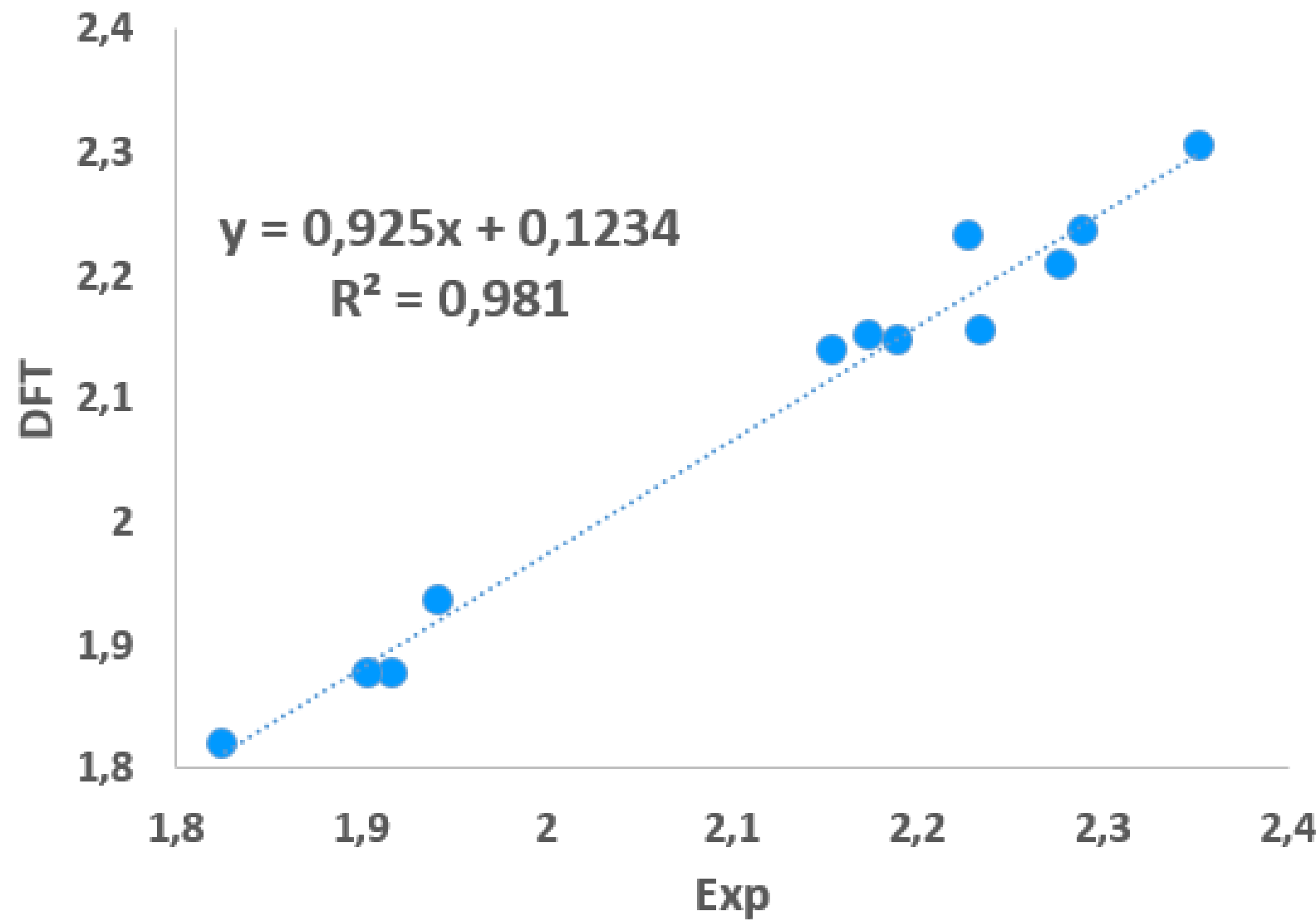
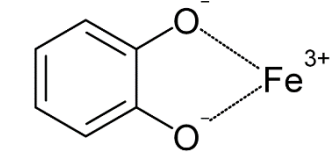
$$L_i \cdot + g_e S_i \quad \Psi_K \quad \Psi_K^*$$

$$\Psi_K$$

$$\Psi_K^*$$

?

Analytical calculation of the g tensor

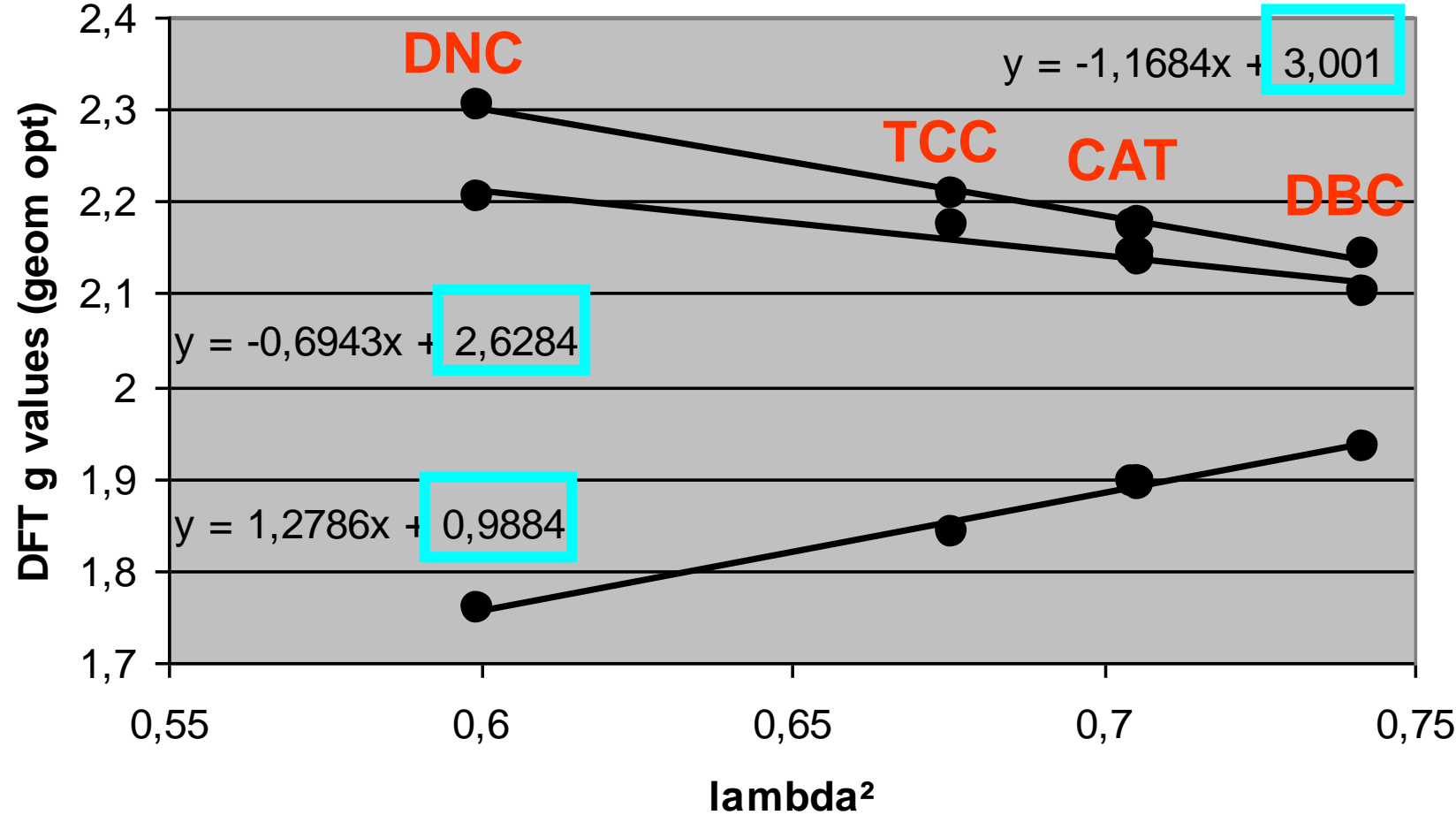


$$[g] = \lambda^2 [g_{\text{Fe(II)SQ}}] + (1 - \lambda^2) [g_{\text{Fe(III)Cat}}]$$

	"HYBRID"	EXP
DBC	1,934 2,138 2,150	1,942 2,155 2,175
CAT	1,875 2,145 2,230	1,918 2,190 2,228
TCC	1,875 2,153 2,234	1,905 2,235 2,290
DNC	1,819 2,206 2,304	1,826 2,278 2,353

Correlations showing non-innocence of catecholate ligands

$$\begin{cases} g_{\min}^{tot} = (1 - \lambda^2)g_{\min}^{Fe}(0) + \lambda^2 \times 2.0023 \\ g_{int}^{tot} = (1 - \lambda^2)g_{int}^{Fe}(0) + \lambda^2 \times 2.0023 \\ g_{max}^{tot} = (1 - \lambda^2)g_{max}^{Fe}(0) + \lambda^2 \times 2.0023 \end{cases}$$



hemoglobins
Biophys. J., 2005, vol.89, 2628) :

$$\begin{aligned} 2.91 < g_{\max} < 3.20 \\ 2.08 < g_{\text{int}} < 2.26 \\ 1.20 < g_{\min} < 1.53 \end{aligned}$$

porphyrins (Bull. Chem. Soc. Jpn, 2004, vol.77, 357) :

$$\begin{aligned} 2.78 < g_{\max} < 3.18 \\ 2.29 < g_{\text{int}} < 2.31 \\ 1.15 < g_{\min} < 1.69 \end{aligned}$$

cytochroms (Phys. Chem. Chem. Phys. 2002, vol.4, p655) :

$$\begin{aligned} 2.93 \approx g_{\max} \\ 2.25 \approx g_{\text{int}} \\ 1.50 \approx g_{\min} \end{aligned}$$

SKIP !

G tensor calculations

- *Bilan* -

- « *ligand field* » approach
 - not rigorous (SOC, gauge)
 - semi-quantitative
- DFT / HF : « *sum-over-states* »
 - gauge correction
 - radicals *versus* metals (3d)
- Linear Response Theory

$$h\nu = \mu_B \bar{\mathbf{B}} \cdot \tilde{\mathbf{g}} \cdot \vec{s}$$

$$\Delta g_{uv} = \frac{1}{\mu_B} \left. \frac{\partial^2 E}{\partial B_{0,u} \partial s_v} \right|_{\mathbf{B}=\mathbf{s}=0}$$

Directly introducing the magnetic field

SKIP !

Stone, A. J., Proc. R. Soc. A, 271, 424 (1963)

**Schreckenbach & Ziegler,
J. Phys. Chem. A, 101, 3388 (1997)**

**→ Application to DFT, with GIAO
(Gauge-Including Atomic Orbital method)**

**Van Lenthe, Wormer & van der Avoird,
J. Chem. Phys., 107, 2488 (1997)**

→ Application of Dirac equation (ZORA)

**Neese & Solomon,
Inorg. Chem. A, 37, 6568 (1998)**

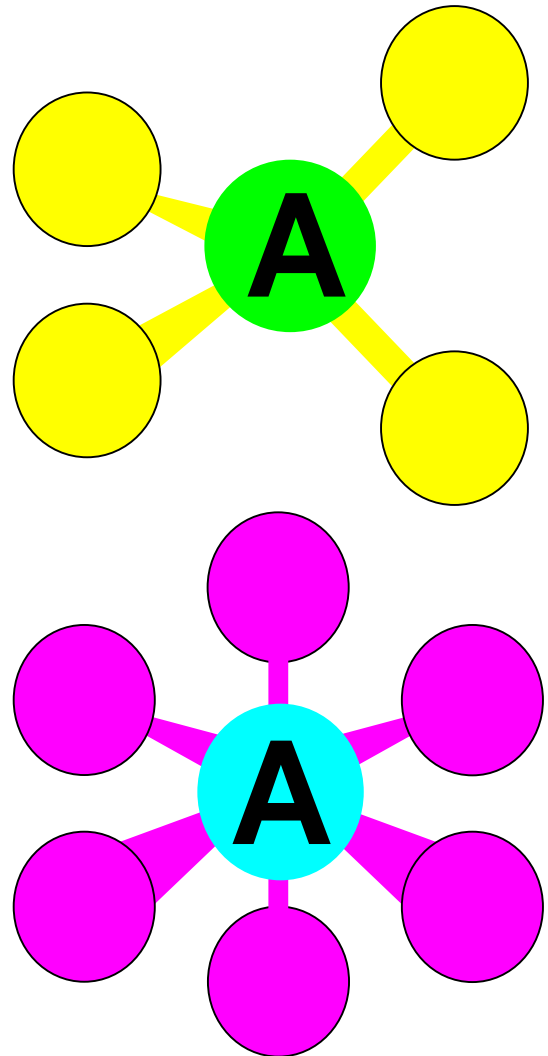
**→ Formulas for g and ZFS ($S \rightarrow S \pm 1$)
implemented with INDO (semi-empirical)
(Intermediate-Neglect of Differential Orbital)**

**Malkina, Malkin, Kaupp et al,
J. Am. Chem. Soc. 122, 9206 (2000)**

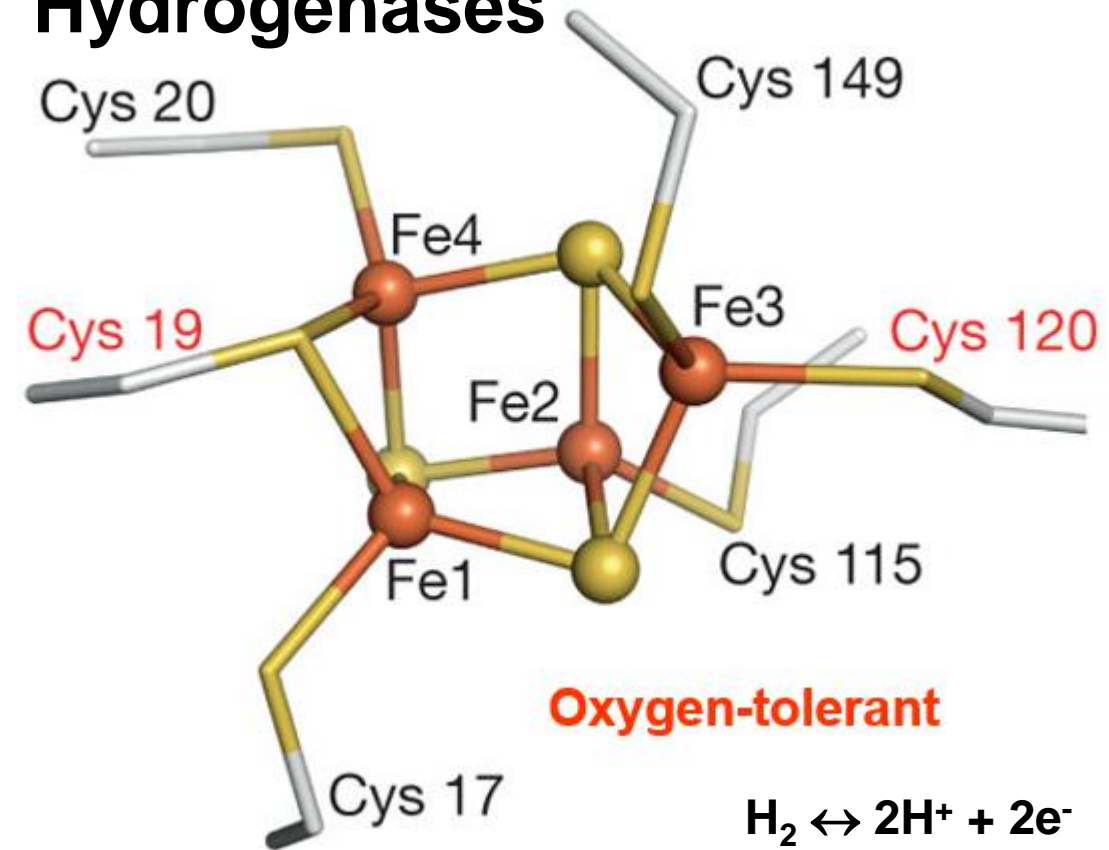
Outline of the lecture

- ***Basic introduction to DFT***
 - Hartree-Fock versus DFT
- ***Application : (mono-metal) g-tensors***
 - Relativistic origin
 - Perturbative & self-consistent approaches
 - When it does not work ...
- ***Polymetallic complexes***
 - Spin-coupling
 - G-tensor (dimer)
 - Hyperfine couplings (dimer)
 - More complex systems : hyperfine & Mössbauer
- ***Conclusions***

Spin coupling & spectroscopies

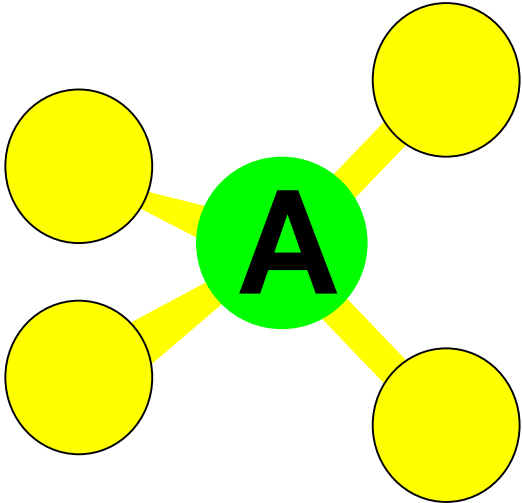


Hydrogenases



$$\text{charge : } \rho_e(\mathbf{r}) = \rho_\alpha(\mathbf{r}) + \rho_\beta(\mathbf{r})$$
$$\text{spin : } \rho_s(\mathbf{r}) = \rho_\alpha(\mathbf{r}) - \rho_\beta(\mathbf{r})$$

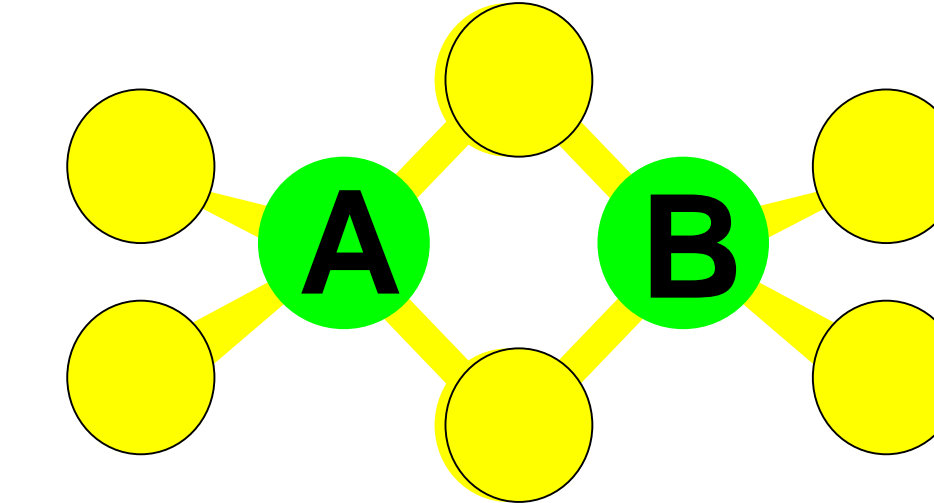
Spin coupling & spectroscopies



Local spins

$$H_A^Z = \beta \vec{H} \cdot \tilde{\vec{g}}_A \cdot \vec{S}_A \quad \vec{S}_A \cdot \tilde{\vec{A}}_A \cdot \vec{I}_A$$

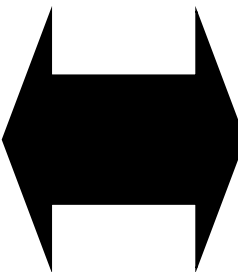
$$H_B^Z = \beta \vec{H} \cdot \tilde{\vec{g}}_B \cdot \vec{S}_B \quad \vec{S}_B \cdot \tilde{\vec{A}}_B \cdot \vec{I}_B$$



Global spin

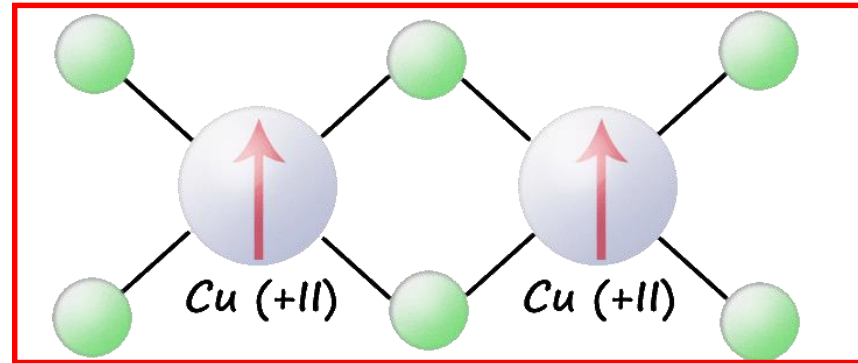
$$H_{tot}^Z = \beta \vec{H} \cdot \tilde{\vec{g}} \cdot \vec{S} \quad \vec{S} \cdot \tilde{\vec{A}}_{A/S} \cdot \vec{I}_A$$

$$H_J = J \vec{S}_A \cdot \vec{S}_B \quad \vec{S} \cdot \tilde{\vec{A}}_{B/S} \cdot \vec{I}_B$$



Case of 2 Cu²⁺(s=1/2) : triplet state (S=1)

$$\Psi_1 = \frac{1}{\sqrt{2}} \begin{vmatrix} \varphi_1(r_1)\alpha_1(s_1) & \varphi_2(r_1)\alpha_2(s_1) \\ \varphi_1(r_2)\alpha_1(s_2) & \varphi_2(r_2)\alpha_2(s_2) \end{vmatrix}$$



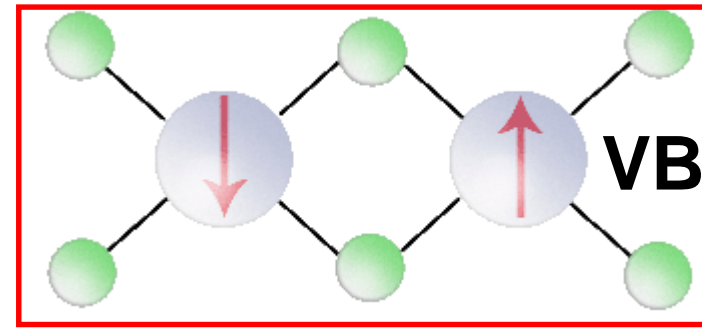
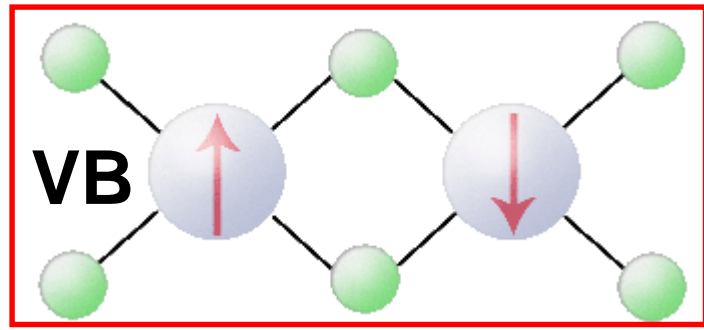
$$[\Phi_1(r_1)\Phi_2(r_2) - \Phi_2(r_1)\Phi_1(r_2)]\alpha(1)\alpha(2)$$

Global spin S=1

Case of 2 Cu²⁺(s=1/2) : singlet state (S=0)

$$\Psi_2 = \frac{1}{\sqrt{2}} \begin{vmatrix} \Phi_1(r_1)\alpha(1) & \Phi_1(r_2)\alpha(2) \\ \Phi_2(r_1)\beta(1) & \Phi_2(r_2)\beta(2) \end{vmatrix}$$

$$\Psi_3 = \frac{1}{\sqrt{2}} \begin{vmatrix} \Phi_1(r_1)\beta(1) & \Phi_1(r_2)\beta(2) \\ \Phi_2(r_1)\alpha(1) & \Phi_2(r_2)\alpha(2) \end{vmatrix}$$



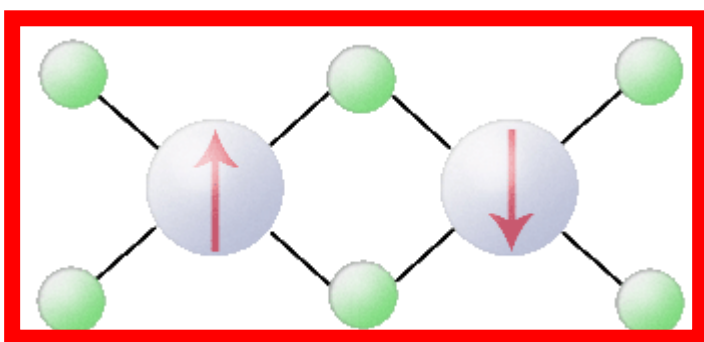
$$[\Phi_1(r_1)\Phi_2(r_2) + \Phi_2(r_1)\Phi_1(r_2)] [\alpha(1)\beta(2) - \beta(1)\alpha(2)]$$

Global spin S=0

Broken symmetry state ($M_s=0$)

$$\Psi_S^{VB} = \frac{1}{\sqrt{2(1+S_{AB}^2)}} [\Phi_A^{VB}(1)\Phi_B^{VB}(2) + \Phi_B^{VB}(1)\Phi_A^{VB}(2)]$$

$$\Psi_T^{VB} = \frac{1}{\sqrt{2(1-S_{AB}^2)}} [\Phi_A^{VB}(1)\Phi_B^{VB}(2) - \Phi_B^{VB}(1)\Phi_A^{VB}(2)]$$

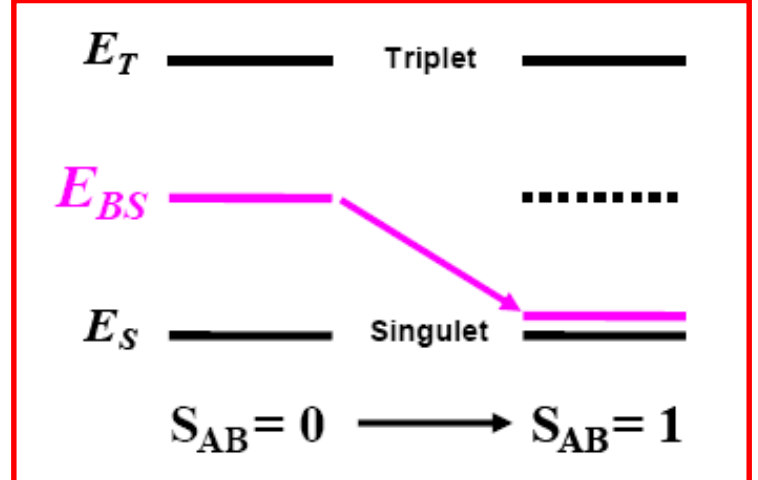


$$\Psi_{BS}^{VB} \equiv \boxed{\Phi_A^{VB}(1)\Phi_B^{VB}(2)} = \sqrt{\frac{1+S_{AB}^2}{2}} \Psi_S^{VB} + \sqrt{\frac{1-S_{AB}^2}{2}} \Psi_T^{VB}$$

$$|S_A, M_A\rangle |S_B, M_B\rangle = |1/2, +1/2\rangle |1/2, -1/2\rangle$$

$$(\alpha\beta - \beta\alpha) |S, M\rangle = |0, 0\rangle$$

$$(\alpha\beta + \beta\alpha) |S, M\rangle = \begin{cases} |1, +1\rangle \\ |1, 0\rangle \\ |1, -1\rangle \end{cases}$$



(3d) Transition metal dimers

Clebsch–Gordan coefficients

Global state

$$|S, M\rangle = \sum_{\{M_A, M_B\}} C_{M, M_A, M_B}^{S, S_A, S_B} |S_A, M_A\rangle |S_B, M_B\rangle$$

$$M_A + M_B = M$$

Local states

Local state

$$|S_A, M_A\rangle |S_B, M_B\rangle = \sum_{\{S\}} C_{M, M_A, M_B}^{S, S_A, S_B} |S, M\rangle$$

$$|S_A - S_B| \leq S \leq S_A + S_B$$

Global state

(3d) Transition metal dimers

Clebsch–Gordan coefficients

$$|S, M\rangle = \sum_{\{M_A, M_B\}} C_{M, M_A, M_B}^{S, S_A, S_B} |S_A, M_A\rangle |S_B, M_B\rangle$$

Cu²⁺- Cu²⁺

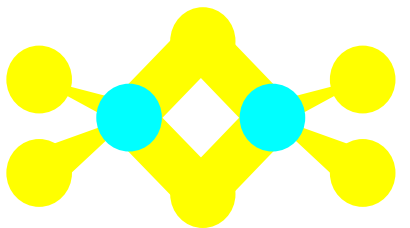
$$\begin{pmatrix} |1,+1\rangle \\ |1, 0\rangle \\ |1,-1\rangle \\ |0, 0\rangle \end{pmatrix} = \begin{pmatrix} 1 & 0 & 0 & 0 \\ 0 & \frac{1}{\sqrt{2}} & \frac{1}{\sqrt{2}} & 0 \\ 0 & 0 & 0 & 1 \\ 0 & \frac{1}{\sqrt{2}} & \frac{-1}{\sqrt{2}} & 0 \end{pmatrix} \cdot \begin{pmatrix} |1/2,+1/2\rangle |1/2,+1/2\rangle \\ |1/2,+1/2\rangle |1/2,-1/2\rangle \\ |1/2,-1/2\rangle |1/2,-1/2\rangle \\ |1/2,-1/2\rangle |1/2,+1/2\rangle \end{pmatrix}$$

$$triplet = \begin{cases} |1,+1\rangle \\ |1, 0\rangle \\ |1,-1\rangle \end{cases}$$

$$singlet = |0,0\rangle$$

$$|5,+5\rangle = |5/2,+5/2\rangle |5/2,+5/2\rangle$$

HS



$$\begin{bmatrix} |5,0\rangle \\ |4,0\rangle \\ |3,0\rangle \\ |2,0\rangle \\ |1,0\rangle \\ |0,0\rangle \end{bmatrix} = \begin{bmatrix} \frac{1}{\sqrt{252}} & \frac{5}{\sqrt{252}} & \frac{5}{\sqrt{63}} & \frac{5}{\sqrt{63}} & \frac{5}{\sqrt{252}} & \frac{1}{\sqrt{252}} \\ \frac{1}{\sqrt{28}} & \frac{3}{\sqrt{28}} & \frac{1}{\sqrt{7}} & -\frac{1}{\sqrt{7}} & -\frac{3}{\sqrt{28}} & -\frac{1}{\sqrt{28}} \\ \sqrt{\frac{5}{36}} & \sqrt{\frac{7}{180}} & -\sqrt{\frac{2}{45}} & -\sqrt{\frac{2}{45}} & -\sqrt{\frac{7}{180}} & \sqrt{\frac{5}{36}} \\ \sqrt{\frac{25}{84}} & \sqrt{\frac{1}{84}} & -\sqrt{\frac{4}{21}} & \sqrt{\frac{4}{21}} & -\sqrt{\frac{1}{84}} & -\sqrt{\frac{25}{84}} \\ \sqrt{\frac{5}{14}} & -\sqrt{\frac{9}{70}} & \sqrt{\frac{1}{70}} & \sqrt{\frac{1}{70}} & -\sqrt{\frac{9}{70}} & \sqrt{\frac{5}{14}} \\ \frac{1}{\sqrt{6}} & -\frac{1}{\sqrt{6}} & \frac{1}{\sqrt{6}} & -\frac{1}{\sqrt{6}} & \frac{1}{\sqrt{6}} & -\frac{1}{\sqrt{6}} \end{bmatrix}$$

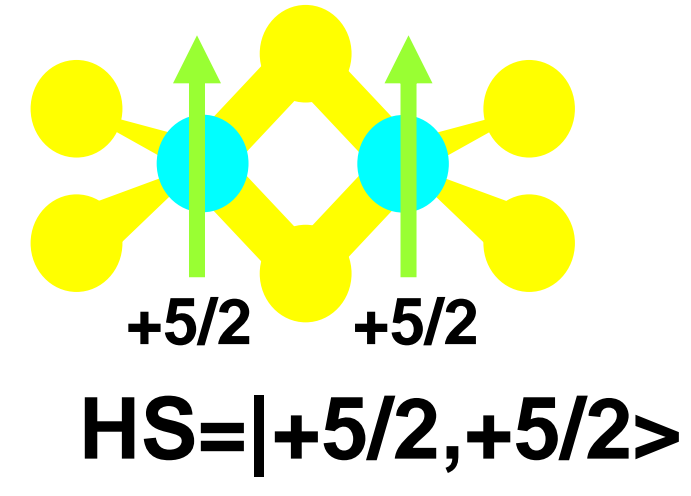
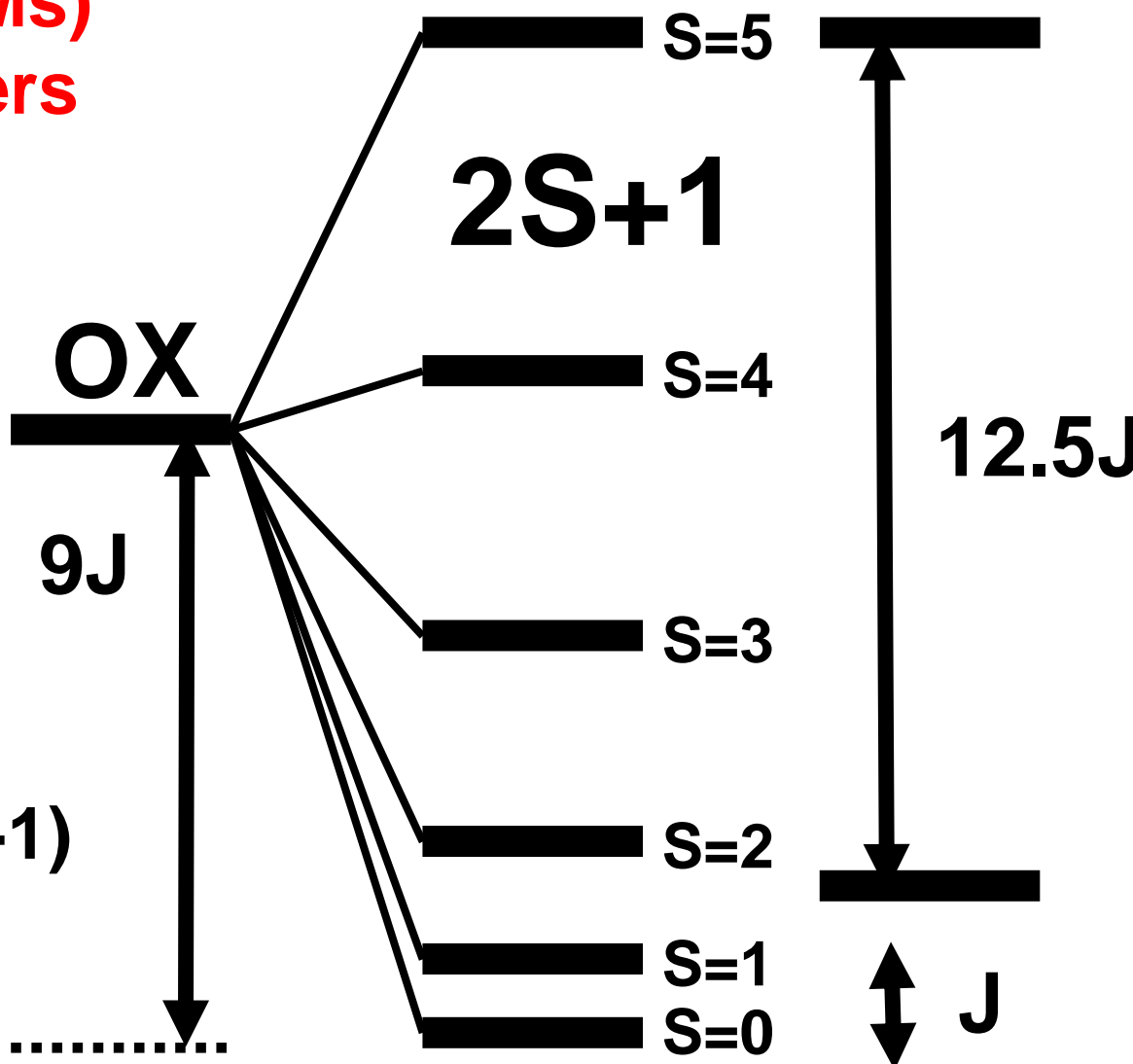
Fe³⁺- Fe³⁺

- $|5/2, 5/2\rangle |5/2, -5/2\rangle$
- $|5/2, 3/2\rangle |5/2, -3/2\rangle$
- $|5/2, 1/2\rangle |5/2, -1/2\rangle$
- $|5/2, -1/2\rangle |5/2, 1/2\rangle$
- $|5/2, -3/2\rangle |5/2, 3/2\rangle$
- $|5/2, -5/2\rangle |5/2, 5/2\rangle$

BS

Broken symmetry state

Artificial state (M_s)
Sum of monomers

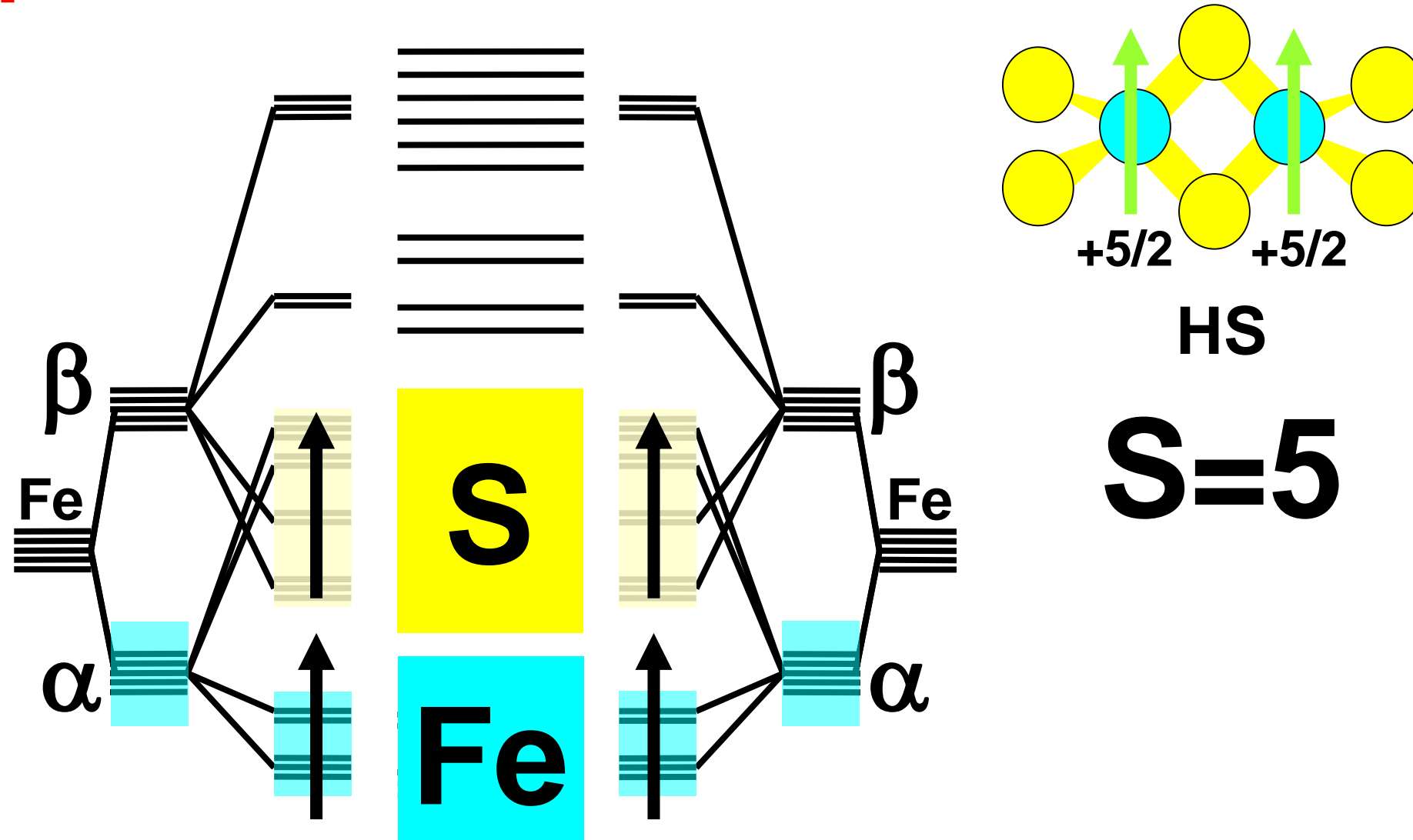


+ spin flip !



High-spin states of [2Fe2S] clusters

SKIP !



$$|9/2, +9/2\rangle = |5/2, +5/2\rangle |4/2, +4/2\rangle \quad \text{HS}$$

$$\begin{bmatrix} |9/2, 1/2\rangle \\ |7/2, 1/2\rangle \\ |5/2, 1/2\rangle \\ |3/2, 1/2\rangle \\ |1/2, 1/2\rangle \end{bmatrix} = \begin{bmatrix} \frac{1}{\sqrt{126}} & \sqrt{\frac{10}{63}} & \sqrt{\frac{10}{21}} & \sqrt{\frac{20}{63}} & \sqrt{\frac{10}{252}} \\ \sqrt{\frac{4}{63}} & \sqrt{\frac{11}{315}} & \sqrt{\frac{4}{105}} & -\sqrt{\frac{14}{45}} & -\sqrt{\frac{64}{315}} \\ \sqrt{\frac{3}{14}} & \sqrt{\frac{6}{35}} & \sqrt{\frac{8}{35}} & 0 & \sqrt{\frac{27}{70}} \\ \sqrt{\frac{8}{21}} & -\sqrt{\frac{2}{105}} & -\sqrt{\frac{2}{35}} & \sqrt{\frac{5}{21}} & -\sqrt{\frac{32}{105}} \\ \frac{1}{\sqrt{3}} & \frac{-2}{\sqrt{15}} & \frac{1}{\sqrt{5}} & -\sqrt{\frac{2}{15}} & \sqrt{\frac{1}{15}} \end{bmatrix}$$

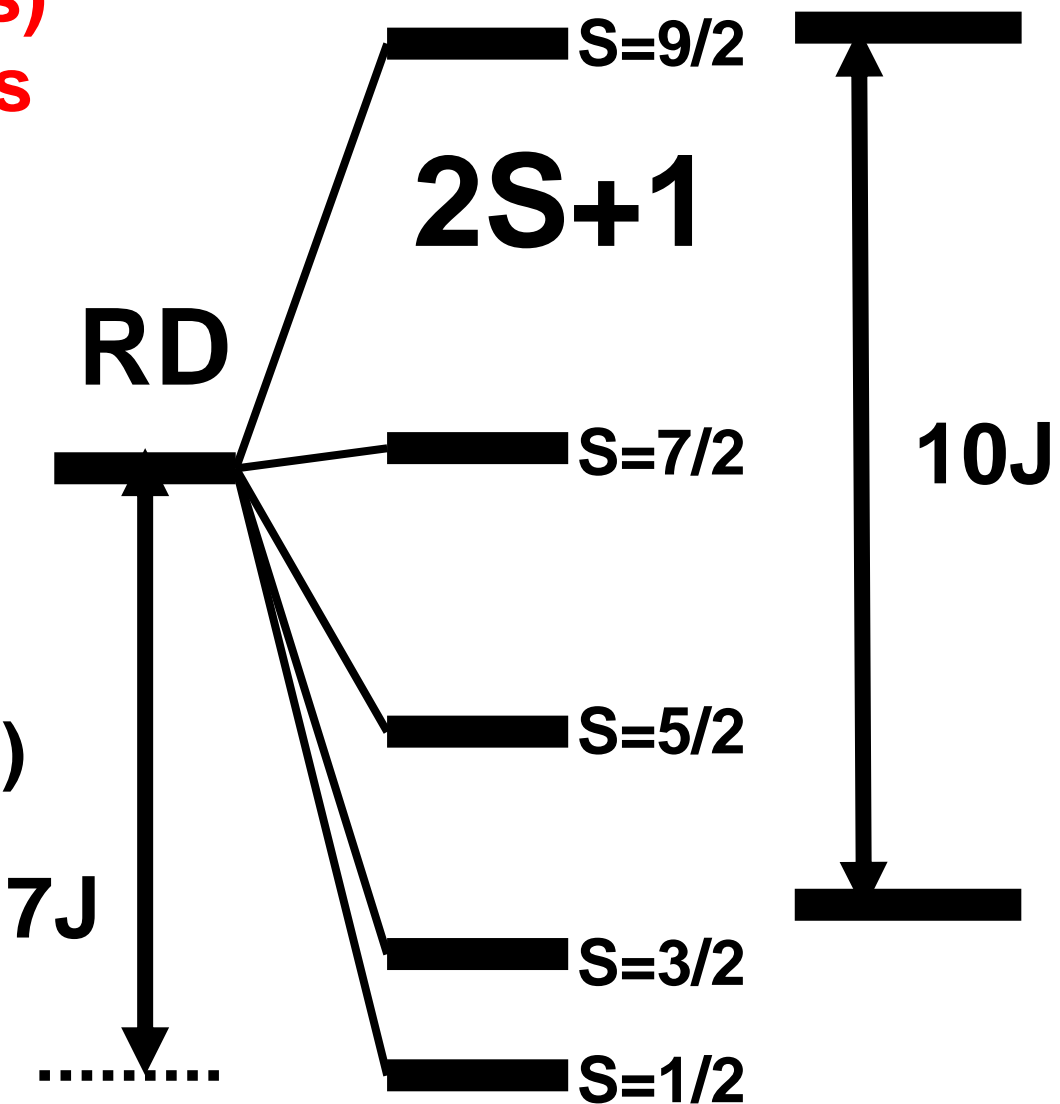
Fe³⁺- Fe²⁺

$$\bullet \begin{bmatrix} |5/2, 5/2\rangle |2, -2\rangle \\ |5/2, 3/2\rangle |2, -1\rangle \\ |5/2, 1/2\rangle |2, 0\rangle \\ |5/2, -1/2\rangle |2, 1\rangle \\ |5/2, -3/2\rangle |2, 2\rangle \end{bmatrix}$$

BS

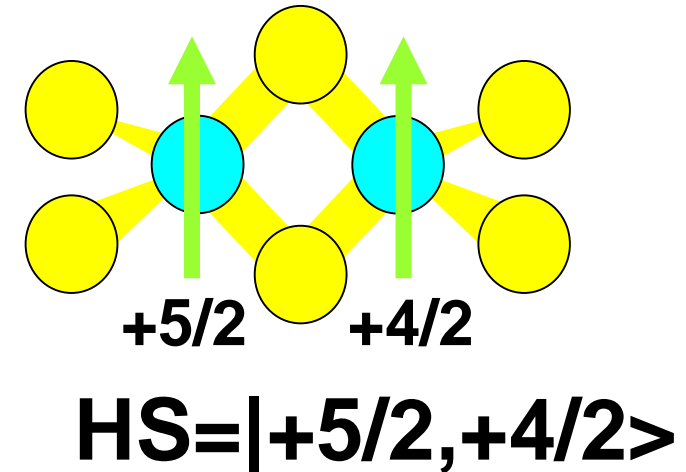
Broken symmetry state

Artificial state (M_s)
Sum of monomers

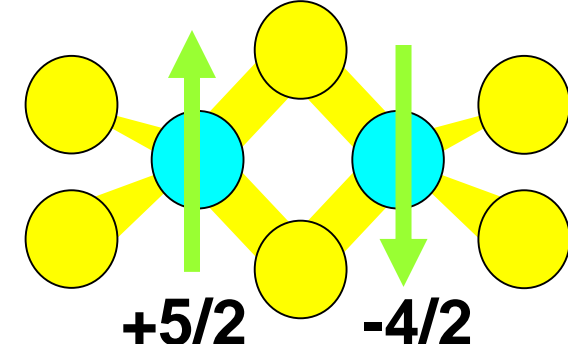


$$H_{\text{Heis.}} = J \mathbf{S}_1 \cdot \mathbf{S}_2$$

$$E_{\text{Heis.}} = (J/2) S(S+1)$$

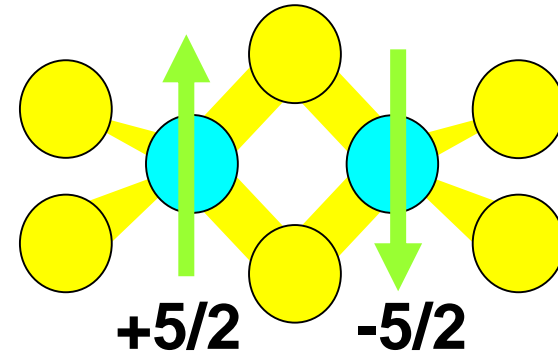
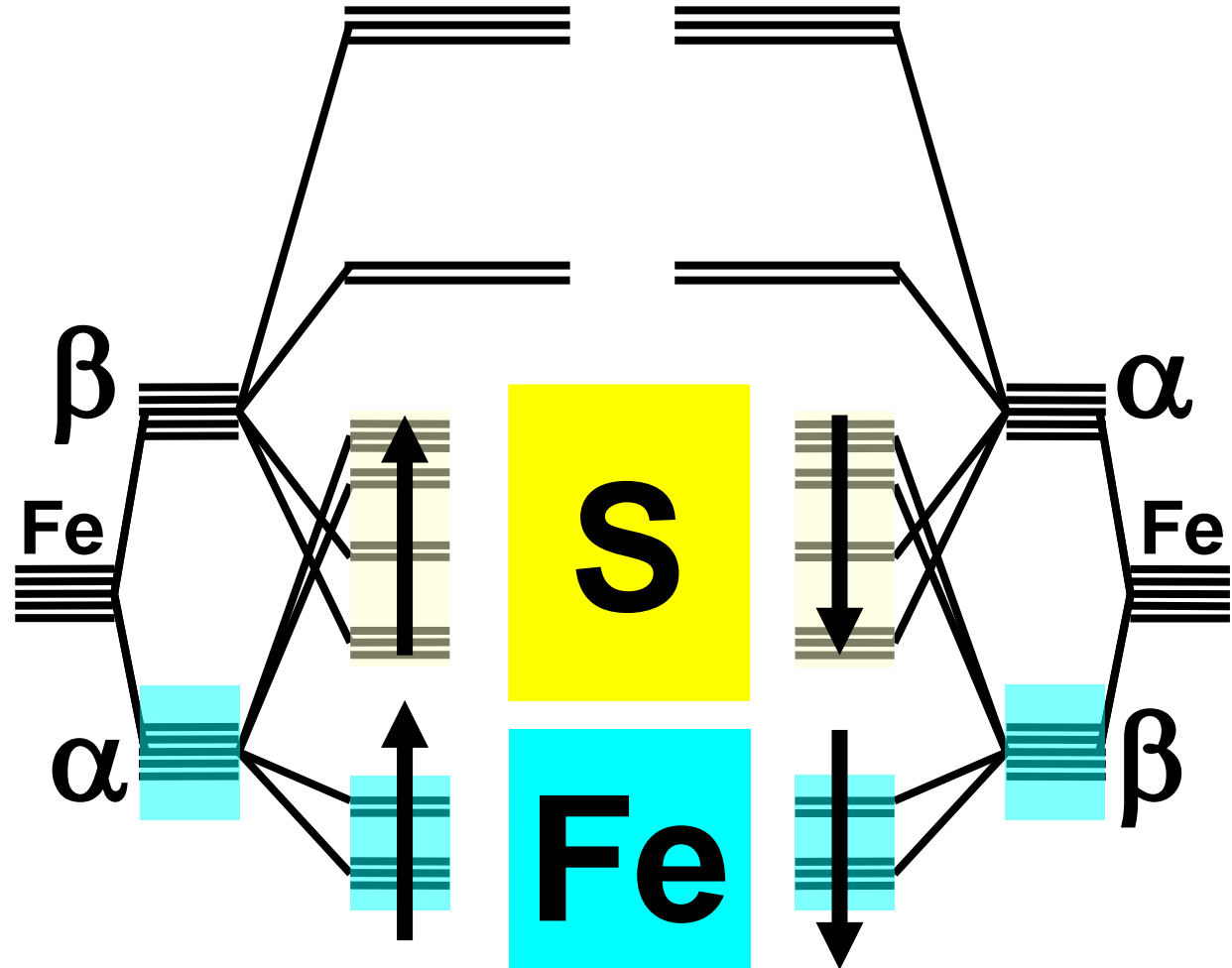


+ spin flip !



SKIP !

BS states of [2Fe2S] clusters



BS

$M_{SA} = 5/2$

Spin coupling

$$|S, M\rangle = \sum_{\{M_A, M_B\}} C_{M, M_A, M_B}^{S, S_A, S_B} |S_A, M_A\rangle |S_B, M_B\rangle$$

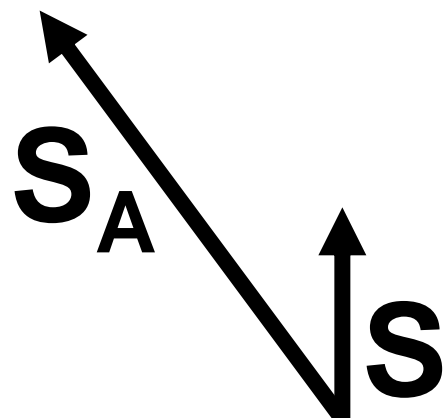
**Global
representation**



**Local
representation**

$$\langle S, M | S_z | S, M \rangle = M$$

$$\langle S, M | S_{Az} | S, M \rangle = \sum_{\{M_A, M_B\}} M_A (C_{M, M_A, M_B}^{S, S_A, S_B})^2$$



$$\tilde{A}_{global} \equiv \underbrace{\frac{\langle S, M | S_{Az} | S, M \rangle}{\langle S, M | S_z | S, M \rangle}}_{K_A} \tilde{A}_{local}$$

$$\vec{S}_A \cdot \tilde{\vec{A}}_{local} \cdot \vec{I}_A$$



$$\vec{S} \cdot \tilde{\vec{A}}_{global} \cdot \vec{I}_A$$

Spin coupling

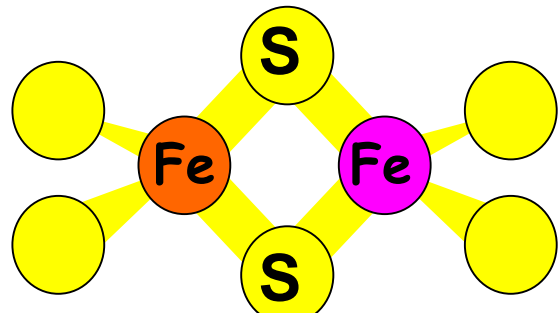
$$\mathbf{S}_A + \mathbf{S}_B = \mathbf{S}$$

$$K_A \equiv \frac{S(S+1) + S_A(S_A+1) - S_B(S_B+1)}{2S(S+1)}$$

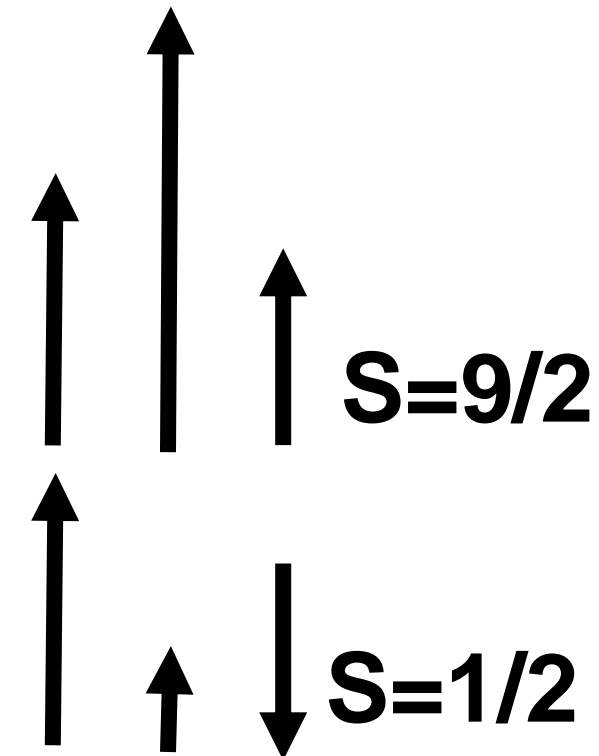
$$\mathbf{K}_A + \mathbf{K}_B = 1$$

$$K_B \equiv \frac{S(S+1) + S_B(S_B+1) - S_A(S_A+1)}{2S(S+1)}$$

$$\begin{aligned} S_A &= 5/2 \\ S_B &= 2 \end{aligned}$$



S	K_A	K_B
$9/2$	$+5/9$	$+4/9$
$7/2$	$+37/63$	$+26/63$
$5/2$	$+23/35$	$+12/35$
$3/2$	$+13/15$	$+2/15$
$1/2$	$+7/3$	$-4/3$



SKIP !

Spin coupling and EPR/ENDOR spectroscopies

$$|S, M\rangle = \sum_{\{M_A, M_B\}} C_{M, M_A, M_B}^{S, S_A, S_B} |S_A, M_A\rangle |S_B, M_B\rangle$$

Global
representation



Local
representation

$$H_A^Z = \beta \vec{H} \cdot \tilde{\vec{g}}_A \cdot \vec{S}_A$$

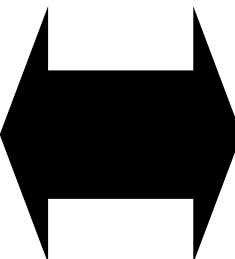
$$\vec{S}_A \cdot \tilde{\vec{A}}_A \cdot \vec{I}_A$$

$$H_{tot}^Z = \beta \vec{H} \cdot \tilde{\vec{g}} \cdot \vec{S}$$

$$\vec{S} \cdot \tilde{\vec{A}}_{A/S} \cdot \vec{I}_A$$

$$H_B^Z = \beta \vec{H} \cdot \tilde{\vec{g}}_B \cdot \vec{S}_B$$

$$\vec{S}_B \cdot \tilde{\vec{A}}_B \cdot \vec{I}_B$$



$$H_J = J \vec{S}_A \cdot \vec{S}_B$$

$$\vec{S} \cdot \tilde{\vec{A}}_{B/S} \cdot \vec{I}_B$$

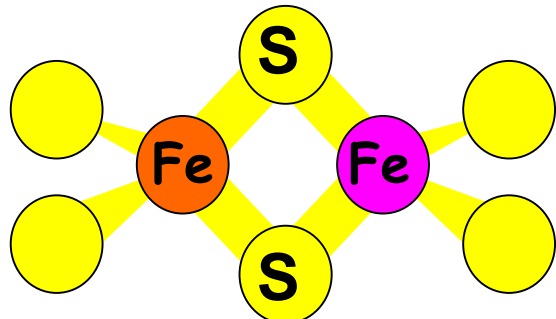
Spin coupling and EPR/ENDOR spectroscopies

$$S_A + S_B = S$$

$$\tilde{g} = K_A \tilde{g}_A + K_B \tilde{g}_B$$

$$S_A = 5/2$$

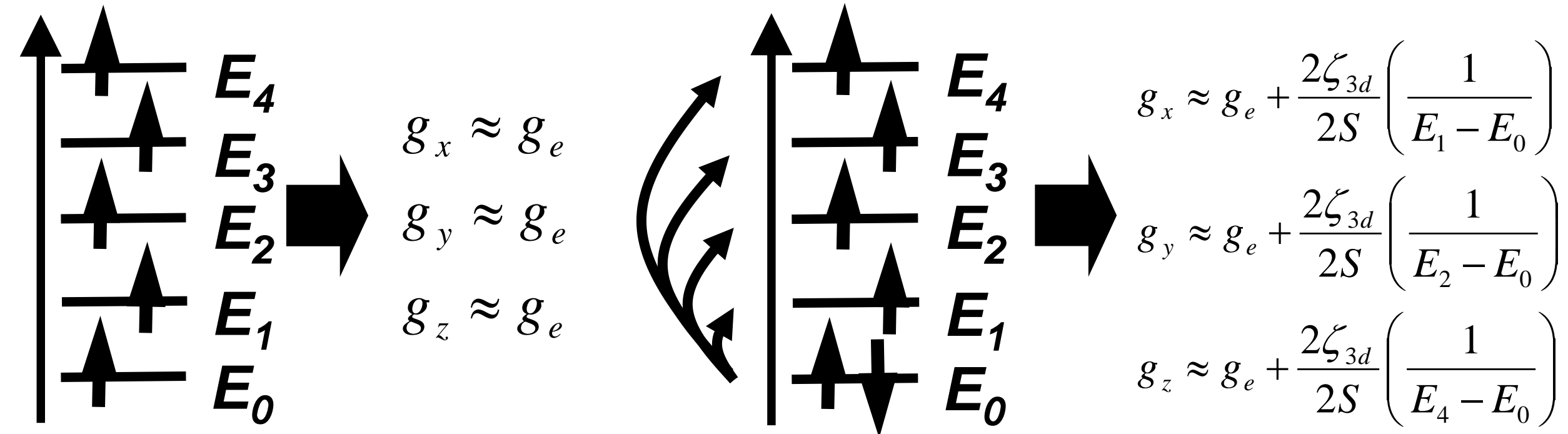
$$S_B = 2$$



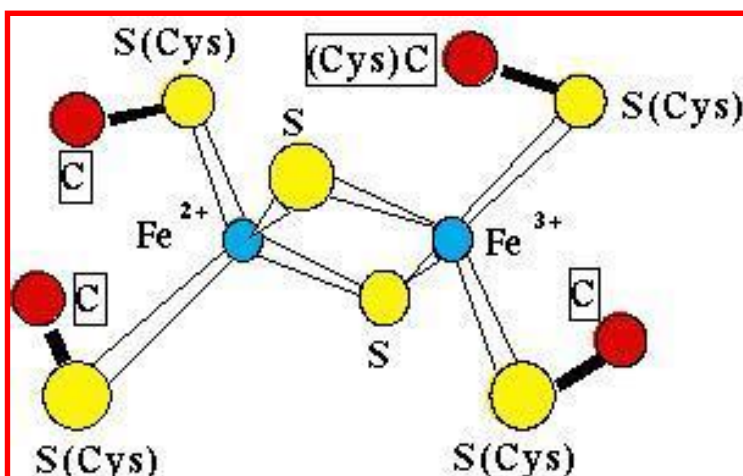
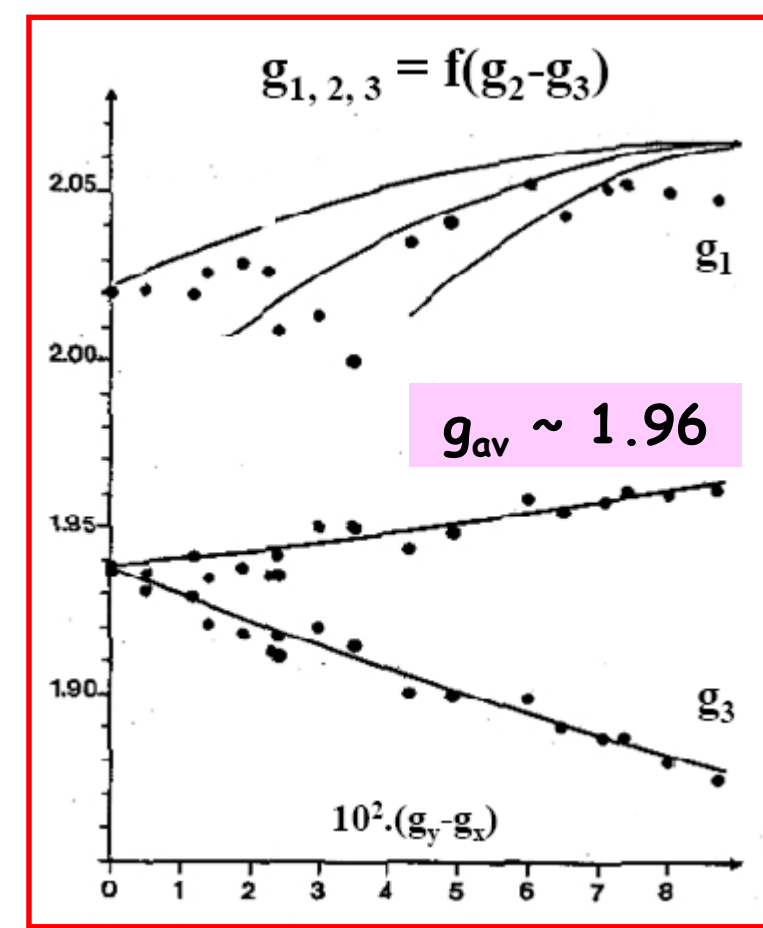
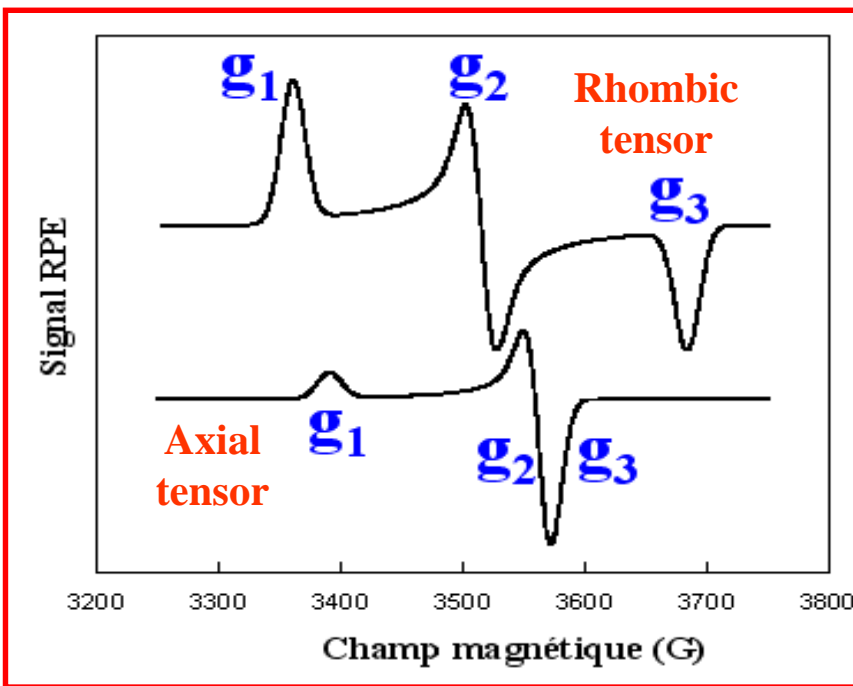
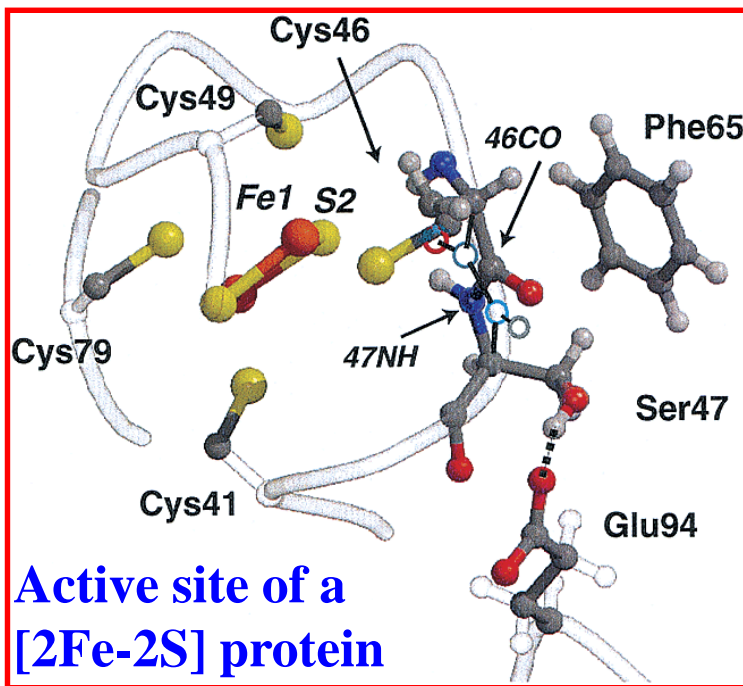
S	K_A	K_B
9/2	+ 5/9	+ 4/9
7/2	+ 37/63	+ 26/63
5/2	+ 23/35	+ 12/35
3/2	+ 13/15	+ 2/15
1/2	+ 7/3	- 4/3

Spin coupling and EPR/ENDOR spectroscopies

$$\tilde{g} = (7/3)\tilde{g}_A - (4/3)\tilde{g}_B$$



Example of magneto-structural correlation



Correlation between the Magnetic g Tensors and the Local Cysteine Geometries for a Series of Reduced [2Fe-2S*] Protein Clusters. A Quantum Chemical Density Functional Theory and Structural Analysis

Serge Gambarelli* and Jean-Marie Mouesa*

Inorg. Chem. 2004, 43, 1441–1451

Variation of Average g Values and Effective Exchange Coupling Constants among [2Fe-2S] Clusters: A Density Functional Theory Study of the Impact of Localization (Trapping Forces) versus Delocalization (Double-Exchange) as Competing Factors

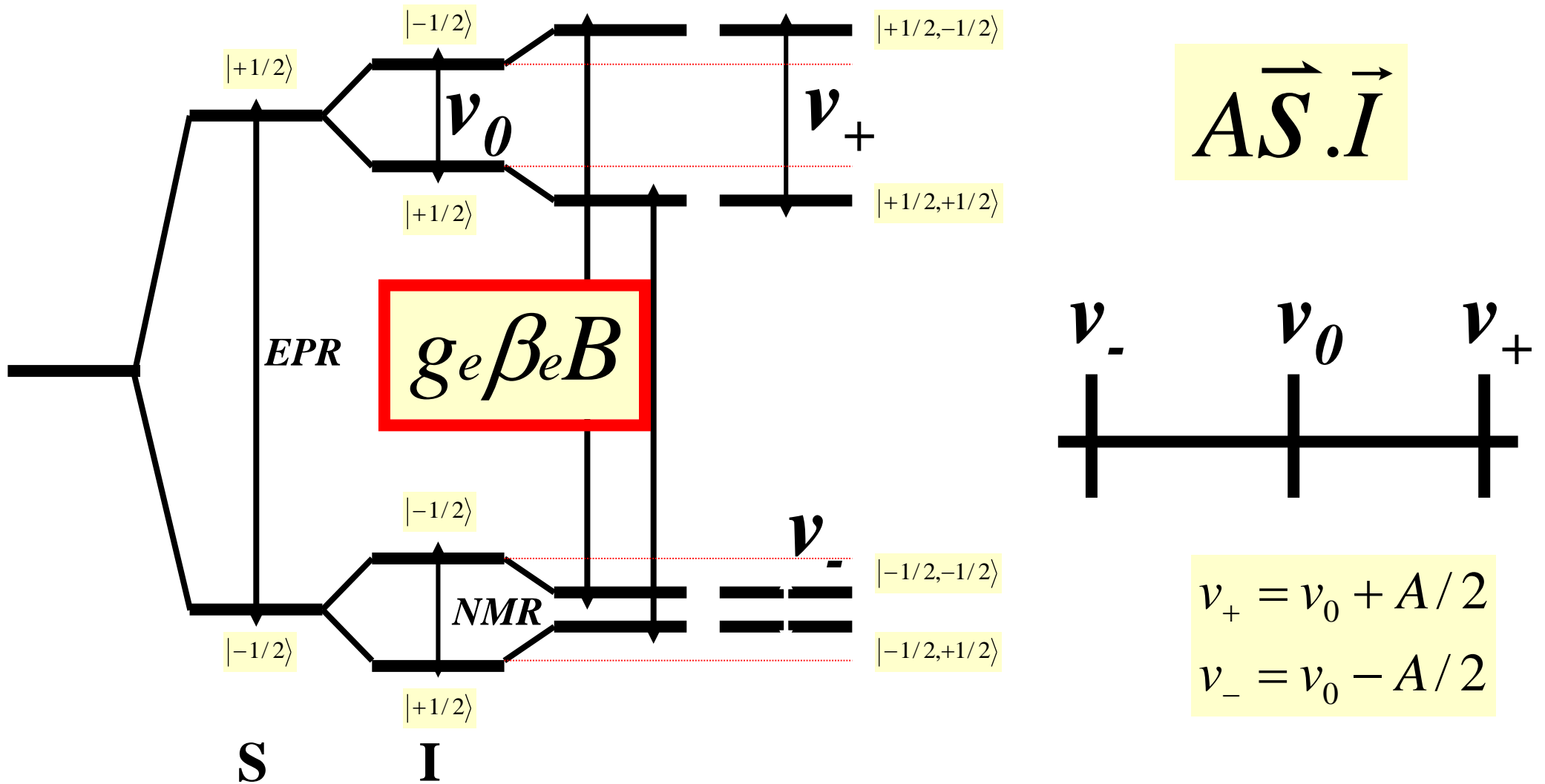
Maylis Orio and Jean-Marie Mouesa*

Inorg. Chem. 2008, 47, 5394–5416

P. Bertrand and J.-P. Gayda,
Biochim. Biophys. Acta 579,
p.107 (1979)

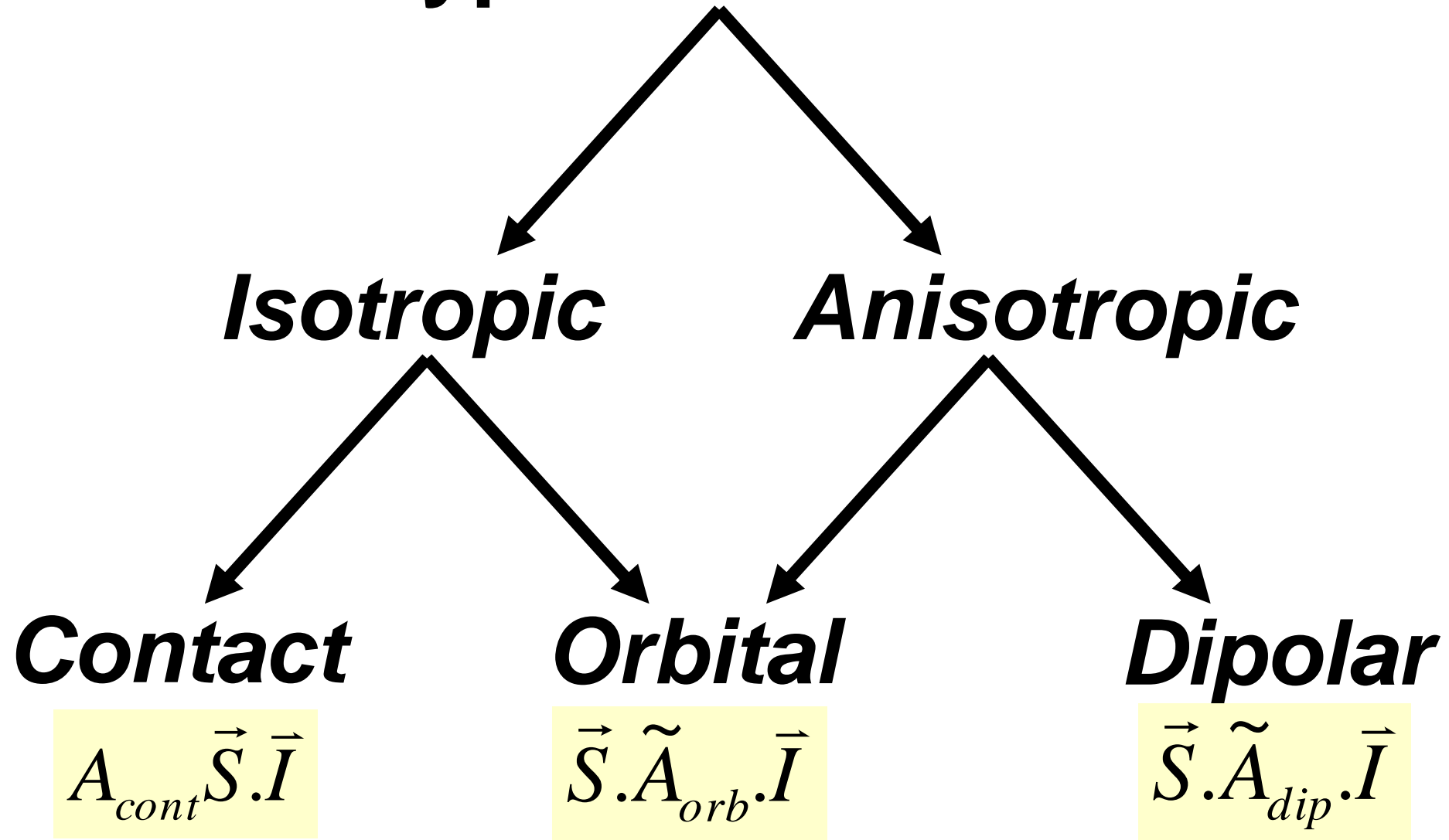
SKIP !

Zeeman interactions + hyperfine couplings



SKIP !

Hyperfine tensor



SKIP !

Hyperfine couplings

$$\vec{S} \cdot \tilde{\vec{A}}_I \cdot \vec{I}$$

Fermi contact

$$A_{cont} \vec{S} \cdot \vec{I}$$

$$A_{cont} = \frac{1}{2S} \frac{8\pi}{3} g_e \beta_e g_I \beta_I \Psi^2(r_I)$$

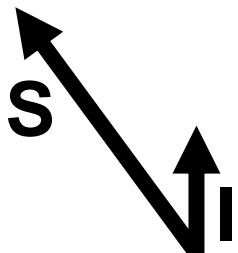
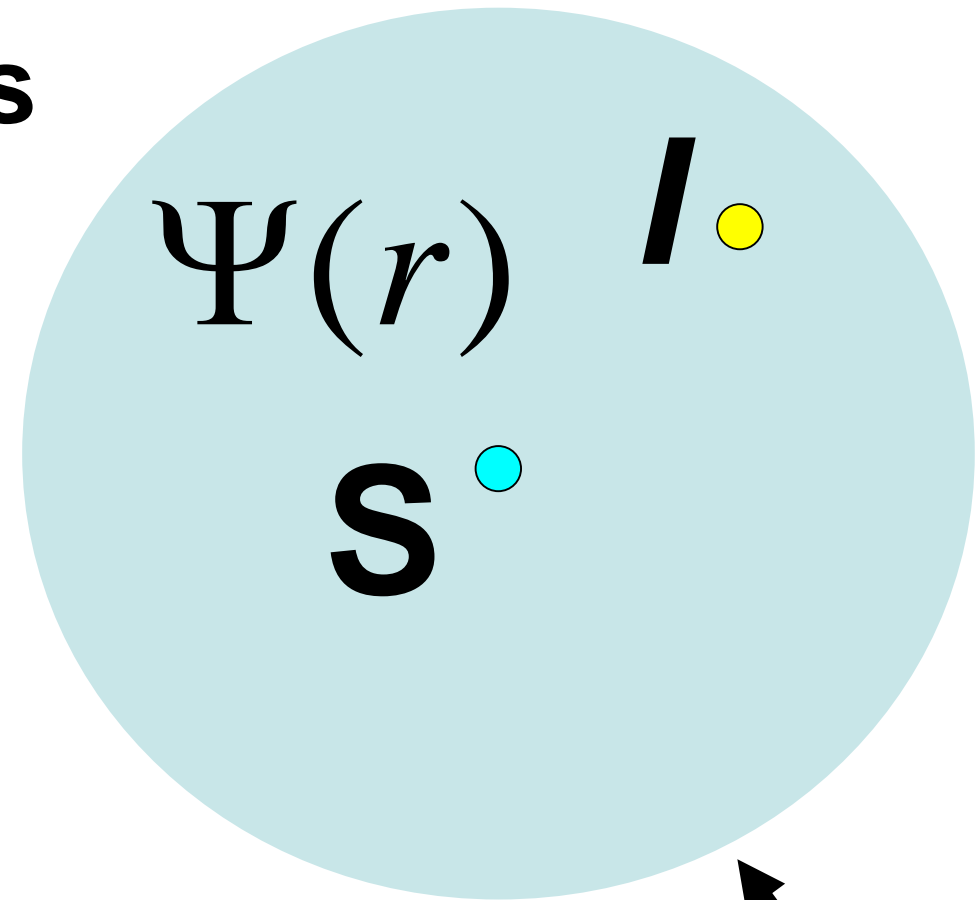
$$\vec{S} \cdot \tilde{\vec{A}}_{orb} \cdot \vec{I}$$

$$\tilde{\vec{A}}_{orb} = \vec{S} \cdot \left[\frac{1}{g_e} \left(\tilde{g} - g_e \tilde{I} d \right) \tilde{\vec{A}}(\text{dip}) \right] \cdot \vec{I}$$

Pseudo-contact

$$\vec{S} \cdot \tilde{\vec{A}}_{dip} \cdot \vec{I}$$

$$\tilde{\vec{A}}_{dip} = \frac{g_e \beta_e g_I \beta_I}{2S} \iiint_r \frac{1}{r^5} \left[-\vec{S} \cdot \vec{I} r^2 + 3(\vec{S} \cdot \vec{r})(\vec{I} \cdot \vec{r}) \right] \Psi^2(r) dr$$



SKIP !

Hyperfine couplings

$$\vec{S} \cdot \tilde{\vec{A}}_I \cdot \vec{I}$$

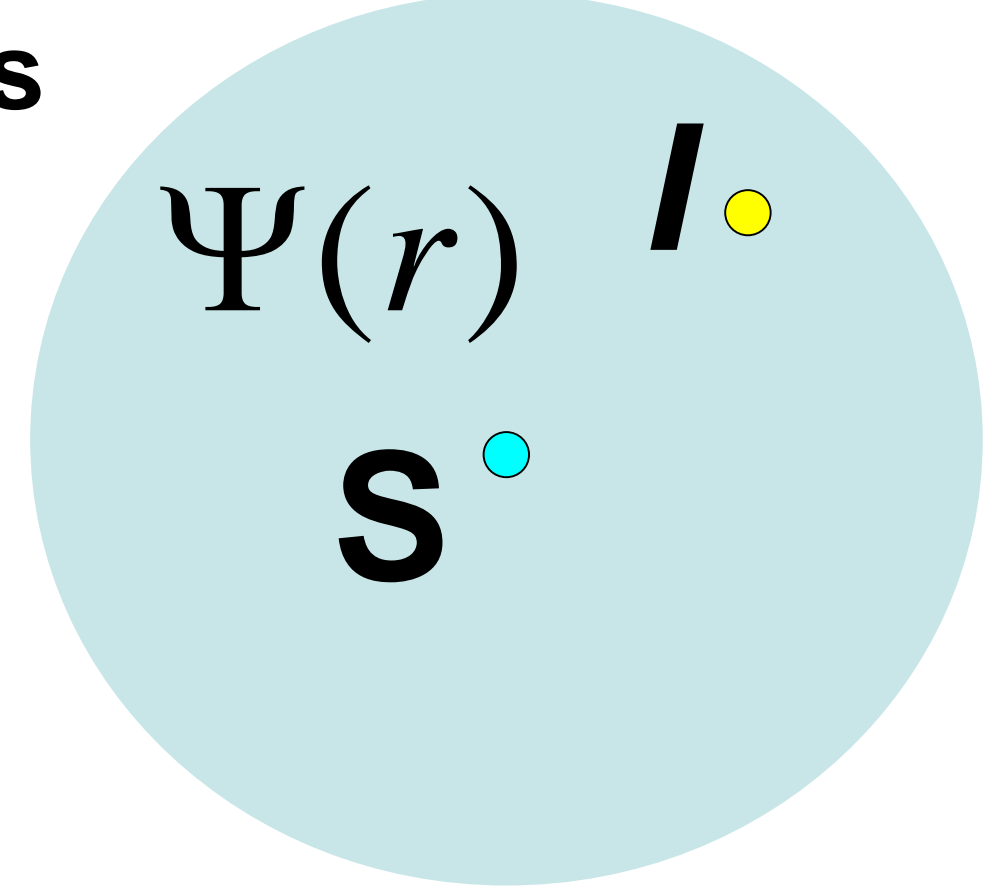
$$A_{cont} \vec{S} \cdot \vec{I}$$

$$A_{cont} = \frac{1}{2S} \frac{8\pi}{3} g_e \beta_e g_I \beta_I (\Psi_\alpha^2(r_I) - \Psi_\beta^2(r_I))$$

$$\left(\frac{\mu_0}{4\pi} \right) g_e \beta_e g_I \beta_I / (hr^3)$$

In MHz:

Proton (1H)	79.1
Carbone (^{13}C)	19.9
Nitrogen (^{14}N)	5.7
Fer (^{57}Fe)	2.55



${}^1H(1s : 100\%)$
 $\rightarrow 1420 \text{ MHz}$

SKIP ! Organic radicals versus Metallic complexes

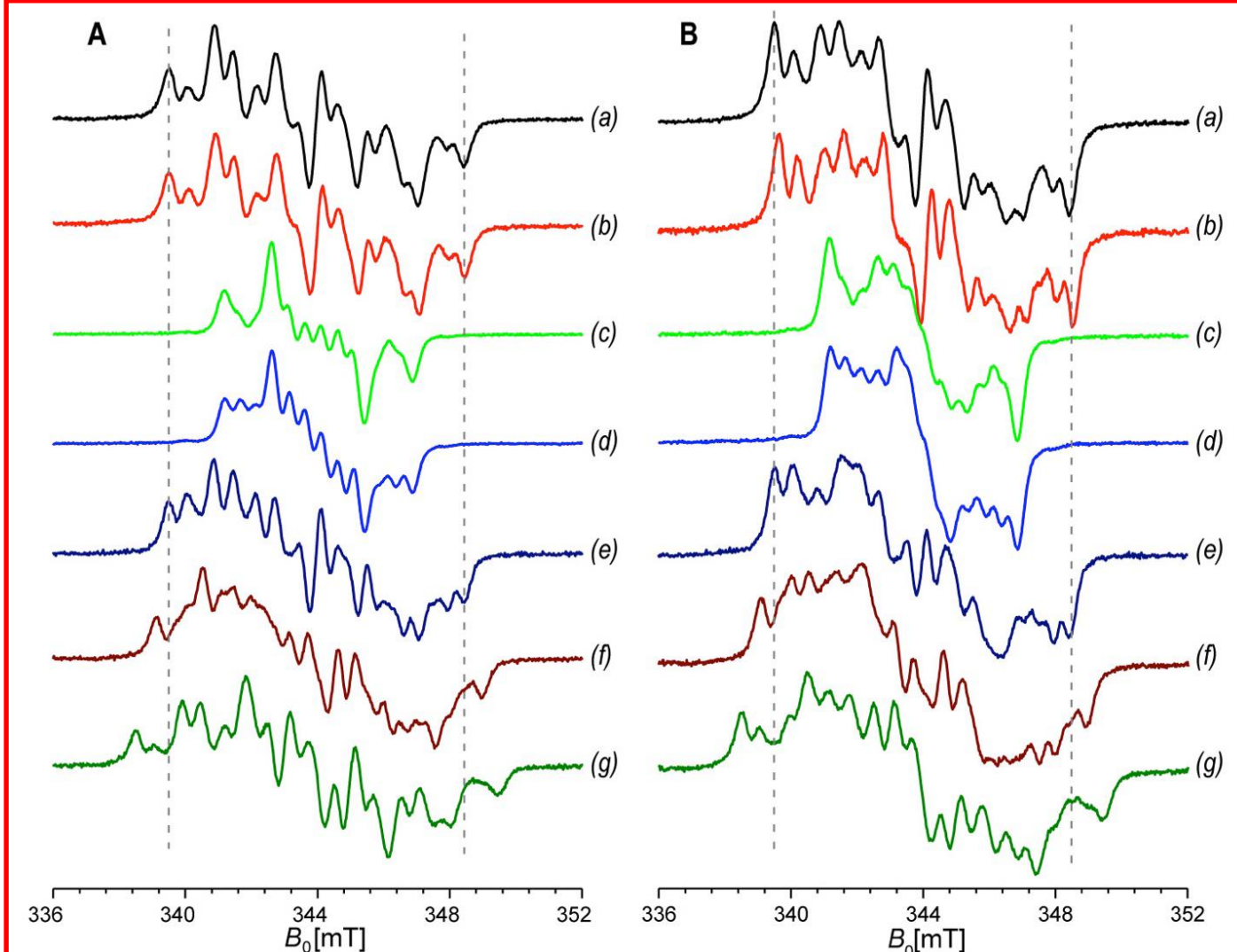
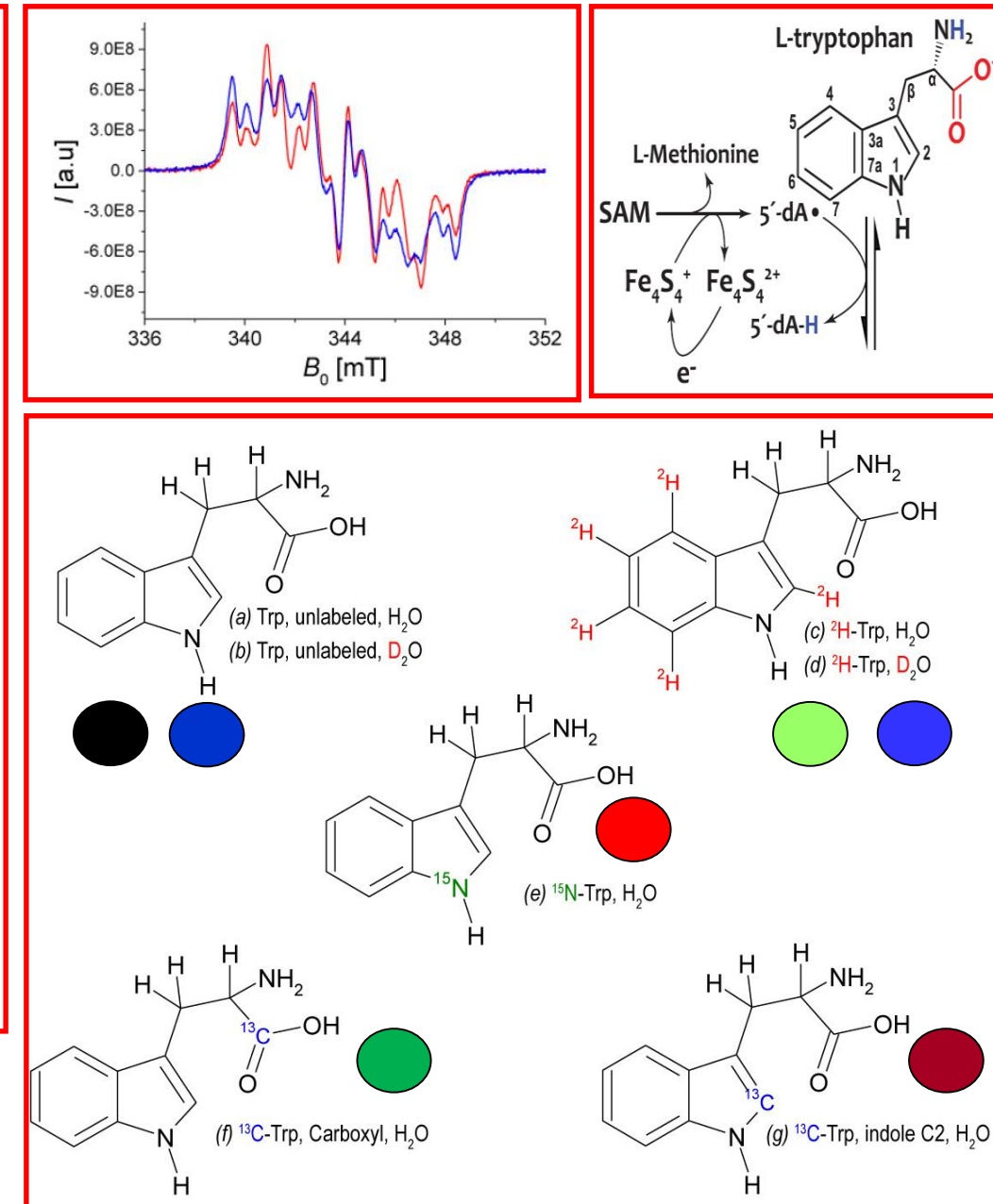
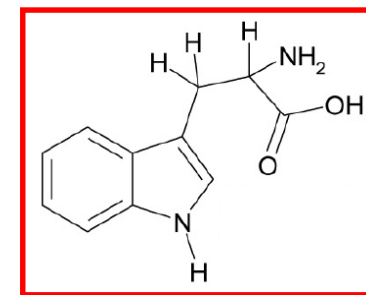
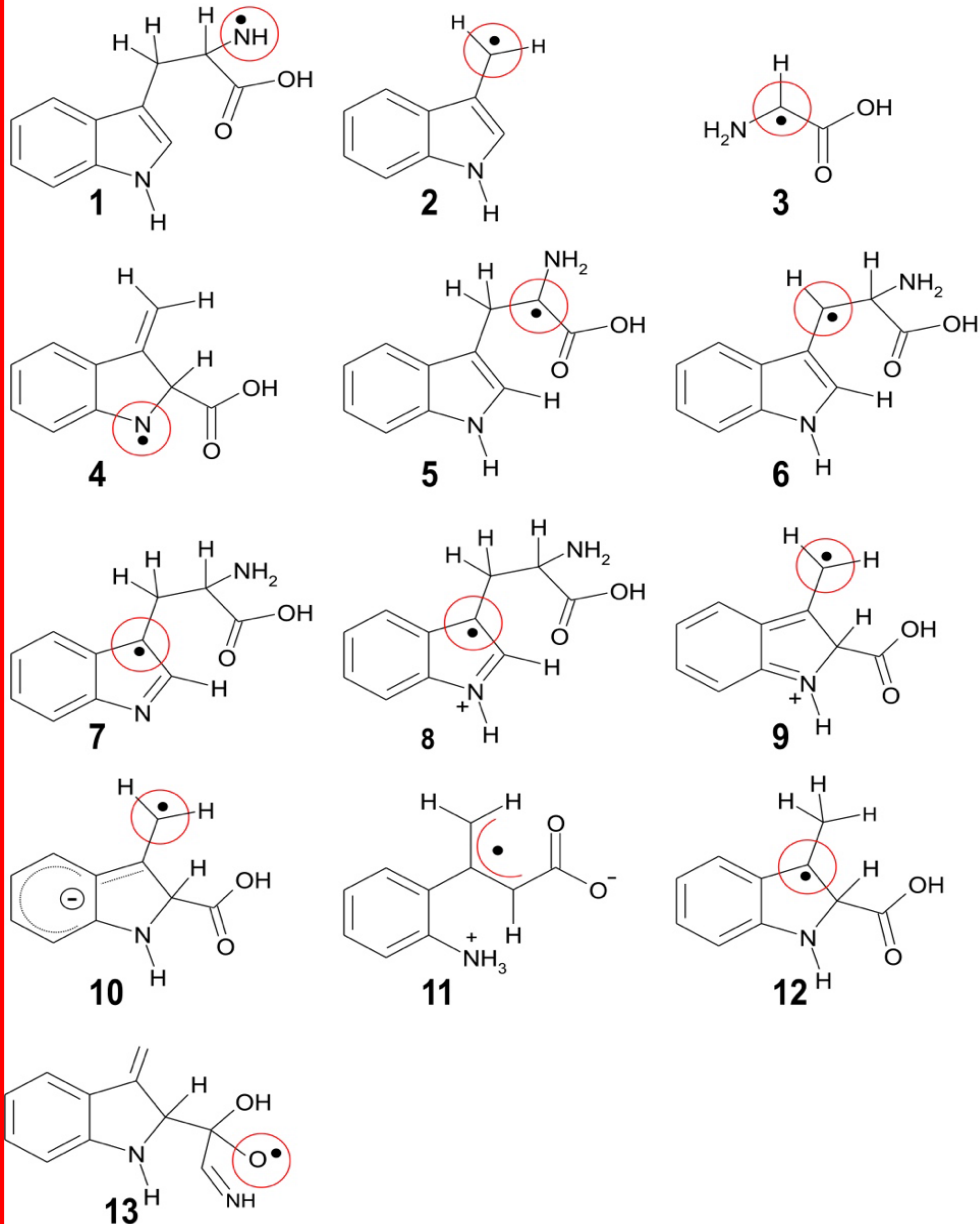


Figure S6. Raw spectra (X-band, 9.65 GHz) for unlabeled L-tryptophan (Trp) in H_2O (a, black), ^{15}N -Trp (b, red), ^2H -Trp in H_2O (c, light green), ^2H -Trp in D_2O (d, blue), unlabeled Trp in D_2O (e, navy), ^{13}C -Trp (f, indole, brown), ^{13}C -Trp (g, COOH, dark green); quenching time of the reaction: 45 s. (A) temperature 80 K, (B) temperature 60 K.

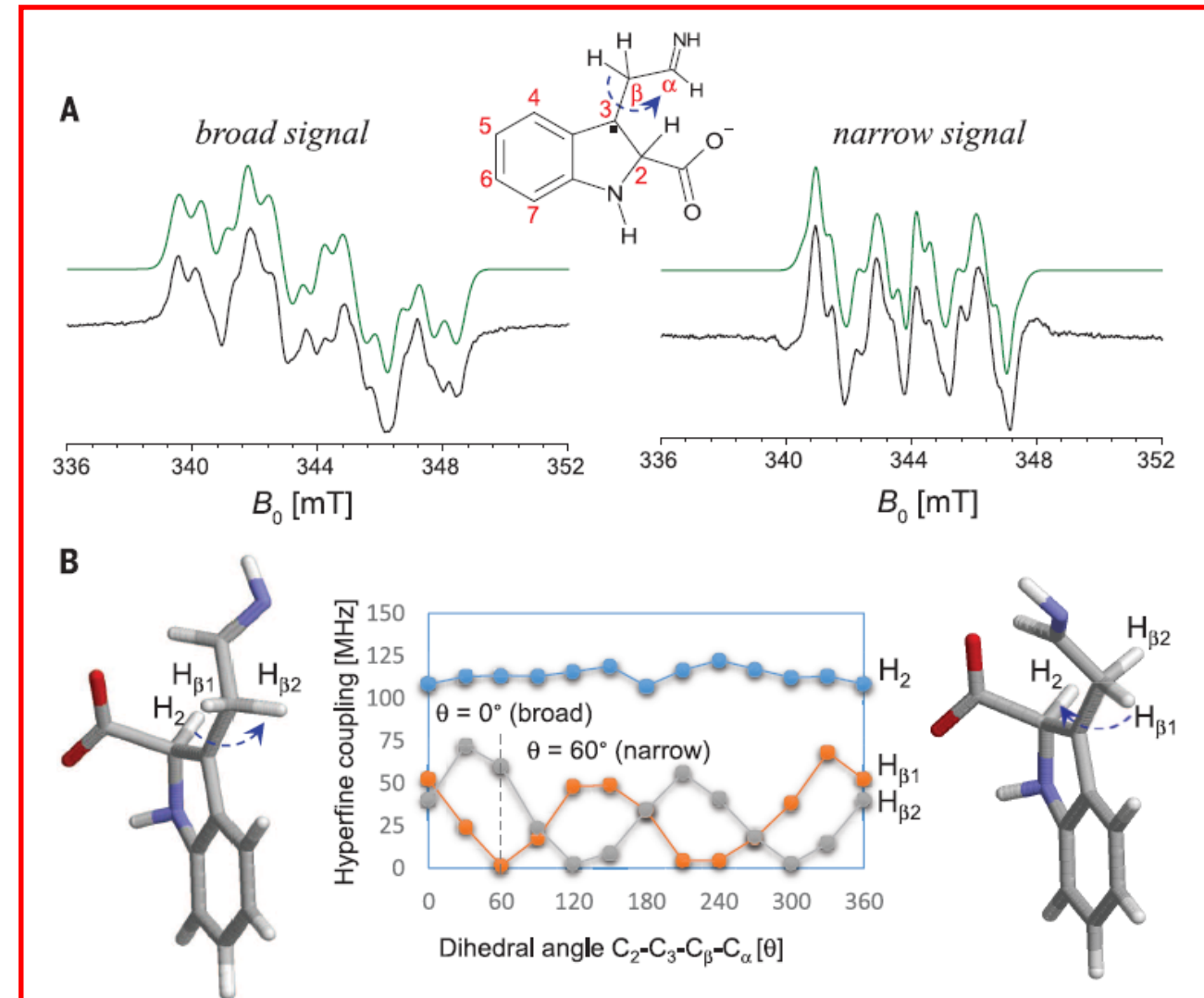


SKIP !



Fine-tuning of a radical-based reaction by radical S-adenosyl-L-methionine tryptophan lyase *Science* 2016, vol.351, p.1320

Giuseppe Sicoli,^{1,2} Jean-Marie Mouesa,^{1,2} Laura Zeppieri,³ Patricia Amara,³ Lydie Martin,³ Anne-Laure Barra,⁴ Juan C. Fontecilla-Camps,³ Serge Gambarelli,^{1,2*} Yvain Nicolet^{3*}



3s

Organic radicals versus Metallic complexes

2s

1s

$$FC = A_{cont}$$

$$PC = A_{orb}$$

Ions	1s	2s	3s	total
Fe ²⁺	+0.07	+2.37	-1.44	≡ 1.00
Fe ³⁺	+0.09	+2.83	-1.91	≡ 1.00

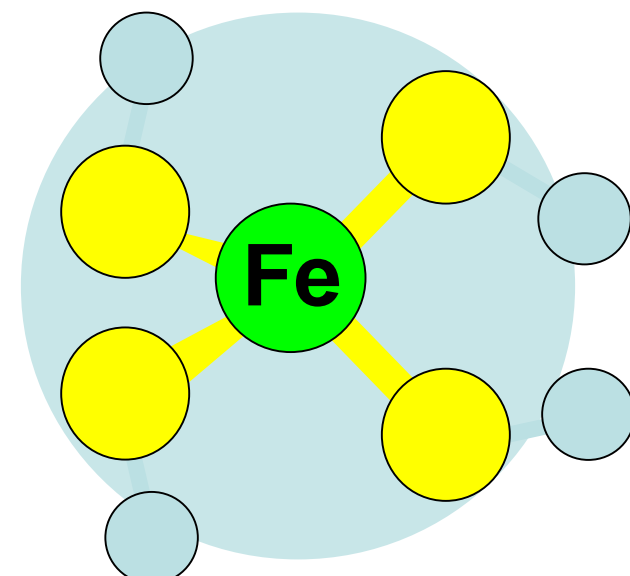
Watson & Freeman (1961)

The Mössbauer Parameters of the Proximal Cluster of Membrane-Bound Hydrogenase Revisited: A Density Functional Theory Study

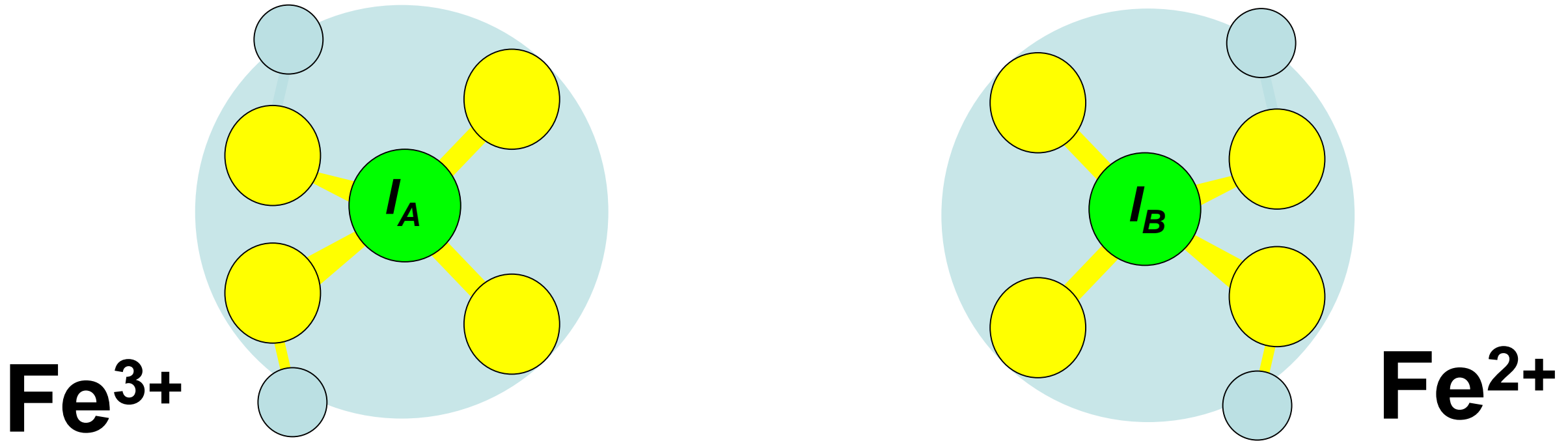
Shadan Ghassemi Tabrizi,[†] Vladimir Pelmenschikov,[†] Louis Noodleman,[‡] and Martin Kaupp^{*†}

	FC	PC	FC+PC	FC ^{scal}	PC ^{scal}	FC ^{scal} +PC ^{scal}	A _{iso} ^{exp}
Fe ^{II} PorOAc	-18.5	+1.3	-16.8	-35.9	+4.7	-31.2	-21.8
Fe ^{II} SR3	-14.7	+2.3	-12.4	-28.5	+8.3	-20.2	-14.9
Fe ^{III} Az	-15.8	+4.6	-11.1	-30.7	+16.6	-14.0	-13.47
Fe ^{III} OEPPy	-16.6	+6.2	-10.4	-32.2	+22.4	-9.8	-6.8
Fe ^{III} MAC	-3.2	+1.0	-2.1	-6.2	+3.6	-2.6	-15.4
Fe ^{III} PorOAc	-16.6	+0.1	-16.4	-32.2	+0.4	-31.8	-27.5
Fe ^{III} PorO ₂	-13.3	+0.7	-12.6	-25.8	+2.5	-23.3	-32.1
Fe ^{IV} PorO	-9.6	-0.7	-10.4	-18.6	-2.5	-21.2	-25.2
Fe ^{IV} MAC	-8.2	+0.3	-7.9	-15.9	+1.1	-14.8	-20
Rd _{red} Fe ²⁺	-13.49	+1.37	-12.12	-26.2	+4.9	-21.2	-23.4
Rd _{ox} Fe ³⁺	-12.19	+0.61	-11.58	-23.6	+2.2	-21.4	-22.5

J. Chem. Theory Comput. 2016, 12, 174–187



Spin coupling



Fe³⁺

$$\vec{S}_A \cdot (\tilde{A}_{cont}(loc)_{AA}) \cdot \vec{I}_A$$

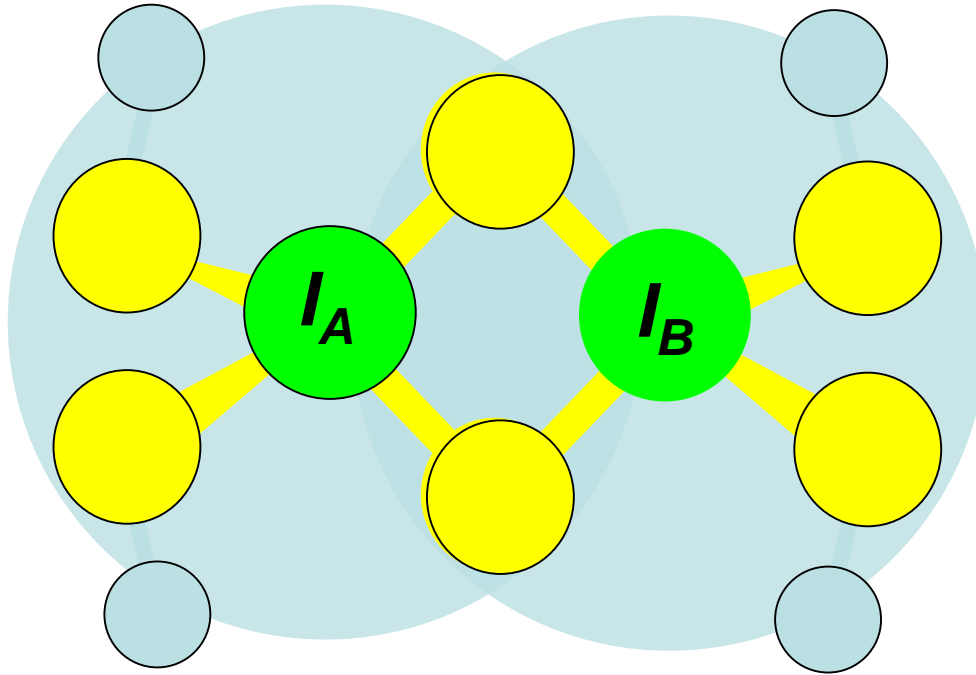
$$\tilde{A}_{cont}(loc)_{AA} \approx -22 \text{ MHz}$$

Fe²⁺

$$\vec{S}_B \cdot (\tilde{A}_{cont}(loc)_{BB}) \cdot \vec{I}_B$$

$$\tilde{A}_{cont}(loc)_{BB} \approx -23 \text{ MHz}$$

Spin coupling



57Fe

$$K_A = +7/3$$

$$K_B = -4/3$$

$$K_A \tilde{A}_{cont}(loc)_{AA} = -51 \text{ MHz}$$

$$K_B \tilde{A}_{cont}(loc)_{BB} = +27 \text{ MHz}$$

S=1/2

Spin coupling effect on hyperfine couplings

Exp.	14.6	[-3.2, -0.5, 3.6]	[11.4, 14.1, 18.2]
	13.0	[-1.5, -1.5, 3.0]	[11.5, 11.5, 16.0]

BS State	Model	$A_{\text{iso}}^{\text{UBS}}$	T^{UBS}	$A^{\text{UBS}} = A_{\text{iso}}^{\text{UBS}} + T^{\text{UBS}}$
BS12	S-OX _P ⁵⁺	38.0	[-8.0, -1.6, 9.5]	[30.0, 36.4, 47.5]
	S-OX _D ⁵⁺	34.4	[-10.4, 3.1, 7.3]	[24.0, 37.5, 41.7]
	S-OX _{D-H} ⁵⁺	35.8	[-9.8, 0.8, 9.0]	[26.1, 36.6, 44.8]
BS13	S-OX _P ⁵⁺	41.2	[-8.7, -1.8, 10.5]	[32.5, 39.5, 51.7]
	S-OX _D ⁵⁺	35.2	[-10.8, 3.1, 7.8]	[24.3, 38.2, 43.0]
	S-OX _{D-H} ⁵⁺	37.1	[-10.4, 1.1, 9.3]	[26.8, 38.2, 46.4]
BS34	S-OX _P ³⁺	9.5	[-4.5, 0.2, 4.3]	[5.0, 9.7, 13.7]
	S-OX _D ⁵⁺	-2.5	[-7.0, 2.0, 5.0]	[-9.4, -0.5, 2.5]
	S-OX _{D-H} ⁵⁺	-5.3	[-6.1, 2.0, 4.1]	[-11.4, -3.3, -1.3]

$$\vec{S}_A \cdot (\tilde{A}_{\text{cont}}(\text{loc})_{AA}) \cdot \vec{I}_A$$

$$\tilde{A}_{\text{cont}}(\text{loc})_{BS12} \sim 36 \text{ MHz}$$

$$\tilde{A}_{\text{cont}}(\text{loc})_{BS13} \sim 37 \text{ MHz}$$

$$\tilde{A}_{\text{cont}}(\text{loc})_{BS14} \sim -5 \text{ MHz}$$

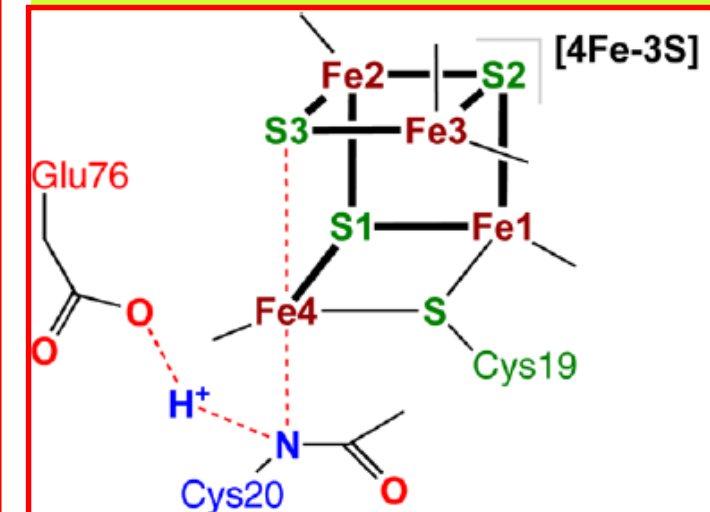


Table S9. ‘Raw’ Unrestricted Broken-Symmetry (UBS) DFT Hyperfine Parameters (MHz) of the Fe4-bound Cys20 Amide Nitrogen Atom N20 in Different Structural Arrangements of the Superoxidized Proximal Cluster Computed using PBE and B3LYP Functionals for the Broken-Symmetry States BS12, BS13, and BS34^a

Spin coupling effect on hyperfine couplings

Redox-Dependent Structural Transformations of the [4Fe-3S] Proximal Cluster in O₂-Tolerant Membrane-Bound [NiFe]-Hydrogenase: A DFT Study

Vladimir Pelmenschikov and Martin Kaupp,
J. Am. Chem. Soc. 2013, 135, 11809–11823

Signal/DFT Model	BS State	A_{iso}	\mathbf{T}	$A = A_{\text{iso}} + \mathbf{T}$
N _{C20} (ENDOR) ¹⁹	–	14.6	[-3.2, -0.5, 3.6]	[11.4, 14.1, 18.2]
N1 (HYSCORE) ²⁰	–	13.0	[-1.5, -1.5, 3.0]	[11.5, 11.5, 16.0]
S-OX _{D-H} ⁵⁺ (B3LYP)	BS12	16.8	[-4.6, 0.4, 4.2]	[12.3, 17.2, 21.1]
	BS13	17.5	[-4.9, 0.5, 4.4]	[12.6, 18.0, 21.8]
	BS34	-1.8	[-2.0, 0.7, 1.4]	[-3.8, -1.1, -0.4]

$$K_{ij} \tilde{A}_{\text{cont}}(\text{loc})_{BSij}$$

$$K_{BS12} = 0.47$$

$$K_{BS13} = 0.47$$

$$K_{BS34} = 0.33$$

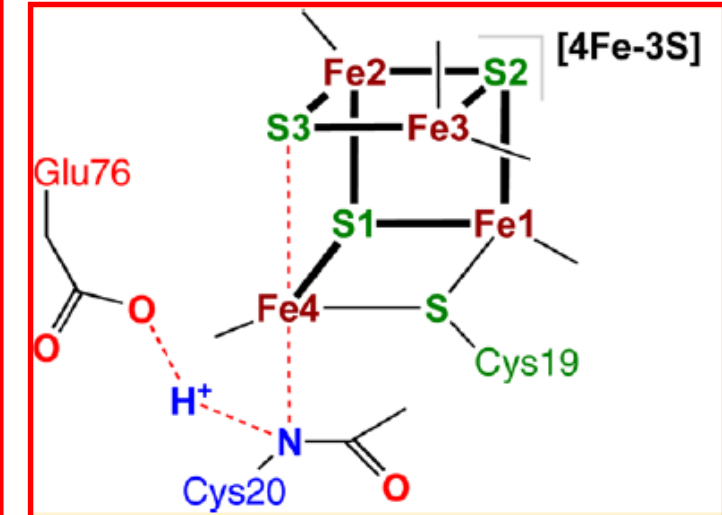


Table S10. Spin-Projected ¹⁴N Hyperfine Parameters (MHz) of the Fe4-bound Cys20 Amide Nitrogen Atom N20 in Different Structural Arrangements of the Superoxidized Proximal Cluster Computed using B3LYP Functional for the Broken-Symmetry States BS12, BS13, and BS34, Compared to ENDOR and HYSCORE Data^a

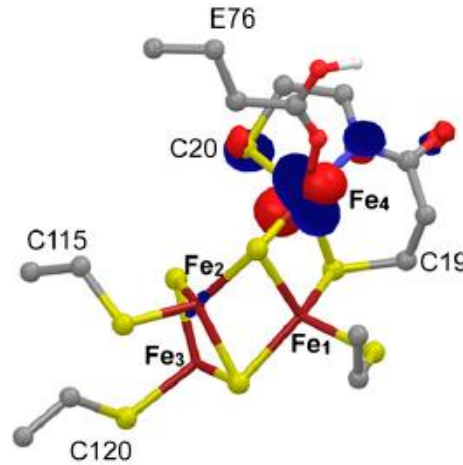
Spin coupling effect on charges (Mössbauer)

X-ray crystallographic and computational studies of the O₂-tolerant [NiFe]-hydrogenase 1 from *Escherichia coli*

PNAS 2012, vol. 109, p.5305–5310

Anne Volbeda^{a,1}, Patricia Amara^{a,1}, Claudine Darnault^a, Jean-Marie Mouesca^b, Alison Parkin^c, Maxie M. Roessler^{c,d}, Fraser A. Armstrong^{c,d}, and Juan C. Fontecilla-Camps^{a,2}

Exp 2.41 0.60 0.60 1.23



BS13	-4/2	+5/2	-5/2	+5/2
BS24	+5/2	-5/2	+5/2	-4/2
BS34	+5/2	+5/2	-5/2	-4/2
BS23	+5/2	-4/2	-5/2	+5/2
BS12	-4/2	-5/2	+5/2	+5/2
BS14	-5/2	+5/2	+5/2	-4/2

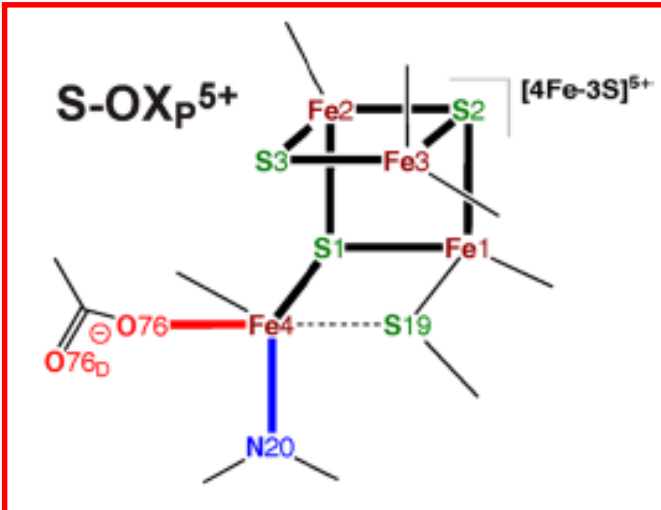
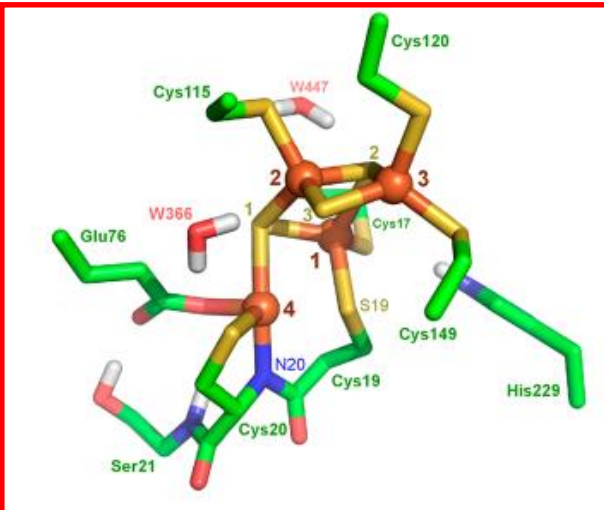
Electronic State	Relative energies (kJ/mol)	ΔE_Q Fe ₁ (η)	ΔE_Q Fe ₂ (η)	ΔE_Q Fe ₃ (η)	ΔE_Q Fe ₄ (η)
BS13	8.1	2.36 (0.21)	0.31 (0.44)	-0.31 (0.29)	0.96 (0.60)
BS24	0.0	2.14 (0.21)	0.27 (0.45)	-0.35 (0.24)	2.09 (0.77)
BS34	9.9	1.65 (0.93)	0.49 (0.52)	-0.20 (0.46)	2.12 (0.51)
BS23	58.7	0.56 (0.62)	1.11 (0.68)	0.72 (0.40)	1.35 (0.40)
BS12	1.4	1.54 (0.97)	0.44 (0.33)	-0.24 (0.22)	0.80 (0.83)
BS14	60.4	1.23 (0.70)	0.37 (0.97)	-0.45 (0.37)	1.55 (0.28)

Spin coupling effect (Mössbauer & hyperfine)

The Mössbauer Parameters of the Proximal Cluster of Membrane-Bound Hydrogenase Revisited: A Density Functional Theory Study

Shadan Ghassemi Tabrizi,[†] Vladimir Pelmenschikov,[†] Louis Noodleman,[‡] and Martin Kaupp^{*†}

J. Chem. Theory Comput. 2016, 12, 174–187



	site	$A_{\text{iso}}^{\text{a}}$	$A_{\text{iso}}^{\text{b}}$	T_{xx}^{c}	T_{yy}	T_{zz}
BS13 S- OX_p^{5+}						
	$\text{N}_{\text{C}20}$	+16.0	—	-3.5	+0.1	+3.5
^{14}N exp.	$\text{N}_{\text{C}20}^{\text{ENDOR}}$	+14.6		-3.2	-0.5	+3.6
	$\text{N}_{\text{C}20}^{\text{HYSCORE}}$	+13.0		-1.5	-1.5	+3.0

Table 3. Computed Mössbauer Parameters for the S- OX_p^{5+} Model at PBE/B3LYP Levels in Different BS States As Compared to Experimental Data^a

S- OX_p^{5+} PBE/B3LYP Mössbauer parameters					
state	site	ΔE_Q (mms ⁻¹)	δ (mms ⁻¹)	η	A_{iso}
S- OX_p^{5+} exp. ²⁰	S	(+)2.45	0.46	0.5	+25.7
		(+)0.70	0.39	1.0	-47.9
		(+)0.60	0.28	0.3	+33.4
		(-)1.00	0.40	0.7	-33.6
BS12	$\text{Fe}1^{2+}$	+1.67/+2.51	0.48/0.50	0.93/0.70	+
	$\text{Fe}2^{3+}$	-0.55/-0.66	0.37/0.35	0.71/0.86	+
	$\text{Fe}3^{3+}$	-0.41/+0.47	0.32/0.29	0.89/0.95	-
	$\text{Fe}4^{3+}$	-1.63/-1.66	0.58/0.47	0.39/0.20	-
BS13	$\text{Fe}1^{2+}$	+2.51/+3.42	0.48/0.55	0.21/0.35	+
	$\text{Fe}2^{3+}$	+0.54/+0.53	0.32/0.30	0.42/0.57	-
	$\text{Fe}3^{3+}$	+0.66/+0.78	0.36/0.33	0.87/0.66	+
	$\text{Fe}4^{3+}$	-1.34/-1.26	0.59/0.50	0.85/0.85	-
BS34	$\text{Fe}1^{2+}$	+1.82/+2.70	0.50/0.51	0.69/0.50	-
	$\text{Fe}2^{3+}$	-0.54/-0.64	0.41/0.40	0.16/0.64	-
	$\text{Fe}3^{3+}$	+0.37/+0.46	0.33/0.31	0.78/0.68	+
	$\text{Fe}4^{3+}$	+2.51/+2.89	0.53/0.51	0.25/0.19	+

DFT codes are very useful ... But they are not black boxes !

- Some cases are « easily » treated :
 - Most organic molecules
 - Most (metallic) monomeric complexes
 - g-tensors, hyperfine couplings ... but also ZFS
 - « most » → possible degenerescence problems
- Polymetallic complexes :
 - Beware of spin coupling !
 - Computation of Broken Symmetry states
- Almost each problem is unique
 - Know your system before DFT calculations

Original papers

- *Inhomogeneous Electron Gas*, P. Hohenberg and W. Kohn, Phys. Rev. **136**, B864 (1964).
- *Self Consistent Equations Including Exchange and Correlation Effects*, W. Kohn and L.J. Sham, Phys. Rev. **140**, A1133 (1965).

Review Articles

- *Nobel Lecture: Electronic structure of matter-wave functions and density functionals*, W. Kohn, Rev. Mod. Phys. **71**, 1253 (1998).
- *The density functional formalism, its applications and prospects*, R.O. Jones and O. Gunnarsson, Rev. Mod. Phys. **61**, 689 (1989).

Books

- *Density-Functional Theory of Atoms and Molecules*, R.G Parr and W. Yang, Oxford University Press, New York (1989).
- *A Chemist's Guide to Density Functional Theory*, W. Koch and M.C. Holthausen, WILEY-VCH (2001).

REPORT

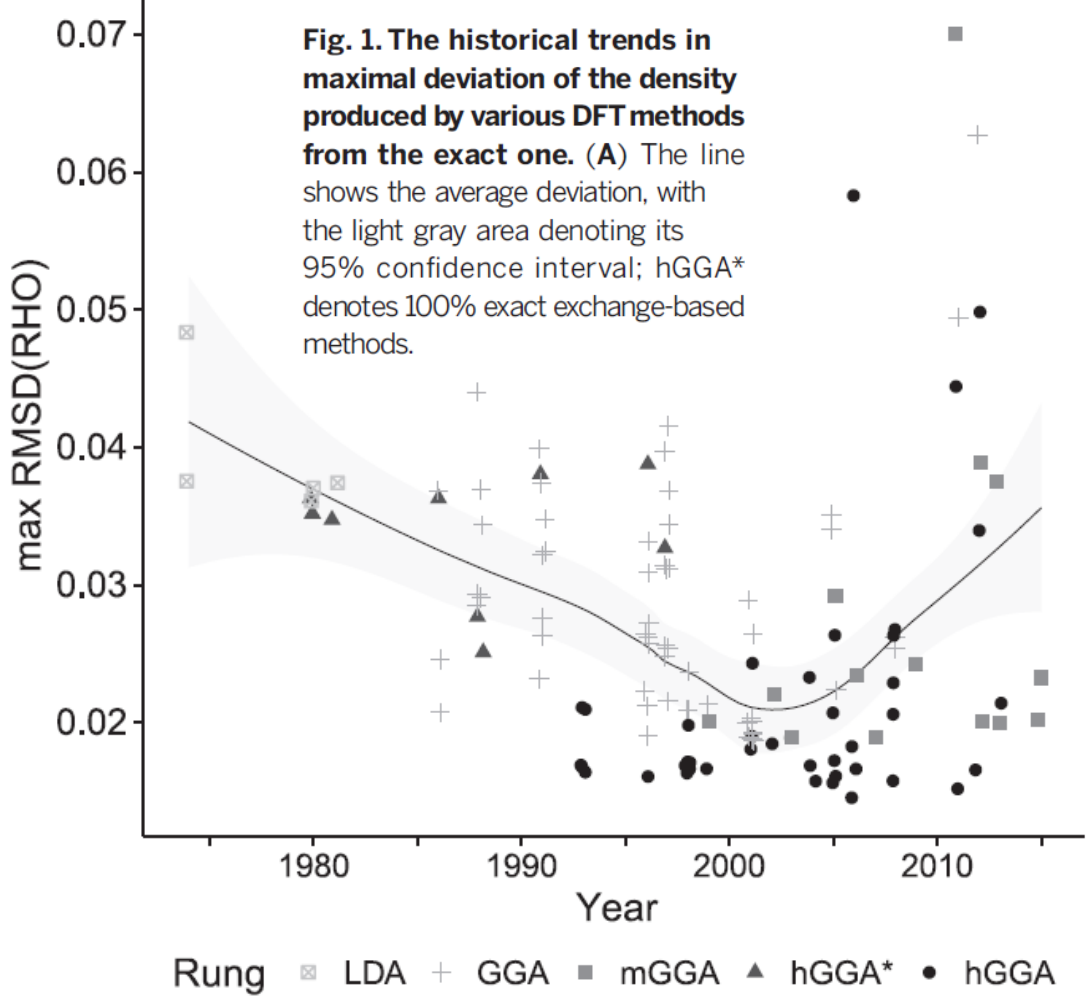
THEORETICAL CHEMISTRY

Density functional theory is straying from the path toward the exact functional

Michael G. Medvedev,^{1,2,3*}† Ivan S. Bushmarinov,^{1*}† Jianwei Sun,^{4‡}
John P. Perdew,^{4,5†} Konstantin A. Lyssenko^{1†}

The theorems at the core of density functional theory (DFT) state that the energy of a many-electron system in its ground state is fully defined by its electron density distribution. This connection is made via the exact functional for the energy, which minimizes at the exact density. For years, DFT development focused on energies, implicitly assuming that functionals producing better energies become better approximations of the exact functional. We examined the other side of the coin: the energy-minimizing electron densities for atomic species, as produced by 128 historical and modern DFT functionals. We found that these densities became closer to the exact ones, reflecting theoretical advances, until the early 2000s, when this trend was reversed by unconstrained functionals sacrificing physical rigor for the flexibility of empirical fitting.

ORIGINAL ARTICLE Medvedev, M. G. et al.
Density functional theory is straying from the path toward the exact functional. *Science* **355**, 49–52 (2017)



QUANTUM CHEMISTRY

DFT's midlife crisis

Gabriella Graziano

Nature Reviews Chemistry

Published online 1 Feb 2017

doi:[10.1038/s41570-017-0019](https://doi.org/10.1038/s41570-017-0019)

Review

Prediction of molecular properties and molecular spectroscopy with density functional theory: From fundamental theory to exchange-coupling

Frank Neese

Lehrstuhl für Theoretische Chemie, Universität Bonn, Institut für Physikalische und Theoretische Chemie, Wegelerstrasse 12, D-53115 Bonn, Germany

Coordination Chemistry Reviews 253 (2009) 526–563

Coordination Chemistry Reviews

Volume 253, Issues 5–6, Pages 523–826 (March 2009)

Theory and Computing in Contemporary Coordination Chemistry

Edited by A. Ghosh

REVIEW ARTICLE

www.rsc.org/pccp | Physical Chemistry Chemical Physics

Density functional theory for transition metals and transition metal chemistry

Christopher J. Cramer* and Donald G. Truhlar*

Phys. Chem. Chem. Phys., 2009, 11, 10757–10816

Chem. Rev. 2004, 104, 419–458

Electronic Structures of Metal Sites in Proteins and Models: Contributions to Function in Blue Copper Proteins

Edward I. Solomon,*[†] Robert K. Szilagyi,[†] Serena DeBeer George,[‡] and Lipika Basumallick[†]

Challenges for Density Functional Theory

Aron J. Cohen,* Paula Mori-Sánchez,* and Weitao Yang*

June 1998

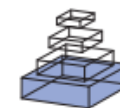
Density functional theory of one-dimensional two-particle systems

H. L. Neal

American Journal of Physics 66, 512 (1998); <http://doi.org/10.1119/1.18892>

REVIEW ARTICLE

published: 29 April 2014
doi: 10.3389/fchem.2014.00014



Applications of density functional theory to iron-containing molecules of bioinorganic interest

Hajime Hirao *, Nandun Thellamurege and Xi Zhang



International Journal of
Molecular Sciences



Int. J. Mol. Sci. 2016, 17, 519; doi:10.3390/ijms17040519

Review

Challenging Density Functional Theory Calculations with Hemes and Porphyrins

Sam P. de Visser ^{1,*} and Martin J. Stillman ^{2,*}

Essentials of
Computational Chemistry Second Edition
Theories and Models

Christopher J Cramer

